2015

Study of Escherichia Coli ADP-Glucose Pyrophosphorylase Catalysis: Investigating Critical Roles of Conserved Arg32 and Lys42 Residues

Angela Lynn Mahaffey
Loyola University Chicago

LOYOLA UNIVERSITY CHICAGO

STUDY OF *ESCHERICHIA COLI* ADP-GLUCOSE PYROPHOSPHORYLASE CATALYSIS: INVESTIGATING CRITICAL ROLES OF CONSERVED ARG32 AND LYS42 RESIDUES

A DISSERTATION SUBMITTED TO

THE FACULTY OF THE GRADUATE SCHOOL

IN CANDIDACY FOR THE DEGREE OF

DOCTOR OF PHILOSOPHY

PROGRAM IN CHEMISTRY

BY

ANGELA L. MAHAFFEY

CHICAGO, IL

DECEMBER 2015

ACKNOWLEDGEMENTS

The author would like to acknowledge, with sincere gratitude, the assistance and support of the following persons and organizations: Debra Mahaffey, M.A. (Mother), Dr. Miguel A. Ballicora, Dr. Kenneth W. Olsen, Dr. David Crumrine, Dr. Dali Liu, Dr. Jeffrey Doering, Dr. Duarte Mota de Freitas, Dr. Carlos M. Figeuroa, Dr. Misty L. Kuhn, Dr. Linda McCabe-Smith, Ligin Solamen, Saleh Aiyash, Ana Cristina Ebrecht, Stacey Lind, Marcela Gallegos, Dr. Samuel Attoh, Loyola University Chicago Graduate School and Department of Chemistry and Biochemistry, National Science Foundation, IBHE-DFI Fellowship Program, Nazarene All Nations Church, Ms. Cynthia Wells and Mr. George H. and Mrs. Alice T. Robinson.

For Mom,
Truly you have been a support, of which there is no worldly measure.
I am grateful that God has bestowed such a treasure upon
HIS humble scientific researcher.

And Nathanael said unto him, Can there any good thing come out of Nazareth?
Philip saith unto him, Come and see.

—John 1:46, KJV

TABLE OF CONTENTS

LIST OF TABLES

LIST OF FIGURES

ABSTRACT

Carbohydrates have been most notable as energy sources for mammals, bacteria (glycogen) and plants (starch) – and in many other species. As such the biosynthesis of carbohydrates is essential to the sustainability of many forms of life, on earth. Adenosine-‘5-diphosphate glucose pyrophosphate (ADP-Glc pyrophosphorylase; ADP-Glc PPase) is the allosterically controlled “first committed step” in both the biosynthetic pathways of starch (~25% amylose and ~75% amylopectin, in plants and algae) and glycogen (in bacteria), preceding the starch/glycogen synthase reaction. By catalyzing the following reaction, ATP + α –D-Glc-1P ⇌ ADP-Glc + PP_i , ADP-Glc PPase functions as the primary enzyme in the reaction that provides the glycosyl precursor for the elongation of α-1,4-polyglucans. ADP-Glc PPase is a tetrameric allosterically regulated enzyme. The structure of this enzyme is homotetrameric in enteric bacteria (*Escherichia coli*) – α4, and heterotetrameric in plants and other photosynthetic eukaryotes – consisting of two small subunits (50-52 kDa) and two large subunits (~60kDa): ($\alpha_2\beta_2$). The plant ADP-Glc PPases are allosterically regulated: mainly by 3-phosphoglycerate (3PGA) as an activator and inhibited in the presence of inorganic phosphate (Pi). There is an allosteric disparity in the bacterial enzyme’s counterpart. For instance, the *E. coli* ADP-Glc PPases enzyme is activated by fructose-1,6-bisphosphate (FBP) and inhibited by adenosine-‘5-

monophosphate (AMP). All ADP-Glc PPases, to date, are noted to have a divalent metal ion cofactor (Mg^{+2}).

Comparative modeling of the *E. coli* ADP-Glc PPase with ATP bound in the active site predicted critical interactions for Lys42. In the model, this residue interacts with the catalytic Asp142 and the β-phosphate of the ATP substrate, which comprises the reaction "leaving group". Lys42 is highly conserved in the ADP-Glc PPases known to be catalytic, but absent in plant subunits that are catalytically deficient. It is also conserved in other homologues of the sugar-nucleotide pyrophosphorylase superfamily. To investigate the role of Lys42 in *E. coli* ADP-Glc PPase, we performed site-directed mutagenesis. As a result, we observed a markedly decreased k_{cat} (>3 orders of magnitude lower than the wild type (WT)). We analyzed another conserved residue that interacts with the phosphates of ATP (Arg32). In mutating the Arg32 residue, we observed the $S_{0.5}$ of the ATP substrate for the mutants was only two to three times higher than that of the WT. But more significant was the marked decrease in specific activity (and k_{cat}) for the Arg32 mutants (1 -3 orders of magnitude). Our results indicate that the interaction of Arg32 guanidinium moeity and structural length of the Arg32 side chain is critical for overall catalysis. Modeling of the *E. coli* enzyme WT and Arg32 mutants suggest that two nitrogen atoms of the Arg32 guanidinium side chain may interact with the γ-phosphate of the ATP substrate making the PP_i product a more stable leaving group. These results show that both residues in the *E. coli* ADP-Glc PPase are catalytic (Lys42), important for orientation and positioning of the ATP substrate (Arg32) and overall essential for the production of ADP-glucose.

CHAPTER ONE

INTRODUCTION

The biosynthesis of carbohydrates is essential to the sustainability of many forms of life on earth. The role of starch grains (as a food source; *rhizhomes* of *Typha*) was identified from grinding stones in Europe and dated over 30,000 years ago (Revedin, Aranguren et al. 2010). Continued scientific studies of genetics in starch producing plants and starch biosynthesis can be dated back to the early 1900s (Hanes 1940a, Hanes 1940b, Mangelsdorf, Jones 1926, Wentz 1925). Another essential carbohydrate is glycogen. As an α-1,4-polyglucan, glycogen provides an essential "energy-storage" for mammals, fungi and bacteria when carbon nutrients are lacking. The biosynthesis of glycogen is also advantageous to the bacterial, fungi and mammalian cells in that it's high molecular weight (and various properties as a polysaccharide) yield little to no effect in altering any osmotic pressure of the cell .

Glycogen is the energy store of choice in a number of bacterial species: gram negative, gram-positive, cyano-bacterial and archaebacterial (genera *Sulfolobus*, *Thermoproteus*, *Desulfurococcus* and *Thermococcus*) (Konig, Skorko et al. 1982) cells – *to note a few*. The branched polyglucan consists of monomers in which 90% are α-1,4 linkages and the remaining α-1,6 linkages. Most bacteria synthesize glycogen during the "stationary" stage – with a few exceptions *Rhodopseudomonus capsulata, Streptococcus mitis* and *Sulfolobus solfataricus.* In most cases the level of glycogen increases with the

availability of carbon in the "growth media" or when bacterial growth is hindered by the lack of other nutritional elements (sulfur, phosphates, nitrogen, etc.). It has been noted that given optimal conditions a bacterial cell can store up to 50% in its dry weight of the polyglucan, as an energy source (Ballicora, Iglesias et al. 2003). Another α-1,4-polyglucan, starch, is an unparalleled source of energy, and often termed the "storehouse" of energy for a number of organisms (Leloir, Cardini 1957). Over fifty percent (50%) of carbohydrates consumed by humans is from starch. Although, starch appears as granules in plants, when processed (or manufactured) for human consumption, it is in a white powder form. Starch can be used as a stiffening agent (which corresponds with the root of the word "starch", derived from "sterchen" which is defined as stiffen). There are a variety of uses for starch, such as: starch employed in the printing industry, moldings, laundry starch, glue and biofuel (via fermentation glucose units of starch can be converted to ethanol).

Biosynthesis of Starch and Sucrose: ADP-Glc vs. UDP-Glc

Preceding the works of the Argentine Physician and Biochemist Luis Leloir, it was believed that the synthesis of the α,1-4 a glucosidic linkage in plants was catalyzed by phosphorylases (reaction 1) (Hanes 1940a, Hanes 1940b, Preiss 1980):

$$\text{Glucose-1-P} + (\text{glucosyl})_n \rightleftharpoons P_i + (\text{glucosyl})_{n+1} \quad (1)$$

In contrast, it was discovered that the starch synthase reaction was responsible for the production and polymerization of the starch molecule, in the following proposed reaction

(Reaction 2) (Hanes 1940a, Hanes 1940b, Preiss 1980, RECONDO, LELOIR 1961, RECONDO, DANKERT et al. 1963):

$$\text{ADP(UDP)glucose} + (\text{glucosyl})_n \rightleftharpoons \text{ADP(UDP)} + (\text{glucosyl})_{n+1} \quad (2)$$

Both UDP-glucose (UDP-Glc) and ADP-glucose (ADP-Glc) are described in the aforementioned reaction; however, ADP-Glc has been noted to be a more viable glucose donor (substrate), during starch synthesis reaction. ADP-Glc has exemplified a higher maximum velocity as well as substrate affinity – versus that of UDP-Glc. Moreover, UDP-Glc comparatively lacked a functional role in both bacterial glycogen synthases and leaf starch synthases. In comparison to ADP-Glc activity, the UDP-Glc activity was 1% or less (Preiss 1980).

Both UDP-Glc and ADP-Glc (glucose donors) are products of pyrophosphorylase reactions (by ADP-Glc PPase and UDP-Glc PPase). Additionally, both nucleotide phosphate sugars can also be synthesized via reverse sucrose synthase reaction (reactions 3a, 3b, 4a and 4b) (Hanes 1940a, Hanes 1940b, Preiss 1980, Recondo, Leloir 1961, Recondo, Dankert et al. 1963, Delmer, Albersheim 1970, Baroja-Fernandez, Munoz et al. 2004):

$$\text{NTP} + \text{glucose-1-P} \rightleftharpoons \text{NDP-glucose} + PP_i \quad (3a)$$

$$\text{ATP(UTP)} + \text{glucose-1-P} \rightleftharpoons \text{ADP(UDP)glucose} + PP_i \quad (3b)$$

$$\text{NDP-glucose} + \text{fructose} \rightleftharpoons \text{sucrose} + \text{NDP} \quad (4a)$$

$$\text{sucrose} + \text{ADP(UDP)} \rightleftharpoons \text{fructose} + \text{ADP(UDP)glucose} \quad (4b)$$

These pyrophosphorylase enzymes are both found throughout the plants and bacteria (Figure 1) and are allosterically controlled by carbon metabolites of glycolytic pathways (Figure 2) (Preiss 1980, Recondo, Leloir 1961, Recondo, Dankert et al. 1963, Baroja-Fernandez, Munoz et al. 2004, Ventriglia, Ballicora et al. 2007, Yep, Ballicora et al. 2006, Ballicora, Dubay et al. 2005, Ballicora, Iglesias et al. 2004).

The previous notes two mechanisms for the production of α,1-4 glucosidic linkages in plants: UDP-Glc and ADP-Glc reactions – with ADP-Glc being the principal mechanism. The dominant presence, specificity and activity of the ADP-Glc substrate in plant leaves (for starch bound or soluble starch synthases) and bacteria has been noted in previous studies. The UDP-Glc substrate has been found to exhibit a glucosyl transfer rate in biosynthesis of starch equivalent to 10% to 33% of that of the ADP-Glc glucosyl donor, in plant leaves. Further, bacterial glycogen synthases have appeared to be inactive in the presence of UDP-Glc substrate (Preiss 1980, Recondo, Leloir 1961).
Intermediates from the Calvin-Benson Pathway lead into the starch synthesis and ADP-Glc production pathways in the chloroplast of plant leaves. Following the aforementioned glucosyl donor, products of the Calvin-Benson cycle (triose-phosphate) also feed into the sucrose synthesis pathway (another critical biosynthetic carbohydrate pathway) in the cytoplasm of plant leaves (Preiss 1980, Recondo, Leloir 1961, Baroja-Fernandez, Munoz et al. 2004, Ballicora, Iglesias et al. 2004, Preiss 1984) (Figure 3). In regard to both starch and glycogen polyglucans, synthesis of the α-1,6 linkages in the amylopectin

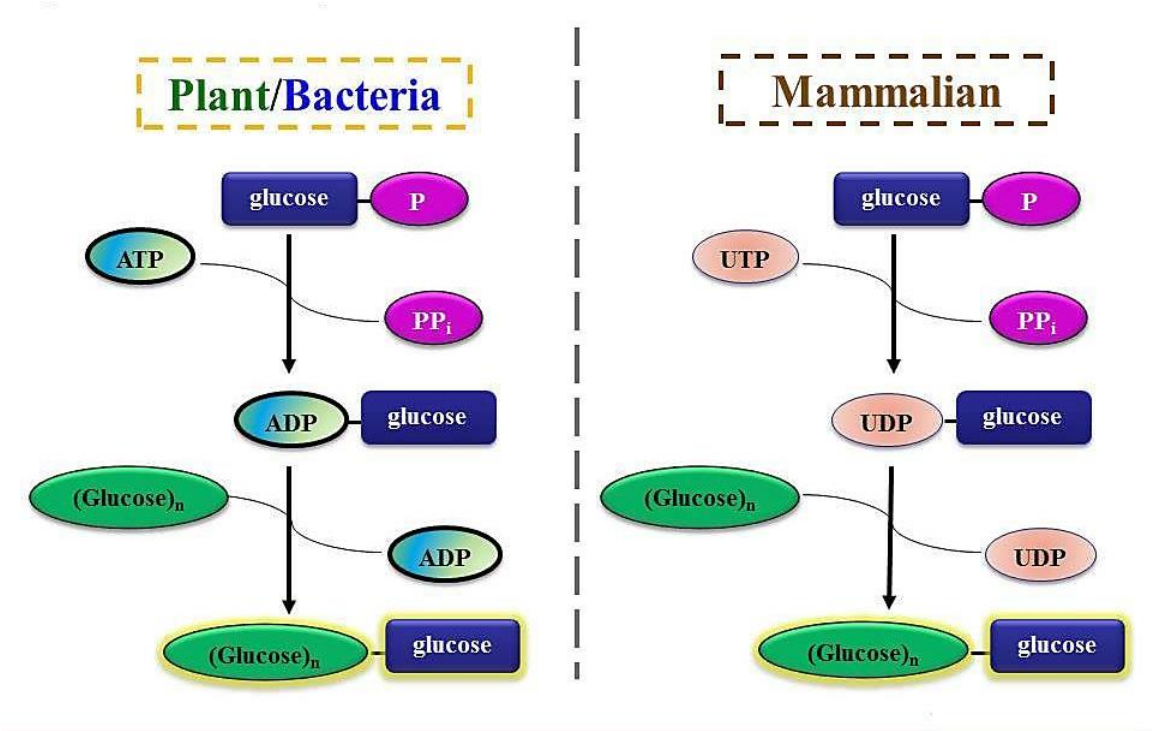

Figure 1. Synthesis of Polysaccharides: Comparison of ADP-Glc (Plant/Bacteria) and UDP-Glc (Mammalian) Pyrophosphorylases.

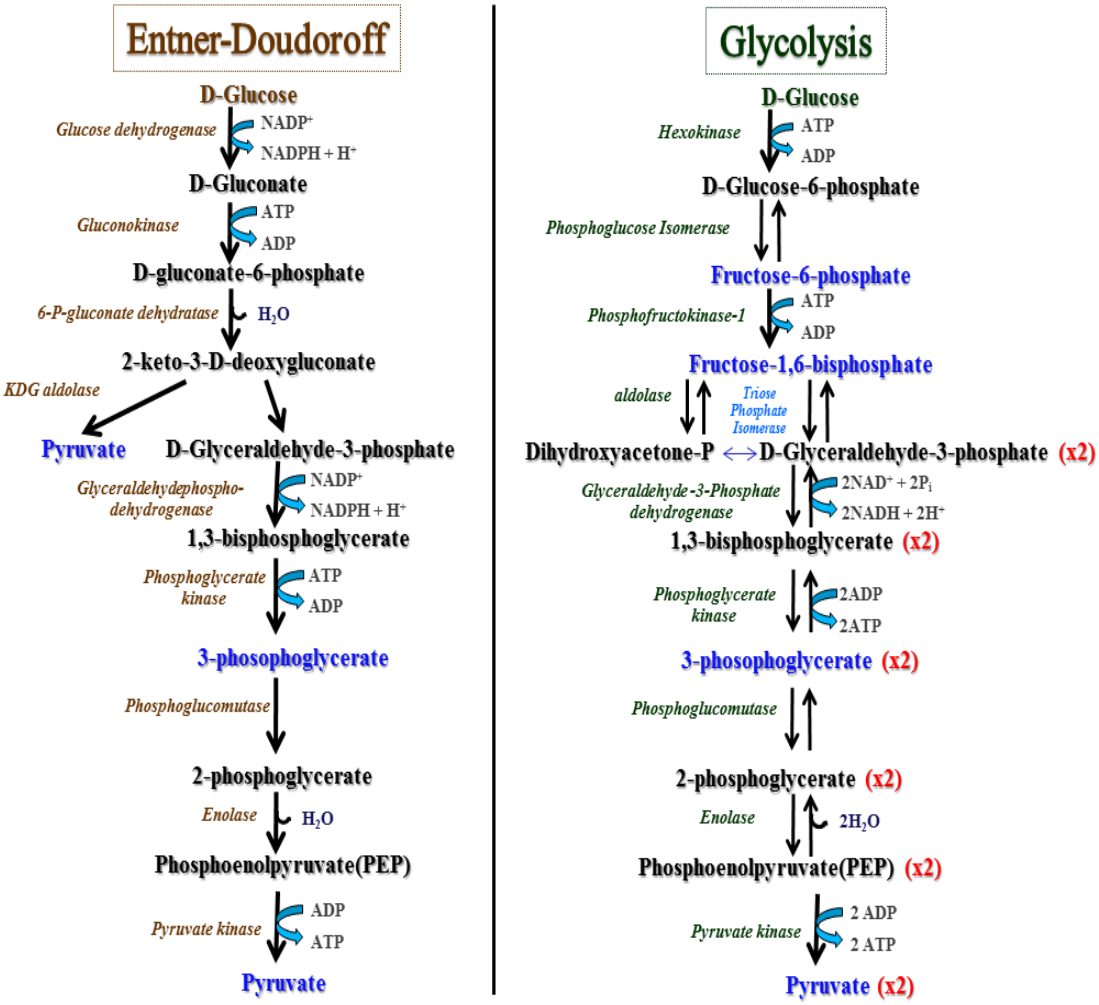

Figure 2. Glycolysis Cycle/Entner-Doudoroff. Depiction of the Entner-Doudoroff and Glycolysis Pathways. ADP-Glc PPase allosteric effectors (for both starch and glycogen synthesis; plant and bacterial species) synthesized in the Entner-Doudoroff in *E. coli* (Conway 1992) and Glycolysis pathways are noted in blue.

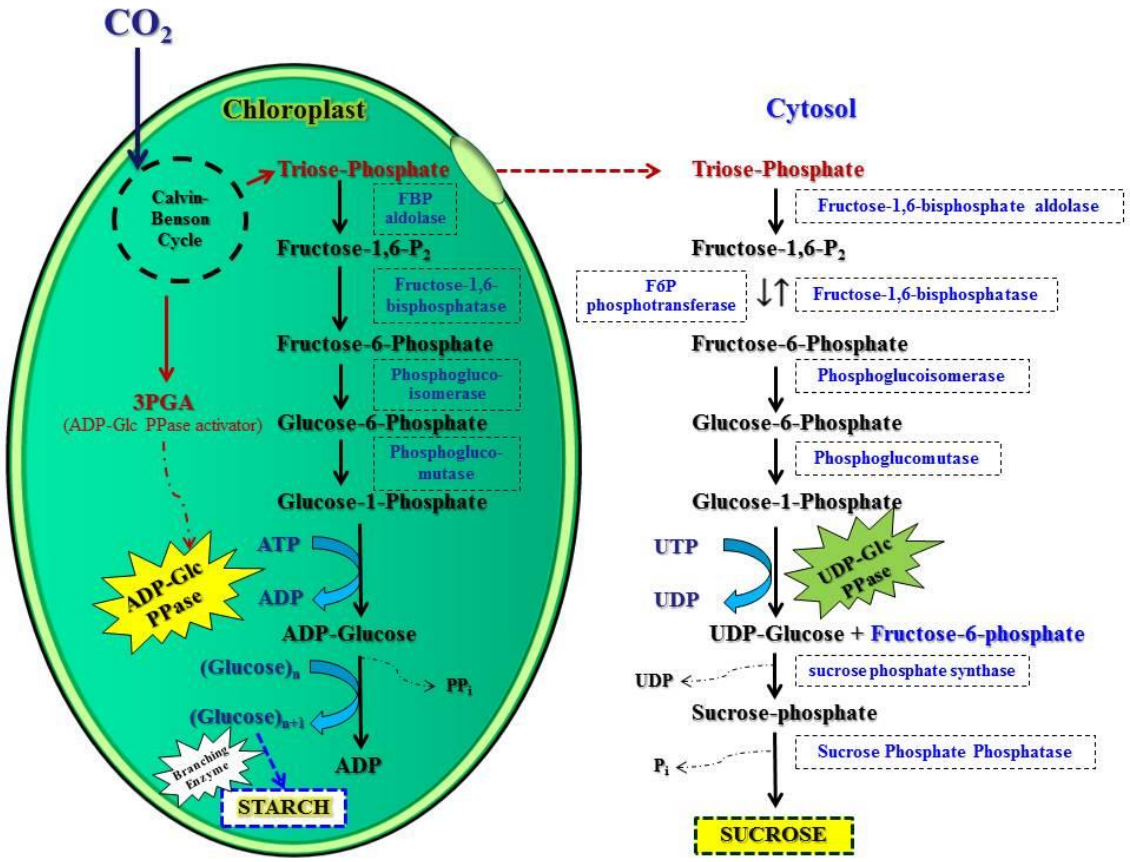

Figure 3. Starch/Sucrose Synthesis. Starch synthesis in the chloroplast and sucrose synthesis in the cytosol of plant leaves (modified depiction of Baroja-Fernández et al.) (Baroja-Fernandez, Munoz et al. 2004)).

(of starch) and glycogen (Figure 4) (Berg, Tymoczko et al. 2012) is incorporated via the branching enzyme (glgB gene) (Figure 5).

The biosynthesis of sucrose was found to be the product of UDP-Glc and Fructose-6-P (Reactions 5 and 6) (Preiss 1980, Recondo, Leloir 1961, Cardini, Leloir et al. 1955, Leloir, Cardini 1955):

$$\text{UDP-Glc} + \text{fructose} \rightleftharpoons \text{sucrose} + \text{UDP} \quad (5)$$

$$\text{UDP-Glc} + \text{fructose-6-Phosphate} \rightleftharpoons \text{sucrose-6-Phosphate} + \text{UDP} \quad (6)$$

The sucrose synthase reaction was found to be pH dependent, as seen with starch synthesis. Oddly, the sucrose synthase reaction also utilizes ADP-Glc, TDP-Glc, dTDP-Glc, CDP- Glc and GDP- Glc as glucosyl donors. Nevertheless, the affinity for the UDP-Glc substrate is much higher, for sucrose synthase. Significantly, for the reverse sucrose synthase reaction UDP functions as an inhibitor by preventing the production of ADP-Glc. Thus, outlining the significance of one glucosyl donor (UDP-Glc) over another (ADP-Glc) in a sucrose synthase reaction (Preiss 1980). Another relationship (as seen with pH dependence) between starch and sucrose synthesis is the conversion of "starch-sucrose" postulated to occur in plant tissues via a reaction mechanism where sucrose and ADP(UDP) are the substrates for sucrose synthase yielding a ADP(UDP)-Glc produce to be utilized as a substrate for starch synthesis, as a glucosyl donor (Preiss 1980). To sum, it has been previously noted sucrose synthase has a much greater affinity for UDP than ADP; alternatively, starch synthase prefers ADP-Glc moreso than UDP-Glc. As such we begin to see the roles of both UDP-Glc and ADP-Glc in sucrose (and starch) synthesis.

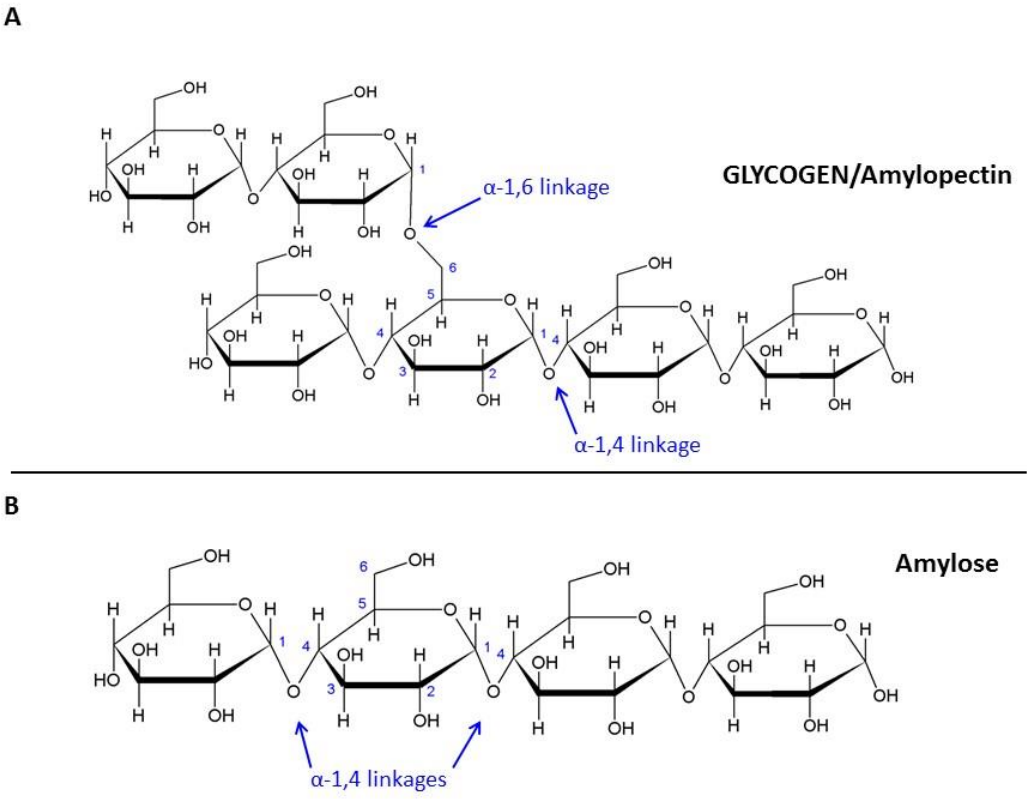

Figure 4. Starch and Glycogen. The α-glycosidic linkages of starch and glycogen. (A) Starch and glycogen are polymers of α,1-4-glycosidic linked units with amylopection/glycogen α,1-6-glycosidic branching (Devillers, Piper et al. 2003). Glycogen has a higher number of branching than starch. Starch is made of Amylose (B) an Amylopectin.

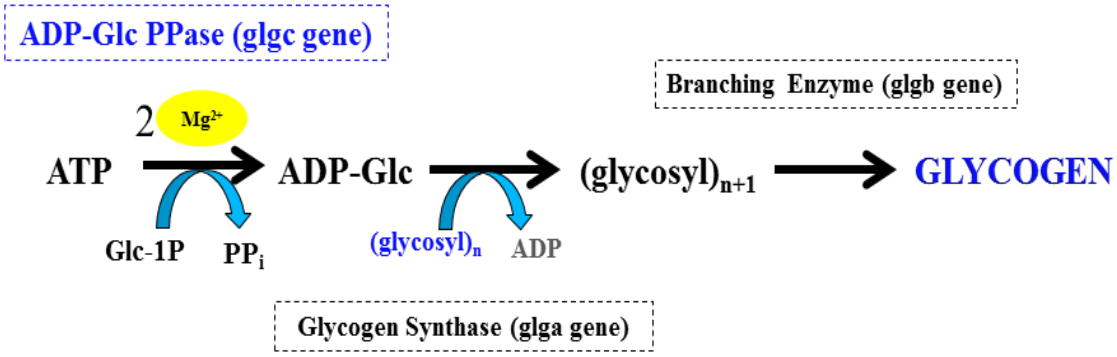

Figure 5. ADP-Glc PPase Reaction Scheme.

The production of sucrose is pertinent for plants, as sucrose is a key source of carbohydrates produced as well as essential for the production of plant cell walls. As such, we see the crucial role of the NDP-sugar phosphorylases in organisms, regarding the biosynthesis of carbohydrates.

Biosynthesis of Bacterial Glycogen: ADP-Glc

Glycogen, a α-1,4-polyglucan, provides an essential "energy-storage" for mammals, fungi and bacteria utilized when carbon nutrients are lacking. This is advantageous in that its high molecular weight yields little to no effect in altering any osmotic pressure of the cell. The synthesis of polyglucans is dependent upon the synthesis of ADP-Glc. The primary regulatory step of the glycogen synthesis pathway is driven by ADP-glucose pyrophosphorylase (ATP: α-D-glucose-1-phosphate adenylyltransferase, E.C:2.7.7.27; ADP-Glc PPase) (Ballicora, Iglesias et al. 2003). The biosynthesis of glycogen is dependent upon the construction of the α1,4 glucosidic linkages, and the synthesis of these linkages rely upon the production of the glucosyl donor α-ADP-Glc (via ATP), in bacteria (Reaction 7). Following production, a transfer of the glucose monomer to a pre-existing polyglucan occurs and is succeeded by α1,6 branching via the glgB gene expressed branching enzyme (Devillers, Piper et al. 2003). Approximately 10% of the glucosidic linkages in bacterial glycogen are α1,6 (Preiss 1984). The production of the α-ADP-Glc (glucosyl donor) is mediated by the ADP-Glc PPase enzyme (expressed from the glgC gene) in the presence of a divalent magnesium cation (Figure 5). For bacteria, glycogen is postulated to be employed as a source of both

energy and carbon, when carbon is lacking in media or surrounding environment – as well as RNA and protein production, mobility, regulation of pH within the bacterial cell and osmotic regulation (Yep, Ballicora et al. 2006, Preiss 1984, Machtey, Kuhn et al. 2012, Yep, Ballicora et al. 2004b, Furlong, Preiss 1969). Furthermore, in some species of *Clostridia* glycogen makes up 60% of the dry weight in these bacterial cells. Moreover, a substantial degradation in cellular glycogen, of these bacteria, has been observed during periods of sporulation. This implies that glycogen is useful for the sporulation process of the *Clostridia* cells, and as such, is necessary for bacterial cell survival - as sporulation is a process used by bacterial cells for conservation in environments lacking necessary nutrients for proliferation. Finally, it has been stated that glycogen serves as both a "reserve" and a source of energy and carbon during non-prolific periods, for bacterial cells (Preiss 1984).

Biosynthesis of Mammalian Glycogen: UDP-Glc

The synthesis of the α1,4 glucosidic linkages of mammalian glycogen is produced via a different precursor: UDP-Glc. However, plant starch synthesis and bacterial glycogen synthesis both involve a glucosyl donor, such as ADP- Glc. Additionally, in mammalian cells glycogen synthase (expressed from the glgA gene) is involved in the regulatory step of glycogen synthesis. During gluconeogenesis, the rate limiting step is catalyzed via glycogen synthase. Glycogen synthase is inhibited when phosphorylated, but active in its dephosphorylated stage (which can occur in the presence of a number of intracellular phosphatases). Glycogen synthase, in the absence of glucose-6-phosphate, is

active in skeletal muscle cells - in its dephosphorylated form - but high levels of glycogen obviously inhibit the glycogen synthase enzyme – as synthesis of glycogen is not needed during times of increased intracellular glycogen concentrations (Preiss 1984). One of the major differences in mammalian glycogen synthesis is that one of the roles of the glycogen synthase enzyme is to catalyze reaction where covalent modification and allosteric control is needed. As UDP-Glc has not only been observed as a precursor for the synthesis of glycogen, but also functions in a number of different roles, crucial to mammalian cell proliferation. UDP-Glc has also been noted to be employed by mammalian cells in the synthesis of a number of other sugar nucleotides, such as UDP-galactose, UDP-glucuronate, UDP-xylose, and functioning in the transference of other glucose to various intermediates for the production of glycoproteins (Preiss 1984, Degeest, de Vuyst 2000). Whereas, it has been observed that the major purpose of the ADP-Glc in bacteria is to provide a glucosyl donor for the elongation of a α1,4 polyglucan. As such, the role of UDP-Glc in mammalian cells is inherently different and serves a more diverse role of pertinence than the ADP-Glc glucosyl donor in bacteria and plant carbohydrate biosynthesis. Still, both are crucial sugar nucleotides.

ADP-glucose Pyrophosphorylase

(ATP: α-D-glucose-1-phosphate adenylyltransferase; ADP-Glc PPase)

The ADP-glucose pyrophosphorylase (E.C:2.7.7.27; ADP-Glc PPase) mechanism is the allosterically controlled “1st committed step” in both the biosynthetic pathways of starch (~25% amylose and ~75% amylopectin) in plants, photosynthetic bacteria and

green algae and glycogen in animals, bacteria, fungi, cyanobacteria and archaebacteria, preceding the starch/glycogen synthase reaction (Preiss 1973). By catalyzing the reaction:

$$ATP + \alpha\text{–D-Glc-1P} \rightleftharpoons \text{ADP-Glc} + PP_i \quad (7)$$

ADP-glucose pyrophosphorylase functions as the primary enzyme in the irreversible in vivo (reversible in vitro) reaction that provides the glycosyl precursor for the elongation of α-1,4-polyglucans (Leloir, Cardini 1957, Preiss 1980, RECONDO, LELOIR 1961, Dhalla, Li et al. 1994, Gomez-Casati, Iglesias 2002, Fox, Kapust et al. 2001, Smidansky, Clancy et al. 2002, Charng, Sheng et al. 1995).

The synthesis of ADP-Glc is important as revealed by the fact that (in vivo) the rate of glucose transfer from ADP-Glc occurs ten times faster than the UDP-Glc transfer to the α-1,4-glucan, in plants (Fox, Routzahn et al. 2003). ADP-Glc PPase is a tetrameric allosterically regulated enzyme. The structure of ADP-Glc PPase is homotetrameric in enteric bacteria (*E. coli*) – α4 (200kDa), and heterotetrameric ($\alpha_2\beta_2$) in plants and photosynthetic organisms – consisting of two small subunits (50-52 kDa) and two large subunits (51-60kDa) deriving from a common ancestor (Figures 6 and 7). In firmicutes, it has also been observed in heterotetrameric form (Asencion Diez, Demonte et al. 2013, Takata, Takaha et al. 1997). ADP-Glc PPase is regulated by "small effector molecules" that indicate elevated (activator) or decreased (inhibitor) carbon and energy levels in the cells. Numerous bacterial enzymes can be activated or inhibited by various intermediates of the glycolysis pathway. In the *E. coli* glycogen synthesis pathway a key activator for the *E. coli* ADP-Glc PPase is fructose 1,6-bisphosphate (FBP).

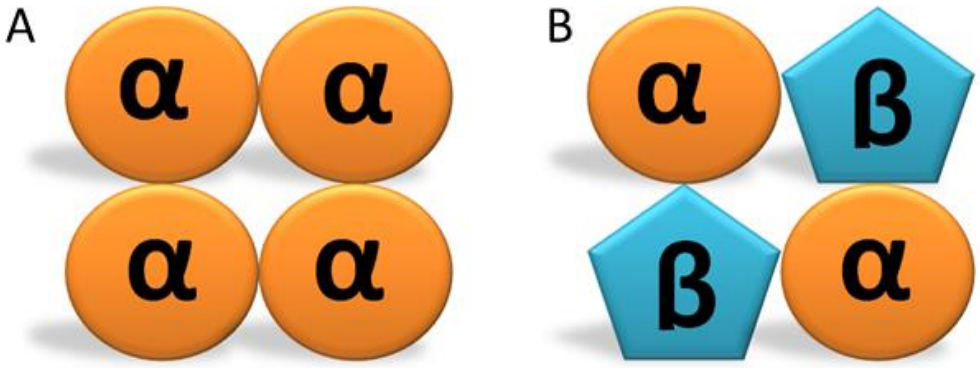

Figure 6. Plants and *E. coli* ADP-glucose Pyrophosphorylase Tetramers. (A) Enteric Bacteria; homotetramer (α_4) and (B) Plant species; heterotetrameric with two large (β) subunits (60kDa) and two small (α) subunits (50-52kDa): $\alpha_2\beta_2$.

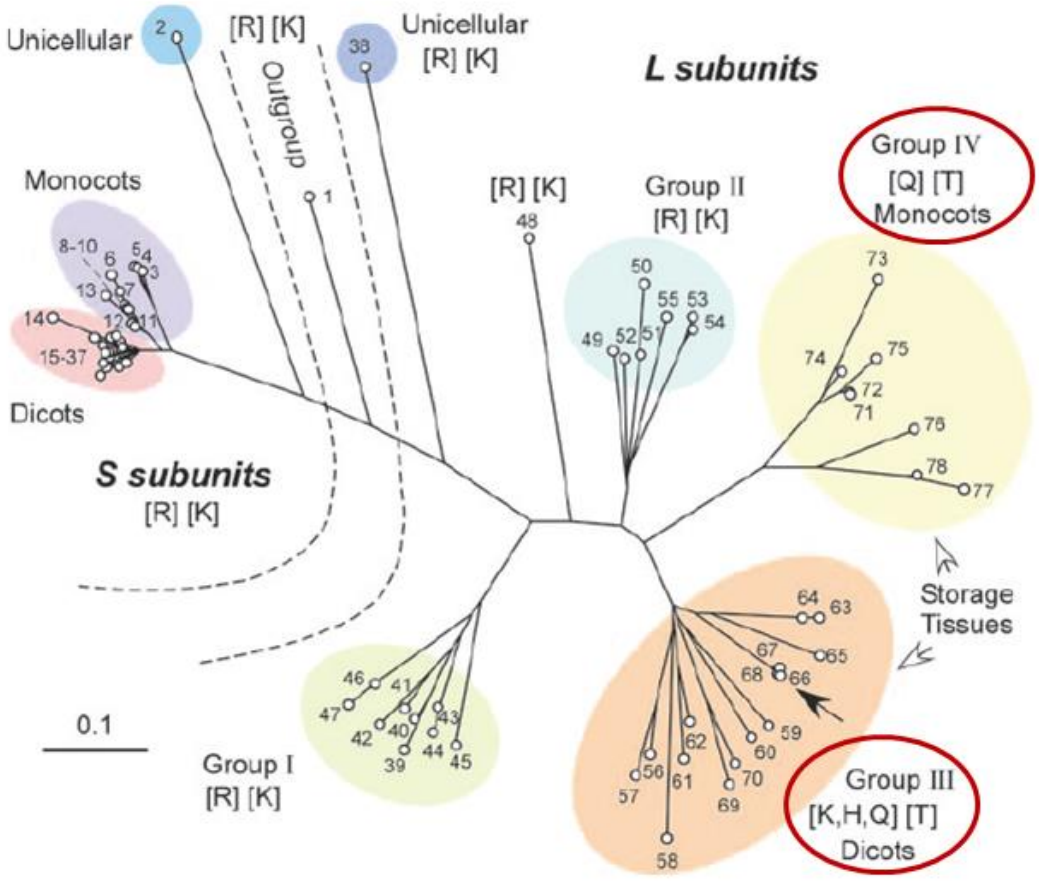

Figure 7. Phylogenetic relationship of ADP-Glc PPases from photosynthetic eukaryotes. Brackets indicate residues conserved in each group**.** Residues of interest circled in red. Image courtesy of Ballicora et al. (Ballicora, Dubay et al. 2005)

In contrast, the glycogen accumulation process via ADP-Glc PPase in the bacteria cells is inhibited by the presence of high levels of AMP (Preiss 1984). Sugar nucleotide PPases allosterically controlled by Fru6P and FBP, are affected by metabolites from the Entner-Doudoroff or glycolysis cycle (Figure 2), which is a major carbon assimilation pathway, for the bacterial cell (Preiss 1980). On the other hand, the plant ADP-Glc PPases are predominantly allosterically activated by 3-phosphoglycerate (3PGA) and inhibited by inorganic phosphate (P_i) (Preiss 1982). This inhibition of the plant ADP-Glc PPase has been observed in both leaf and green algae species (Preiss 1980). They consist of L-subunit and S-subunits that may have differentiated roles. In certain cases, one is a catalytic subunit and the other is not - the regulatory role has been observed in the non-catalytic subunit (Ballicora, Dubay et al. 2005, Crevillen, Ballicora et al. 2003, Kuhn, Falaschetti et al. 2009). Both subunits are nearly fifty percent identical which implies common ancestry.

The effect of the concentration dependence on P_i in spinach leaves was noted in 1966, by Ghosh et al. It was observed that in the presence of 22μM of inorganic phosphate, and absence of activator (3PGA), 50% of the function for the Spinach Leaf ADP-Glc PPase was inhibited. However, in the presence of 1mM 3PGA 1.3mM Pi was necessary to acquire 50% inhibition of the enzyme, in spinach leaves. Here we see a 450-fold decrease in inhibition, when the 3PGA activator is present for a plant-form ADP-Glc PPase. Experimental procedures were performed at pH 7.5 (Preiss 1980, Furlong, Preiss 1969, Ghosh, Preiss 1966, Ozbun, Hawker et al. 1972).

High concentrations of 3PGA observed during the starch synthesis cycle of plant leaves (periods of photosynthesis; daytime) illustrate optimal conditions for activation of the ADP-Glc PPase, as well as production of ADP-Glc. In contrast, lower levels of P_i is observed during photosynthetic (starch production) cycles. At night, however, higher levels of P_i in plant leaves have been observed, which is not conducive to the production of the glycosyl donor (ADP-Glc). The aforementioned lends credence to the notion that ADP-Glc PPase plays a major role in the production of starch in plant leaves, considering the presence of the enzyme's allosteric effectors and reaction product during the diurnal starch production cycle (Preiss 1980, Ballicora, Iglesias et al. 2004, Ventriglia, Kuhn et al. 2008, Iglesias, Ballicora et al. 2006, Dawar, Jain et al. 2013, Figueroa, Kuhn et al. 2013, Kuhn, Figueroa et al. 2013).

UDP-glucose Pyrophosphorylase

(UTP: α-D-glucose-1-phosphate uridylyltransferase; UDP-Glc PPase)

UDP-Glc PPase, as it has been noted previously, is pertinent for sucrose synthesis (a carbon transport source in plants). UDP-Glc PPase plays a major role, in young and developed plant leaves as a glucosyl donor for the sucrose synthesis pathway, by producing the glucosyl donor (UDP-Glc) for the sucrose phosphate synthetase (reaction 8).

$$\text{UTP} + \alpha\text{-D-glucose-1-phosphate} \rightleftharpoons \text{UDP-Glc} + PP_i \quad (8)$$

UDP-Glc PPase is seemingly ubiquitous enzyme located within animals, bacteria and plants. UDP-Glc PPase of plants are soluble proteins located in the cytosol and can

also be found as a membrane bound enzyme (Martz, Wilczynska et al. 2002). In humans and calf liver UDP-Glc PPase is octameric unlike ADP-Glc, in plants and bacteria (Führing, Cramer et al. 2015, Levine, Illett et al. 1969). In tissues of plants, UDP-Glc PPase plays a role in the degradation of the sucrose, via production of the UDP-Glc moiety. Due to UDP-Glc PPase playing a more active role in the sucrose synthesis pathway, it has not been touted as often as the other NDP-sugar phosphorylases as being largely influential in the biosynthesis of carbohydrates.

UDP-Glc PPase is also necessary for polysaccharide synthesis of cellulose and callose sugars via production of UDP-Glc. Since the UDP-Glc PPase performs a reversible reaction it can be classified as involved in both anabolic and catabolic reactions in cells. Various plant species UDP-Glc PPase have been characterized to date, as well as cDNA sequences; thus, highlighting the importance of investigating this prominent enzyme. Although, unlike ADP-Glc PPase, UDP-Glc PPase is not strictly allosterically regulated by metabolic effectors, post-translational modification and oligomerization have been hypothesized as intracellular control mechanisms for UDP-Glc PPase. Phosphorylation of the enzyme is utilized in yeast cells, as a regulatory method. Also, *O*-glycosylation of UDP-Glc PPase for human and *N*-glycosylation for rice UDP-Glc PPase (Meng, Geisler et al. 2009). Presently, a degree of similarity has been noted among the family of plant UDP-Glc PPases, with 59% to 96% identity among amino acid sequences. Furthermore, a 55% degree of similarity is seen among slime UDP-Glc PPases for amino acids (Kleczkowski, Geisler et al. 2004). In animal tissues,

the presence of UDP-Glc PPase has been observed in response to hypoxia (lack of oxygen reaching tissues), as well as the presence of glucose – as an apparent scarcity of UDP-Glc was seen in "insulin-dependent" tissues of diabetic organisms (Martz, Wilczynska et al. 2002, Robinson, Weinstein et al. 1995, Aw, Jones 1984). The results of further investigation into the role of UDP-Glc PPase – and presence of UDP-Glc - in diabetic tissues can be seen in rat research models, as well (Spiro 1984). As such, we see another example of both the ubiquitous nature and importance of UDP-Glc PPase, in mammals.

TDP-glucose Pyrophosphorylase

(TTP: α-D-glucose-1-phosphate thymidylyltransferase; TDP-Glc PPase)

TDP-Glc PPase is an enzyme that catalyzes the reaction of dTTP and glucose-1-phosphate to dTDP-glucose (reaction 9) (Blankenfeldt, Asuncion et al. 2000b, Zuccotti, Zanardi et al. 2001, Barman 1969):

$$\text{dTTP} + \alpha\text{-D-glucose-1-phosphate} \rightleftharpoons \text{dTDP-glucose} + PP_i \quad (9)$$

TDP-Glc PPase (found in *Escherichia coli*) is a 32 kDa enzyme (Zuccotti, Zanardi et al. 2001). TDP-Glc PPase consists of 431 amino acids and has a genetic similarity to other members of sugar nucleotide phosphorylases. In comparison to the homotetrameric ($\alpha_2\beta_2$) ADP-Glc PPase enzyme, in plants, the *Escherichia coli* TDP-Glc PPase has a 29.5% amino acid similarity. Compared to the N-terminus of the *Escherichia coli* ADP-Glc PPase amino acid sequence, the TDP-Glc PPase has a 27% similarity. The previous is the resulting investigation of TDP-Glc PPase when compared to enzymes from 46 bacterial

backgrounds via protein sequence database, only a 12% conservation of amino acids was observed. Further similarity of TDP-Glc PPase, among the family of glucosyltransferases is seen in 26% amino acid sequence in comparison to *E. coli* UDP-Glc PPase. When compared to the amino acid sequence of the CDP-Glc PPase (α-D-glucose-1-phosphate cytidyltransferase) of *Salmonella enterica* there was an apparent similarity of 27% for both CDP-Glc PPase and TDP-Glc PPase (Blankenfeldt, Asuncion et al. 2000b, Zuccotti, Zanardi et al. 2001).

As the enzyme responsible for catalysis of the dTDP-α-D-glucose synthesis, it produces an important molecule (of the metabolic system) of prokaryotes. The dTDP metabolite serves as a "precursor" for a variety of saccharides synthesized to construct prokaryotic cell surfaces. Markedly, TDP-Glc PPase is the initial enzyme responsible for the production of the precursor dTDP (deoxyTDP)-L-rhamnose, in the biosynthesis of L-rhamnose, which is an important component of gram-positive and gram-negative prokaryote bacterial cell walls, the surface antigens (O-lipopolysaccharides) and the ability of microbes to adhere to host tissues. TDP-L-rhamnose has been isolated from various species, such as *Lactobacillus acidophilus*, *E. coli* and *Streptomyces griseus*, and has been examined since preceeding the 1960s. The production of the dTDP-α-D-glucose molecule, as the eventual precursor of L-rhamnose following the conversion of dTDP-α-D-glucose to dTDP-α-D-rhamnose, is not the only favorable aspect of the TDP-Glc PPase, as dTDP-α-D-glucose may serve as a precursor for a number of mono saccharides, such as 6-deoxy-L-talose, D-fucose, 2,6-dideoxyhexoses, 3-amino-6-deoxyhexoses and

3-C-branched 6-deoxyhexoses (Zuccotti, Zanardi et al. 2001, Kornfeld, Glaser 1961).Although the exact mechanisms of TDP-Glc PPase enzymes have not been completely characterized, the critical role of the enzyme is apparent. In microbes, mutants lacking the TDP-Glc PPase enzymes displayed insufficient synthesis of bacterial cell wall, a decline in integrity of bacterial cells (displayed lower degree of viability) and lack of metabolites (in bacterial cell). As such, inhibitors of the TDP-Glc PPase enzyme have been noted as viable candidates as antimicrobial drugs (Zuccotti, Zanardi et al. 2001).

CDP-glucose Pyrophosphorylase

(CTP: α-D-glucose-1-phosphate cytidylyltransferase; CDP-Glc PPase)

CDP-Glc PPase displays an extraordinary degree of specificity for substrate (CDP- Glc), as such other sugar nucleotides (such as ADP-Glc, UDP-Glc, TDP-Glc and GDP-Glc) did not promote any noteworthy chemical response in for CDP-Glc PPase reaction, for microbes such as *Salmonella paratyphi* A (Preiss 1980). Thus, illustrating how CDP-Glc PPase could only use CDP- Glc as a substrate. Furthermore, in *Azobacter vinelandii* the enzyme was unable to use ATP, GTP, UTP, TTP, dATP, dGTP and dCTP for the synthesis reaction, in the presence of D-glucose-1-phosphate However, this enzyme is comparable to ADP-Glc PPase, as both require the presence of the divalent cation (Mg^{2+}) to function (Barman 1969).

CDP-Glc PPase has also been found useful for the synthesis of saccharides in a number of other organisms: *Salmonella paratyphi*, *Pasteurella pseudotuberculosis* Type

V and *Salmonella typhimurium*. Additionally, it has been observed that the production of CDP- Glc (reaction 10) by this enzymes leads to the synthesis of CDP-paratose in *Salmonella paratyphi*, CDP-ascarylose in *Pasteurella pseudotuberculosis* Type V and CDP-tyvelose in *Salmonella typhimurium*. Furthermore, the production of CDP-2-*o*-methyldeoxyaldose in *A.vinelandii* has implications that the CDP-Glc PPase is necessary for its production (Kimata, Suzuki 1966).

$$\text{CTP} + \alpha\text{-D-glucose-1-phosphate} \rightarrow \text{CDP-glucose} + PP_i \quad (10)$$

A CDP-Glc PPase inhibitor, deoxythymidine, has been found to be semi-competitive with CTP substrate, which is implicit that dTTP may binding to a site alternative to that of the CTP substrate-binding site. Lastly, cytidine nucleotides like 2-*O*-methyldeoxyalsode – and the carboxylic acid ester of this structure – has been found to inhibit the Fraction II CDP-Glc PPase. It is indeed quite interesting that there are two defining Fractions of activity for this NDP-sugar phosphorylase (Barman 1969, Kimata, Suzuki 1966).

GlmU: *N*-acetylglucosamine 1-Phosphate Uridyltransferase

The 49 kDa enzyme, GlmU, is located in the cytoplasm of *E. coli* and plays a key role on the biosynthesis of UDP-*N*-acetylglucosamine (UDP-GlcNAc). The enzyme consists of two domains: pyrophosphorylase (which is homologous throughout residues Met1 to Ala120 with a number of other pyrophosphorylases, including ADP-Glc PPase) and an acetyltransferase domain. This is important because the UDP-GlcNAc molecule is a precursor for peptidoglycan and lipopolysaccharide biosynthesis in gram-positive and

gram-negative bacteria. The UDP-GlcNAc precursor can be found in some O antigens, enterobacterial common antigens. The UDP-GlcNAc precursor has also been observed in the teichoic acids of gram-positive bacteria. As teichoic acids are generally synthesized to fortify the cell walls of gram-positive bacteria, the production of the UDP-GlcNAc precursor serves as an important function of the GlmU enzyme. Furthermore, the biosynthetic process for UDP-GlcNAc production creates a platform for antimicrobial drug development. Mutants lacking the ability to synthesize UDP-GlcNAc exhibited cell lysis under specific growth properties. The production of UDP-GlcNAc from Fructose-6-P utilizes three enzymes (in addition to the GlmU enzyme): GlcN-6-P synthase (GlmS), GlcN-1-P acetyltransferase and a phosphoglucosamine mutase enzyme (G1mM). As with ADP-Glc PPase, the two-step process of the previous enzymes (reaction 11 and 12) must be performed in the presence of Mg^{2+}, for the enzymes to function (Brown, Pompeo et al. 1999):

$$\text{GlcN-1-P} + \text{acetylCoA} \rightarrow \text{GlcNAc-1-P} + \text{CoA} \quad (11)$$

$$\text{GlcNAc-1-P} + \text{UTP} \rightarrow \text{UDP-GlcNAc} + PP_i \quad (12)$$

The acetyltransferase function of the GlmU enzyme is inhibited by “thiol-specific” reagents (Brown, Pompeo et al. 1999). Another use of the GlmU protein has been to generate “azido-substituted nucleotide sugar analogues” to help characterize and identify other glycosyltransferases. Also, GlmU has be utilized to develop a sizeable quantity of N-acetyl-labelled UDP-GlcNAc for use in industrial projects (Brown, Pompeo et al. 1999).

Biofuels, Glycogen Production and Cyanobacteria ADP-Glc PPase *Synechococcus* PCC 7002

Investigation into the production of biofuels has increased over the past few decades, as oil reserves dwindle. As such biorefineries have taken interest in oxygenic photosynthetic microorganisms and microalgae as carbon sources (Lopez, Descles et al. 2005, Ducat, Way et al. 2011, Rosenberg, Oyler et al. 2008). Saccharification is the hydrolysis of polymeric sugars to monosaccharides. Saccharification and fermentation of glycogen produced from cyanobateria (an oxygenic photosynthetic bacteria) and microalgae organisms have been explored for biofuel production. A particular study was performed on the oceanic euryhaline (adaptive to various salinized environments) cyanobacteria *Synechococcus* PCC 7002 carbon source: glycogen (Aikawa, Nishida et al. 2014). Cyanobacteria was further observed to be a prime candidate for biofuel production as this microorganism has the ability of (1) changing solar energy to biomass more effectively than switchgrass (an "energy crop") and (2) the cyanobacteria polyglucans (glycogen) can be fermented into ethanol for biofuel use via yeast fermentation (Melis 2009, Aikawa, Joseph et al. 2013, Choi, Nguyen et al. 2010, Harun, Jason et al. 2011, Ho, Li et al. 2013, Miranda, Passarinho et al. 2012). Aikawa et al. noted that cyanobacteria *Synechococcus* PCC 7002 continued to have glycogen production in the presence of high concentrations of carbon dioxide and light intensity (Ducat, Way et al. 2011, Aikawa, Nishida et al. 2014). Kinetic experimentation was performed on the oceanic microorganism and Goméz-Casati et al found that cyanobacteria glycogen

production is regulated by ADP-Glc PPase in the presence of 3PGA and inhibited during higher concentrations of Pi (Gomez-Casati, Cortassa et al. 2003). As such, Aikawa postulated that 3PGA production was increased due to light intensity and the presence of higher concentrations of carbon dioxide, which would explain the favorable glycogen production during such periods. Notably, we see the crucial role study of the ADP-Glc PPase enzyme and α-polyglucans synthesis play in production of biofuels and "bio-based" chemicals, for biorefineries (Gomez-Casati, Cortassa et al. 2003, Xu, Guerra et al. 2013, Guerra, Xu et al. 2013, Hasunuma, Kikuyama et al. 2013, Aikawa, Izumi et al. 2012, Aoyama, Uemura et al. 1997, De Philippis, Sili et al. 1992, Ernst, Boger 1985, Lehmann, Wober 1976, Erdrich, Knoop et al. 2014, Quintana, Van der Kooy et al. 2011). *E. coli* has multiple metabolic pathways, some of which result in the production of alcohols (ethanol, *n*-butanol and isopropyl alcohol) (Alper, Stephanopoulos 2009, Atsumi, Higashide et al. 2009, Atsumi, Hanai et al. 2008, Atsumi, Cann et al. 2008, Brynildsen, Liao 2009, Hanai, Atsumi et al. 2007, Yomano, York et al. 2008, Zhang, Sawaya et al. 2008, Liu, Vora et al. 2010, Lu, Vora et al. 2008, Ingram, Conway et al. 1987, Steen, Kang et al. 2010, Stephanopoulos 2007). Studies similar to the cyanobacteria *Synechococcus* PCC 7002 and biofuels have been performed in *E. coli* investigating the heterofermentative pathway naturally occurring in the microorganism. Via this pathway *E. coli* has the ability of converting sugars to ethanol (Zhao, Xu et al. 2013, Mazumdar, Clomburg et al. 2010, Liu, Khosla 2010). The hydrolysis of polymeric sugars precede the fermentation step for the production of biofuels. Therefore, synthesis

of starch and glycogen in cyanobateria and *E. coli* are essential to biofuel production – which is the key role of ADP-Glc PPase, the first committed step in synthesis of α-polyglucans (Ventriglia, Ballicora et al. 2007, Yep, Ballicora et al. 2006, Ballicora, Dubay et al. 2005, Kuhn, Falaschetti et al. 2009, Bejar, Ballicora et al. 2006, Jin, Ballicora et al. 2005b) (Figure 8).

Blue-Green Bacterium ADP-glucose Pyrophosphorylase

Synechococcus PCC 6301

Upon investigation of glycogen synthesis in *Synechococcus* 6301, ADP-Glc was found to be the principal sugar nucleotide involved – glucose donor. As such, we see yet another role for the ADP-Glc pyrophosphorylase enzyme (Levi, Preiss 1976). ADP-Glc PPase *Synechococcus* 6301 is activated by 3PGA (8- to 25-fold) (Fredrick 1968). Very much like the green algae species and ADP-Glc PPases in higher plants, we see the blue-green bacterium species is activated by 3PGA (Preiss 1973). More allosteric activators were noted with lower activation fold: fructose-6-phosphate (Fru6P) and FBP. Further characterization of *Synechococcus* 6301 ADP-Glc PPase noted inhibition by inorganic phosphate – and of course, functions in the presence of divalent magnesium cation. Numerous photosynthetic bacterial ADP-Glc PPases are activated by similar effectors (Fru6P, FBP and pyruvate) (Furlong, Preiss 1969, Fredrick 1968, Shen, Preiss 1964). Remarkably, *Synechococcus* 6301 ADP-Glc PPase activation is quite similar to the process observed in ADP-Glc PPase found in higher plants and green algae; however, not similar to the allosteric regulation seen in photosynthetic bacteria.

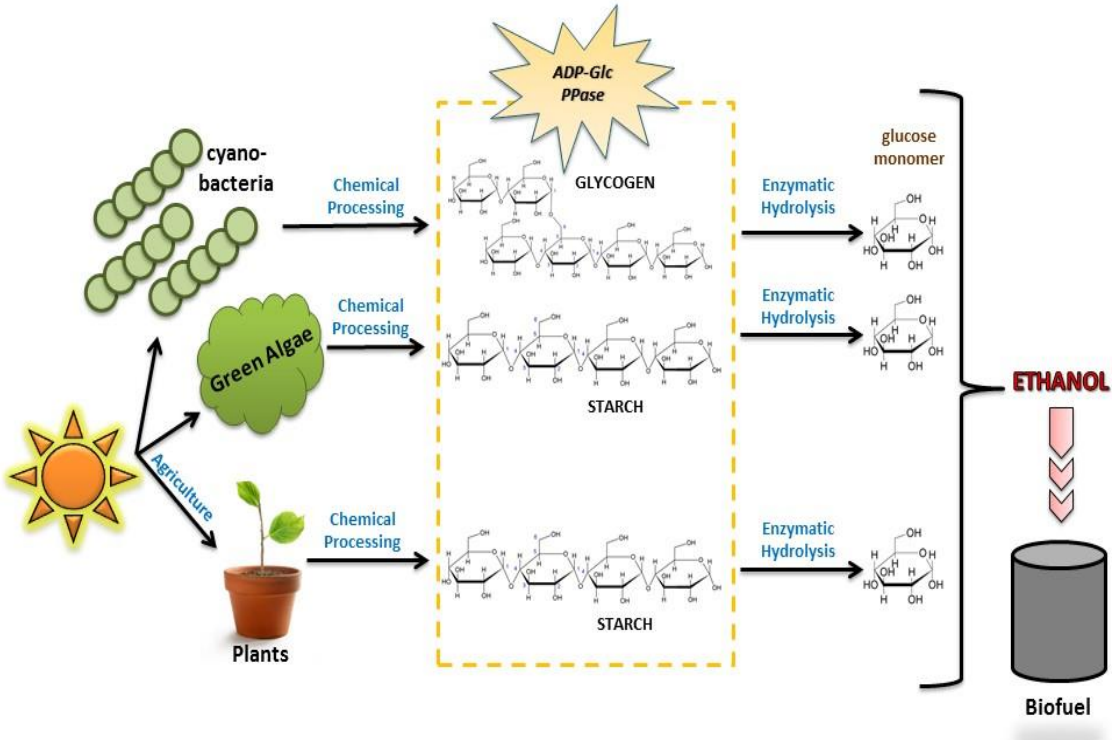

Figure 8. Microbes ADP-Glc PPase and Biofuels. The role of ADP-Glc PPase in Biofuel production.

Furthermore, it has been postulated and observed that the activator/inhibition regulation by 3PGA/P_i is found in green algae, leaf and blue-green bacteria ADP-Glc PPase enzymes (Ghosh, Preiss 1966, Sanwal, Preiss 1967, Sanwal, Greenberg et al. 1968). Consequentially, as the concentration of 3PGA activator increases, the amounts of inorganic phosphate inhibitor has a lower efficacy as an inhibitor. Also, the concentration of 3PGA activator steadies or increases during light to dark transition periods (Hind, Nakatani et al. 1974). Similar observations were noted for concentrations of inorganic phosphate, which are altered during periods of light to dark in green bacteria and green plant leaves (Furlong, Preiss 1969, Fredrick 1968, Shen, Preiss 1964).

E. coli ADP-Glc PPase Substrate (Glc-1P) Binding Site Residues - *Glu^{194}, Ser^{212} Tyr^{216}, Asp^{239}, Phe^{240}, Trp^{274} and Asp^{276}*

As previously stated, the ADP-Glc PPase enzyme interacts with two substrates, ATP and Glc-1P, which are crucial to the synthesis of the glucosyl donor, ADP-Glc. It is important to note that there is a sequential binding process that occurs for the ADP-Glc PPase enzyme, as it interacts with both the ATP and Glc-1P substrates. In 1979, Haugen et al. published a paper outlining their discovery for this process and was able to observe via radioactive binding (equilibrium dialysis) assay that in fact the ATP substrate binds first and then there is a secondary substrate binding of Glc-1P (Haugen, Preiss 1979). In 2006, Bejar and associates identified critical residues in the Glc-1P substrate binding site that are essential for the ADP-Glc synthesis reaction in *E. coli.* She identified seven residues of interest: Glu194, Ser212 Tyr216, Asp239, Phe240, Trp274 and Asp276. The

residues were selected for investigation, as they were conserved throughout the family of ADP-Glc PPases. Alanine scanning was performed via site directed mutagenesis at the residue sites noted, and 1 to 2 order of magnitude decrease in apparent affinity for the Glc-1P substrate was observed for these alanine mutants. Further investigation was performed exploring the "architecture" of the ADP-Glc PPase Glc-1P binding site. Utilizing the homology modelling approach (MODELLER6 v.1) with PPases from *Pseudomonas aeruginosa* (dTDP-Glc PPase) and *Salmonella typhi* (CDP-Glc PPase) they were able to build a model outlining the "architecture" of the Glc-1P substrate binding site, and by doing this they also outlined structural implications of the Glc-1P substrate binding site other NDP-glucose PPases. Bejar found that when superimposing the structures of the Glc-1P substrate binding sites from PPases such as *E. coli* ADP-Glc PPase, *S. typhi* CDP-Glc PPase and *P. aeruginosa* RmlA, a conservation in positioning of side chains was apparent. For example, all three PPases, in comparison to Tyr216 (*E. coli* ADP-Glc PPase), such as the Tyr176 of RmlA (*P. aeruginosa*) and the Phe192 of CDP-Glc PPase (*S. typhi*) overlapped structurally. Additionally, homology modelling revealed that Ser212 residue is involved in a hydrogen bonding network (via the serine side chain and backbone) that may function in the proper positioning of other residues, Glu194 and Lys195, pertinent to the Glc-1P binding site, as the Ser212 residue was spatially close to the Glu194 and Lys195 residues(Bejar, Jin et al. 2006).

Upon examination of mutant kinetics, Bejar noted that the Trp274 alanine mutant (W274A) displayed a 22-fold decrease in apparent affinity for Glc-1P. The

alanine mutant of Ser212 (S212A) displayed a 14-fold decrease in Glc-1P substrate affinity, which was explained by the absence of the serine side chain, and was noted to interact with the O-3 of the ADP-Glc molecule (a substrate for pyrophosphorolysis direction). Any mutagenesis of the Ser212 side chain was accompanied by a decline in enzyme affinity for the Glc-1P substrate. Asp276 was noted as being in close proximity to Glc-1P substrate and that this residue may interact with the ligand via hydrogen bonding. Mutagenesis of the Asp276 residue displayed an approximate decline in substrate binding with Glc-1P of approximately 25- to 100-fold decrease. However, it was also noted that this residue may have other important interactions – not solely Glc-1P binding site (Bejar, Jin et al. 2006).

Tyr216 appeared to be conserved in both ADP-Glc PPases and RmlA transferase (*P. aeruginosa*). Mutating Tyr216, which was examined due to its proximity to the Glc-1P binding site, did result in a 10-fold decrease in V_{max} of the *E. coli* ADP-Glc PPase and a 46-fold decrease in Glc-1P substrate affinity (for the Y216F mutant). This model did not illustrate any interaction of the Tyr216 with the ADP-Glc bound ligand, but biochemical analysis noted that the -OH side chain of the Tyr216 residue may aide in the positioning of the Glc-1P in the substrate "pocket". This was observed in mutating the tyrosine side chain phenylalanine (Y216F), which also resulted in a 1-2-fold decrease in apparent affinity of ATP, Mg^{2+} and FBP for this mutant. Asp239 and Phe 240 were near, but not in direct contact to the ADP-Glc ligand in the models employed, but there were very interesting kinetic analysis resulting from the Asp239 mutant. In investigating the

role of the Asp239 side chain (via alanine mutagenesis) D239A displayed a 31-fold decrease in apparent affinity for Glc-1P and an 11-fold decrease in V_{max}. Likewise, mutating the aspartate side chain to asparagine (D239N) and glutamate (D239E) resulted in a decrease of apparent affinity for the Glc-1P substrate by 16- and 10-fold, respectively. However, the D239N V_{max} decreased 2-fold, but the D239E V_{max} did not display a significant decrease. For the Phe240 residue, mutation at this site for alanine (F240A) and methionine (F240M) resulted in a 12- and 7-fold decrease in apparent affinity for Glc-1P, but no significant change in the V_{max} values compared to that of the wild-type enzyme. Overall, the significant roles of these seven residues were defined, either by homology modelling (structural interactions with ADP-Glc ligand and Glc-1P substrate) or kinetic analysis (illustrating side chain importance and interactions with the Glc-P substrate), which demonstrated the critical functions of these conserved residues for ADP-Glc PPase and in some cases RmlA (Ty216; Tyr176 in RmlA) – plus uncovering a hydrogen bonding network in place to secure the Glc-1P molecule in the substrate pocket (Bejar, Jin et al. 2006)

Important Residue in *E. coli* ADP-Glc PPase for Cofactor (Mg^{2+}) Binding – *Asp^{142}*

All ADP-Glc PPases studied to date, function in the presence of a necessary divalent magnesium cation (Mg^{2+}). This cofactor is required for both the synthesis and pyrophosphorolysis (reverse) reactions of the ADP-Glc PPase enzymes (Ballicora, Iglesias et al. 2003, Preiss 1980, Yep, Ballicora et al. 2006, Ballicora, Dubay et al. 2005,

Ballicora, Iglesias et al. 2004, Preiss 1984, Asencion Diez, Demonte et al. 2013, Iglesias, Ballicora et al. 2006, Diez, Ebrecht et al. 2013, Jin, Ballicora et al. 2005a, Jin, Ballicora et al. 2005a, Yep, Ballicora et al. 2004a, Bejar, Ballicora et al. 2004, Yep, Bejar et al. 2004). In 2001, Frueauf and Ballicora noted an aspartate residue (Asp142) that may demonstrate a pertinent role in positioning of the Mg^{2+} ion of ADP-Glc PPase (Figure 9). During this process, Frueauf performed a comparative review of the RmlA and GmlU phosphorylase crystal structures (Brown, Pompeo et al. 1999, Blankenfeldt, Asuncion et al. 2000a), in conjunction with sequence analysis of ADP-Glc PPases, and found that a number of conserved residues existed among these families of pyrophosphorylases. Of these conserved residues, Asp142 (of *E. coli* ADP-Glc PPase) was analyzed. To fully examine the role of this residue three mutants were designed via site-directed mutagenesis: D142A (alanine), D142N (asparagine) and D142E (glutamate). Kinetic analysis of both the wild-type and mutant enzymes, in both the synthesis and reverse (pyrophosphorolysis) direction was analyzed. A significant decrease of specific activity in mutants was observed at 4 orders of magnitude. For the alanine (D142A) and asparagine (D142N) – in the synthesis direction of the ADP-Glc PPase reaction – mutants there was no effect on the apparent affinities for substrates (ATP; Glc-1P) or activator (FBP). Also, the D142A and D142N mutants exhibited no change in affinity for the cofactor (Mg^{2+}). However, a significant decrease in substrate affinity was observed for D142E. A nearly 12-fold decrease in apparent affinity for ATP and a 46-fold decrease in apparent affinity for the Glc-1P substrate were observed for the D142E mutant.

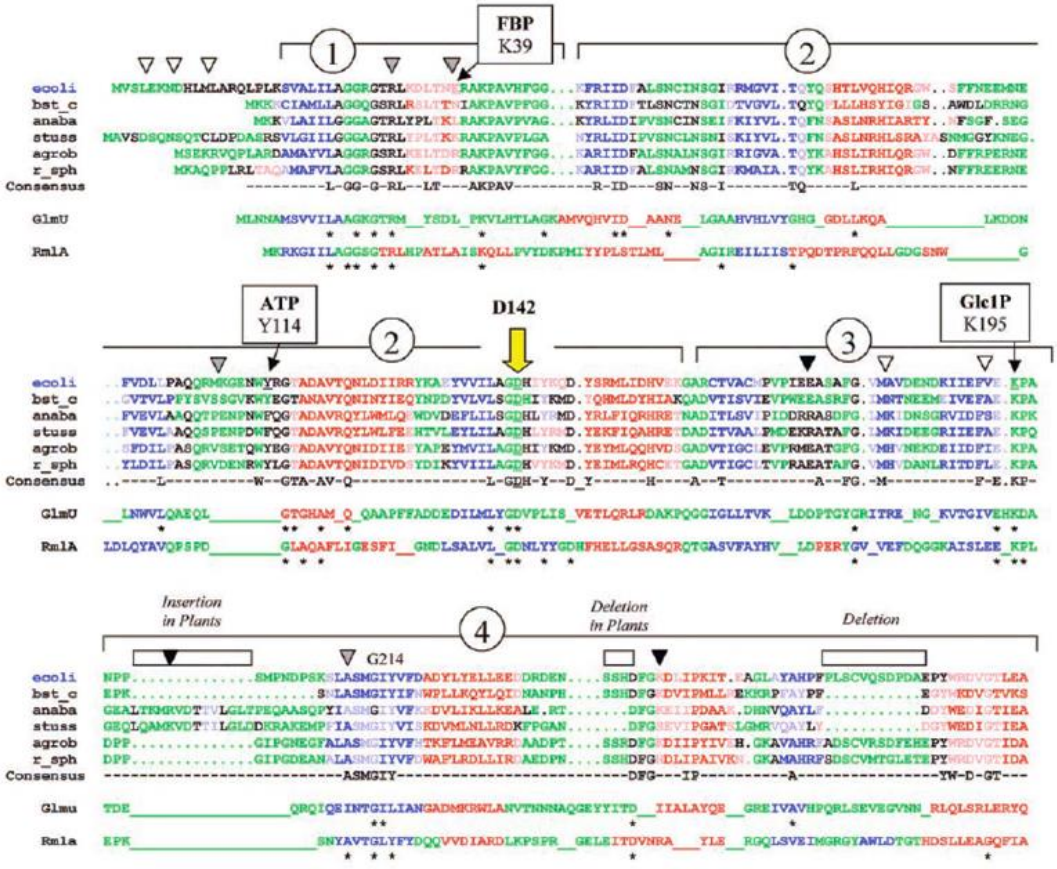

Figure 9. Alignment of ADP-Glc PPases with RmlA and GlmU for comparative analysis of conserved residues and structures. α-helix residues were noted in red and pink. β-sheets were predicted for residues in both blue and light blue. Residues classified as neither a-helix or b-sheets are indicated in green. PHD program was unable to predict structural character of residues in black. Trypsin (grey triangles; black triangles for cutting *Anabaena* ADP-Glc PPase) and protein kinase K (white triangles) were indicated as cutting *E. coli* ADP-Glc PPase at those locations. Finally, (*) indicates a consensus of residues among ADP-Glc PPases, RmlA and GlmU. Image courtesy of Frueauf and Ballicora, 2001 (Frueauf, Ballicora et al. 2001).

Activation by FBP required a 17-fold higher concentration ($A_{0.5}$). Markedly, the effects of altering the Asp142 side chain became apparent with the D142E mutant for cofactor binding, with a 2.5-fold decrease in affinity for Mg^{2+}. All mutants displayed a lower V_{max} than the wild type (D142E, 77-fold decrease; D142A, 5500-fold decrease; D142N, 7200-fold decrease) (Frueauf, Ballicora et al. 2001).

E. coli ADP-Glc PPase Activator (FBP) Binding Site Residue - *Lys*^{39}

Fructose-1,6-bisphosphate functions as the allosteric activator of bacterial ADP-Glc PPase. An analog, PLP (pyridoxal-phosphate), has been noted to also bind at the allosteric activator site. The presence of a Rossmann-type fold structure with three loops facing the ATP substrate binding site were noted within the N-terminus domain of the bacterial ADP-Glc PPase (for glycogen synthesis) (Ballicora, Iglesias et al. 2003, Yep, Ballicora et al. 2006, Bejar, Jin et al. 2006, Figueroa, Esper et al. 2011a, Ballicora, Erben et al. 2007a, Ballicora, Erben et al. 2007b). Previous kinetic assays have demonstrated the important role of a number of residues that are responsible for binding the FBP allosteric effector in the active site of *E. coli* ADP-Glc PPase. In 1989, Gardiol and Preiss identified one such residue: Lys39 (Gardiol, Preiss 1990). One of the N-terminus domain loops actual face the Lys39 residue which has been found to bind both the FBP activator and the PLP analog (Figueroa, Esper et al. 2011a). Other kinetic analysis studies note specific structural characteristic of an effector are needed for activation of bacterial ADP-Glc PPase. Gardiol describes these potential allosteric activators (analogous to FBP) as

having “satisfied” these requirements by having two phosphate moieties (“residues”) within the effector molecule. These particular activators (analogous in function to FBP) are sedoheptulose-1,7-P_2, 1,6-hexanediol-P_2 and NADPH (which has a ribose-2,5-P_2 complex analogous to FBP). There are a number of other bacterial ADP-Glc PPase activators that have only phosphorous group that is accompanied by a carboxyl or aldehyde moiety: PLP, erythrose-4-P, 4-pyridoxic acid-5-P, 2-P-glycerate, and phospoenolpyruvate (PEP). The previous effectors indeed had been kinetically observed as binding at the activation site, of the bacterial ADP-Glc PPases. PLP was also noted as binding the Lys39 residue for *E. coli* ADP-Glc PPase (Gardiol, Preiss 1990).

To examine the effects of altering the Lys39 residue, Gardiol and Preiss performed site-directed mutagenesis to obtain the K39E (glutamate-39) mutant. Kinetic analysis of the K39E mutant was performed. Notably, the NADPH molecule noted previously as being able to bind the active site of the wild-type *E. coli* ADP-Glc PPase was unable to bind the glutamate mutant. Selection of the glutamate mutant was to examine the role of the lysine (-amino) side chain and its effect on binding the FBP activator. By substituting the lysine (basic) for a glutamate (carboxylate) side chain, Gardiol alternates the conditions at the activator binding site-39 for the ADP-Glc PPase enzyme. As such, kinetic analysis demonstrates the critical role Lys39 plays structurally and electrostatically. Activation of the K39E mutant was examined and resulted in only a 2-fold activation for 2-P-glycerate, PLP and FBP, in comparison with the wild-type (15- to 28-fold activation, respectively). The apparent affinity of the K39E mutant for the 2-P-

glycerate, PLP and FBP activators decreased by 5-, 9- and 23-fold in comparison to the wild type. Interestingly, ATP substrate kinetics for the mutant enzyme (K39E) was the same for both with and without the FBP activator – the presence of the activator made little difference here. The K39E mutant exhibited no activation by the wild type activator, NADPH. Moreover, the effect of the AMP inhibitor (for *E. coli* ADP-Glc PPase) did not change ($I_{0.5}$) in the presence of FBP. A 23-fold decrease in affinity for the FBP activator was also observed for the K39E mutant enzyme (Gardiol, Preiss 1990). Gardiol's findings indicate the prominent role of the Lys39 residue and if substituted a hindrance of the activation effect of FBP, substrate binding and inhibition process becomes apparent for *E. coli* ADP-Glc PPase.

Conserved "Gly-X-Gly-(Thr/Ser)-Arg" Motif

Sequence alignment reveals a conserved glycine rich region in the N-terminus of the sugar nucleotidyl transferases superfamily (Charng, Sheng et al. 1995, Okita, Rodriguez et al. 1981, Charng, Kakefuda et al. 1992, Ugalde, Lepek et al. 1998, Uttaro, Ugalde et al. 1998, Igarashi, Meyer 2000), along with other important residues in the active site of bacterial ADP-Glc PPases (including *A. tumefaciens* and *E. coli*), such as Tyr114, Asp142 and Lys195 (Kumar, Ghosh et al. 1989, Kumar, Tanaka et al. 1988, Frueauf, Ballicora et al. 2003, Hill, Kaufmann et al. 1991). A common amino acid motif of this glycine rich region has been found to be GXG(T/S)R (Cupp-Vickery, Igarashi et al. 2008, Cupp-Vickery, Igarashi et al. 2005). A similar review of the domains found in the active sites of *E. coli N*-acetylglucosamine-1-phosphate uridyltransferase (GlmU) and

the *Pseudomonas aeruginosa* and *E. coli* glucose-1-phosphate thymidylyltransferases appear to parallel the characteristics found in this motif, in regard to nucleotide phosphate binding (Blankenfeldt, Asuncion et al. 2000b, Brown, Pompeo et al. 1999, Sivaraman, Sauve et al. 2002, Olsen, Roderick 2001). In 2005, Jin et al. solved the crystal structure of the potato tuber ADP-Glc PPase which also revealed a similar motif, thereby verifying the importance of these aligned residues (Jin, Ballicora et al. 2005a). Similarly, it has been noted that the nucleotide binding may occur in the GXG(T/S)R motif, which is characteristic of substrate binding for the sugar nucleotidyl transferases superfamily (Ballicora, Dubay et al. 2005, Figueroa, Kuhn et al. 2013, Jin, Ballicora et al. 2005a, Figueroa, Esper et al. 2011a, Ballicora, Erben et al. 2007a, Ballicora, Laughlin et al. 1995, Figueroa, Esper et al. 2011b). To illustrate the important role of the aforementioned residues, Gomez-Casati found that the alanine mutation of the "X" (Arg22) and "R" (Arg25) residues of *A. tumefaciens* resulted in a decrease in activity and ATP substrate affinity (Gomez-Casati, Iglesias 2002). As modelling and previous mutagenesis and kinetic analysis in *A. tumefaciens* ADP-Glc PPase suggests, investigation of the GXG(T/S)R motif in the N-terminus of *E. coli* ADP-Glc PPase would be interesting to further define the characteristic of this motif for the bacterial enzymes (Figure 10).

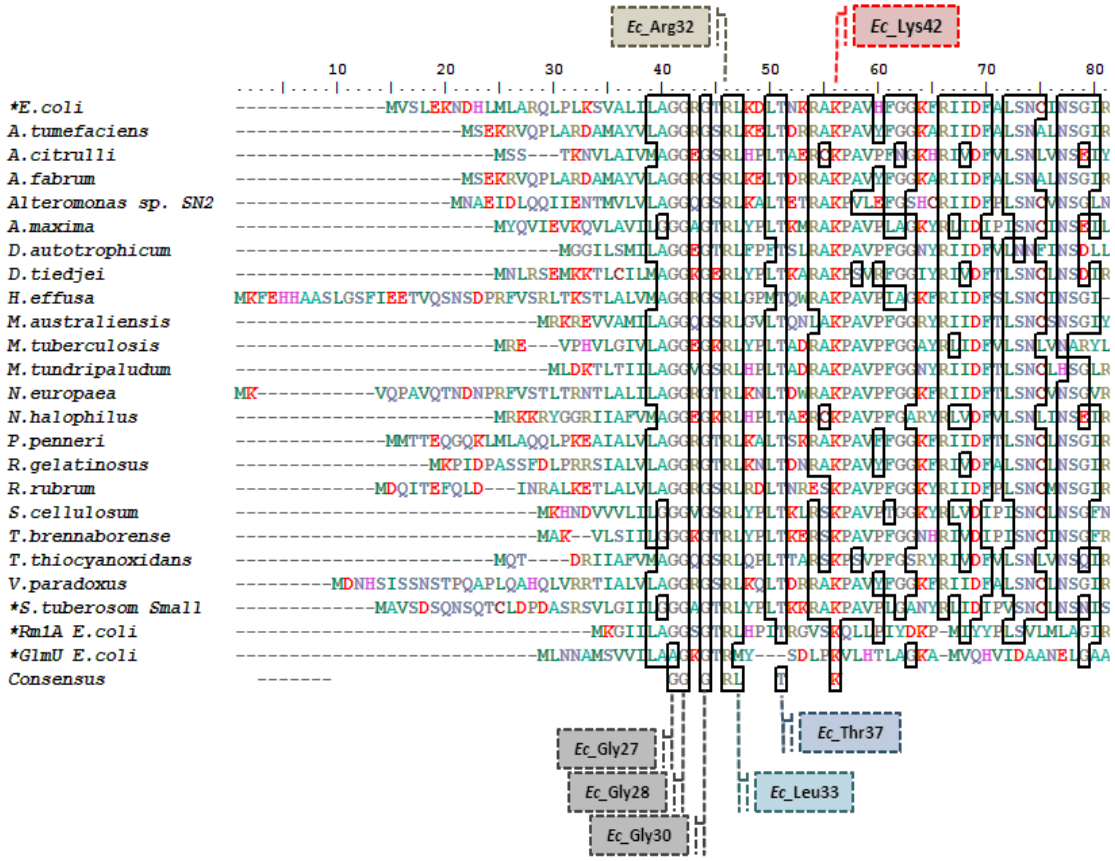

Figure 10. Sequence Alignment of conserved Nterminus Residues of *E. coli* ADP-Glc PPase and comparative enzymes. BioEdit® sequence alignment (Hall 1999) of the *E. coli* ADP-Glc PPase with homologs and consensus alignment. Species and corresponding GI Accession No. available in corresponding chart. A consensus of the residues shared with the wild-type *E. coli* ADP-Glc PPase ("*Ec*_residue#") are outlined in the alignment and in color coordinated text boxes above and below alignment ("*Ec*_Lys42";red, "*Ec*_Gly27", "*Ec*_Gly28", "*Ec*_Gly30"; grey, "*Ec*_Arg32"; olive, "*Ec*_Leu33"; teal and "*Ec*_Thr37"; blue).

E. coli: ADP-Glc PPase Conserved Arg^{32} and Lys^{42} Residues

E. coli is a gram-negative, rod-shaped bacteria. Many strains of *E. coli* are quite harmless. However, some can lead to food poisoning and other diseases. The most common beneficial strain is that which resides in the gut of its host and provides vitamin K (vitamin K_2). Moreover, it creates a balance of bacterial flora, inhibiting extreme growth of foreign bacteria. A common method of pathogenesis occurs via transmission of *E. coli* thru fecal matter to the oral cavity. Being a gram-negative bacterium, glycogen biosynthesis is the optimal carbon energy source storage method for *E. coli.* As such, experimental review of the *E. coli* ADP-Glc PPase offers a platform for understanding bacterial glycogen biosynthesis and the ADP-Glc PPase. A select number of amino acid residues of the *E. coli* ADP-Glc PPase are possibly important to the catalysis of other ADP- Glc PPases. Also, it was noted that the Arginine-32 and the Lysine-42 may possibly play a role in the catalytic funtion of the enzyme. These residues lie within the catalytic pocket of the *E. coli* ADP-Glc PPase enzyme and possibly near the phosphoryl groups of the ATP. With the use of computational homology modeling programs (such as Modeller 9, Swiss PDB Viewer: DeepView®) it is noted that the Arginine-32 and Lysine-42 are conserved residues in the active site of many bacterial ADP-Glc PPase enzymes. Experimentally, genetic mutations of the Arginine-32 and Lysine-42 sites, mutated DNA-vector ligation, cellular sub-cloning of newly synthesized mutated DNA-vector, protein expression and kinetic characterization – as well as Molecular Dynamic Simulations - will clarify its full catalytic function. Ultimately, our goal is to better

understand the overall functions of the individual groups of subunits (whether catalytic or non-catalytic) of the ADP-glucose Pyrophosphorylase Phylogenetic Tree, in intracellular carbohydrate biosynthesis for both photosynthetic (starch or glycogen) and non-photosynthetic organisms (glycogen). We have found that the Arg^{32} and Lys^{42} residues are not only highly conserved, but very important for the whole family of nucleotidyltransferases (Figure 10 and Table S1).

CHAPTER TWO

THE CATALYTIC LYS42 RESIDUE OF *ESCHERICHIA COLI* ADP-GLUCOSE PYROPHOSPHORYLASE

Comparative modeling of the *Escherichia coli* ADP-glucose pyrophosphorylase with ligands bound in the active site predicted critical interactions for Lys42. In the model, this residue interacts with the catalytic Asp142 and the β-phosphorous of the nucleotide triphosphate substrate, which constitutes the leaving group in the reaction. Lys42 is highly conserved in ADP-glucose pyrophosphorylases known to be catalytic, but absent in plant subunits that are catalytically deficient. It is also conserved in other homologues of the sugar-nucleotide pyrophosphorylase superfamily. To explore its role, we replaced Lys42 in the *E. coli* ADP-glucose pyrophosphorylase by other residues with different physicochemical properties. Kinetic analysis of the purified mutants showed k_{cat} decreased more than three orders of magnitude compared to the wild type. Other changes in kinetic parameters, such as apparent affinities for substrates and allosteric effectors, were less significant. These results show that the main role of Lys42 in the ADP-glucose pyrophosphorylase from *E. coli* is catalytic and essential for the enzyme function.

To date, it has been discovered in some plant species and tissues one of the ADP-Glc PPase subunits maintain a catalytic role whereas the other has a regulatory function, but a defective catalysis (Kuhn, Falaschetti et al. 2009, Yep, Bejar et al. 2004, Ventriglia, Kuhn et al. 2008, Crevillen, Ballicora et al. 2003). As a consequence of this functional divergence, there

are conserved and possibly important residues in bacterial ADP-Glc PPases that are lacking in some plant subgroups. One of these is Lys42 (*E. coli*), which is not present in the β subunits from some non-photosynthetic plant tissues, such as tubers and seeds. At this particular site, rather than a Lys there is a Thr residue (Ballicora, Dubay et al. 2005). On the other hand, a homologous Lys in the similar position is well conserved in other NDP-sugar pyrophosphorylases (Blankenfeldt, Asuncion et al. 2000, Brown, Pompeo et al. 1999, Machtey, Kuhn et al. 2012b). This Lys is only few amino acids upstream from the motif GXG(T/S)R proposed to be involved in nucleotide binding (Jin, Ballicora et al. 2005a), and conserved in the whole superfamily (Blankenfeldt, Asuncion et al. 2000, Brown, Pompeo et al. 1999, Jin, Ballicora et al. 2005b, Steiner, Lamerz et al. 2007, Sivaraman, Sauve et al. 2002, Koropatkin, Cleland et al. 2005, Pelissier, Lesley et al. 2010, Maruyama, Nishitani et al. 2007) (Figure 10, Table S1).

In the enzyme family, there is some experimental evidence supporting the importance of Lys at this site. However, there has been no thorough experimental analysis to determine the role of this residue. Mutation of a Thr to a Lys partially resurrected the activity of a catalytically defective β (large) subunit from potato tuber ADP-Glc PPase (Ballicora, Dubay et al. 2005). On the other hand, some data from homologous enzymes make the relevance of this residue less clear. A single Ala mutant of GlmU (UDP-GlcNAc pyrophosphorylase) in the homologous Lys had negligible activity (Mochalkin, Lightle et al. 2007), but another similar experiment in another GlmU only reduced the activity 8-fold (Brown, Pompeo et al. 1999). Some variants of RmlA (dTDP-glucose pyrophosphorylase) from *Salmonella enterica*, which

have this Lys replaced by Gln (Gln26 according to the deposited structures, PDB accession codes 1MP3, 1MP4, 1MP5, 1IIiN, 1IIM), was active enough to be used for synthesis of sugar nucleotides (Barton, Biggins et al. 2002, Barton, Lesniak et al. 2001). However, their k_{cat} values have not been reported to evaluate the degree of catalytic competency of those variants.

Knowing whether Lys42 is important in ADP-Glc PPase and its specific role (catalysis, binding, or regulation) is critical to understand the mechanism of the enzyme. Several studies have been performed, particularly in the *E. coli* enzyme, to characterize the role of various residues (Hill, Wong et al. 2015, Bejar, Jin et al. 2006, Frueauf, Ballicora et al. 2001). However, only Asp142 and Asp276 have been assigned critical roles in catalysis, most likely by their ability to chelate the metal cofactor (Frueauf, Ballicora et al. 2001, Bejar, Ballicora et al. 2006, Gardiol, Preiss 1990).

Here, we built a model of the *E. coli* ADP-Glc PPase with substrates in the active site to survey the possible interactions of Lys42 within the active site. We mutated Lys42 to several residues with different properties to avoid the dangers of assigning roles based on a single alanine mutation as it was previously emphasized (Yep, Kenyon et al. 2008). Based on the models and kinetic characterization of the purified mutants, we propose that the major role for Lys42 is catalytic.

To explore the role of the Lys42 residue we utilized a series of methods and materials ranging from site-directed mutagenesis, protein expression and purification to enzyme kinetics:

Materials

Strataclone™ Blunt PCR cloning kit was purchased from Agilent Technologies, Inc. (Clara, CA). BL21 (DE3) cells were obtained from Novagen. Biochemical reagents were from Sigma-Aldrich Co. New England BioLabs Inc. NEB Turbo® Cells, Restriction enzymes, Phusion® DNA polymerase, and protein markers were purchased from New England Bio Labs.

Site-Directed Mutagenesis

We utilized the pETEC plasmid, a derivative of pET24b (Novagen), for expression of the wild-type and mutant ADP-Glc PPases as described before (Ballicora, Sesma et al. 2002). Using pETEC as a template, site-directed mutagenesis was performed by PCR overlap extension with Phusion DNA polymerase as described before (Kuhn, Figueroa et al. 2010). Oligonucleotides (Table S2) utilized in PCR site-directed mutagenesis were designed using BioEdit® (Hall 1999) and acquired from Integrated DNA Technologies (IDT, San Diego). DNA Sequencing to confirm mutations were performed at the University of Chicago Cancer Research Center (CRC-DNA Sequencing, Chicago).

Expression and Purification of Wild Type and Lys42 Mutant Enzymes

Wild type and pETEC mutants were transformed into BL21(DE3) competent cells. Cells were induced with 0.5 mM isopropyl-β-D-thiogalactoside (IPTG) and incubated for 16 hrs at 25ºC. Cultures were harvested, centrifuged at 10,000 *g* for 20 min at 4 °C and cell pellet resuspended in *Buffer A* (50 mM Hepes, pH 8.0, 5 mM $MgCl_2$, 0.1 mM EDTA, 10% Sucrose). The re-suspended samples were placed on ice and sonicated for three 30-s interval.

The sonicated samples were then centrifuged at 10,000 g for two 15-min intervals at 4ºC, and the supernatants were collected as crude extracts. Purification using DEAE-Sepharose and Source15 Q 4.6/100 PE (GE Healthcare Life Sciences) columns were performed via FPLC as described (Kuhn, Falaschetti et al. 2009). Wild-type and mutant proteins were purified to apparent homogeneity as verified via SDS-PAGE (Figure 11) (Kuhn, Falaschetti et al. 2009). Following protein expression and purification 1L of the BL21 (DE3) mutant cell culture yielded 2–12 mg of purified protein. Protein concentrations were calculated as described before (Asencion Diez, Aleanzi et al. 2014).

Lys42 Mutants Enzyme Assay - Synthesis (Forward) Direction

The assay was performed as described before with minor modifications (Fusari, Demonte et al. 2006). Additionally, the Malachite-Green-Ammonium Molybdate solution was sterile-filtered via a 12 ml NORM-JECT® Luer-Lock syringe and 32 mm syringe filter with 0.2 µm Supor® Membrane from PALL® Life Sciences before the addition of Tween20 to prevent precipitation. Unless stated otherwise, each reaction tube contained 50 mM Hepes buffer (pH 8.0), 7 mM $MgCl_2$, 1 mM Glc-1P, 1.5 mM ATP, 1 mM FBP, 0.5 U/ml pyrophosphatase, 0.2 mg/ml of bovine serum albumin, and water. The reactions were started with addition of 10 µl enzyme to reach a final volume of 50 µl. In a saturation curve for a given effector, the concentration was varied while keeping the rest of the mixture constant. After 10 min at 37ºC, the addition of 0.4 ml Malachite Green-Ammonium Molybdate-Tween 20 solution stopped the reaction and the Mg-phosphate complex was stabilized with 25 µl of a solution 34% sodium citrate.

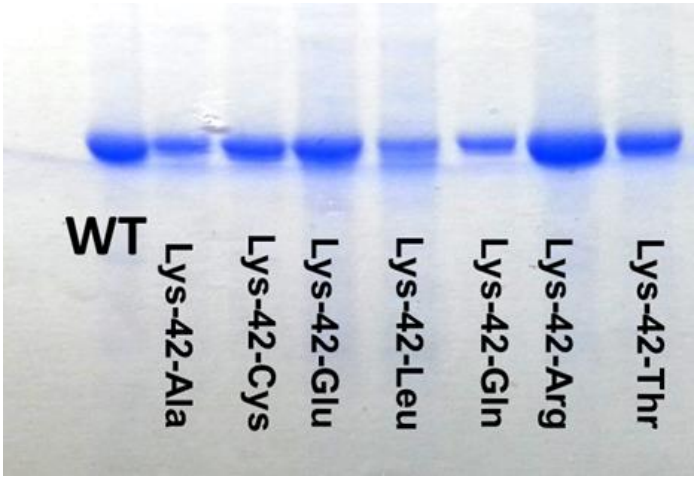

Figure 11. SDS PAGE Verification: WT vs. Lys42 mutants. FPLC chromatography (DEAE and Source15Q - quaternary ammonium; strong anion exchange column) was employed for homogenous purification of the WT and mutant *E.coli* ADP-Glc PPase. All protein samples were eluted from column using Buffer B (running a 1M NaCl elution gradient to 50%). Additionally, Malachite-Green colorimetric assay screening verified collected protein fractions, which were collected, pooled and concentration. SDS-PAGE was loaded with 10μL of 1mg/mL for WT and Lys42 mutants, respectively, to verify protein purification and samples we utilized the New England Biolabs® protein marker #7708S. *E.coli* ADP-Glc PPase SDS bands show at 50-52 kDa.

An aliquot of 0.25 ml was withdrawn and the A595 was measured with a BioTek EL808 microplate reader (Winooski, VT). One unit of ADP-Glc PPase activity was the production of 1 µmol PPi min^{-1}.

Enzyme Assay – Pyrophosphorolysis (Reverse) Direction

The assays in the pyrophosphorolysis direction were performed using a continuous enzyme-coupled spectrophotometric assay, with minor differences, as described before (Hylton, Smith 1992). The reaction mixture contained 80 mM 4-(2-hydroxyethyl)-1-piperazinepropanesulfonic acid (Hepps) buffer (pH 8.0), 5 mM $MgCl_2$, 1 mM FBP, 1 mM ADP-Glc, 0.6 mM NAD, 10 mM NaF, 0.01 mM glucose 1,6-bisphosphate, 2 units/ml phosphoglucomutase rabbit muscle 2 units/ml glucose-6-phosphate dehydrogenase from *Leuconostoc mesenteroides*, 0.2 mg/ml bovine serum albumin and the stated amount of wild-type or mutant *E. coli* ADP-Glc PPase. Assays were initiated by adding 10 µl of sodium PP_i to reach a final volume of 0.150 ml. The final PP_i concentration was held constant at 1.4 mM $NaPP_i$ for ADP-Glc saturation curves. Assays were performed at 37ºC in a 96-well plate and the absorbance was measured at 340 nm using a BioTek EL808 microplate reader (Winooski, VT). In each reaction, A_{340} was recorded every 15 s intervals for a total of 20 min. NADH was used as an external standard to calibrate the relationship between absorbance and concentration of product formation. One unit of enzyme activity was the production of 1 µmol of Glc-1P min^{-1}.

Calculation of Kinetic Parameters

Turnover numbers were calculated per monomer (50 kDa) of enzyme. Therefore, a specific activity of 1.2 U/mg was equivalent to 1 s^{-1}. The $S_{0.5}$, $A_{0.5}$, $I_{0.5}$ values, and their respective standard errors, were calculated by non-linear regression fitting of the data as described before (Hill, Wong et al. 2015). Saturation curves were performed at least twice to verify reproducibility. All data points were quadruplicates.

Homology Modeling

Homology modeling of the *E. coli* ADP-Glc PPase monomer bound to substrates was performed with the program Modeller 9.11 (Sali, Blundell 1993). The procedure used several simultaneous templates, which were the known atomic coordinates of i) *E. coli* dTDP-Glc PPase (RffH) complexed with dTTP and Mg^{2+} (Protein Data Bank code 1MC3) (Sivaraman, Sauve et al. 2002), ii) *Pseudomonas aeruginosa* glucose-1-phosphate thymidylyltransferase (RmlA) complexed with thymidine and Glc-1P (Protein Data Bank code 1G0R) (Blankenfeldt, Asuncion et al. 2000), iii) *S. Enterica* RmlA Q83S variant complexed with dATP (Protein Data Bank code 3PKP) (Moretti, Chang et al. 2011), iv) *S. tuberosum* small subunit ADP-Glc PPase with both subunit A complexed with ADP and B complexed with ADP-glucose (Protein Data Bank code 1YP4) (Jin, Ballicora et al. 2005a), and v) *A. tumefaciens* ADP-Glc PPase (Protein Data Bank code 3BRK) (Cupp-Vickery, Igarashi et al. 2008). Alignment of the target was trivial, since the sequence of the *E. coli* enzyme has no gaps or insertions compared to the *A. tumefaciens* enzyme (56% sequence identity). Afterwards, the alignment of the *A. tumefaciens* enzyme with the other templates served as a guide. In loops in which there is no obvious

structural match between the templates, a gap was introduced so the structural information was inherited only from the *A. tumefaciens* and potato tuber enzymes. The only two exceptions were in loops 103-115 and 232-243 in which the structure of the *A. tumefaciens* enzyme was not resolved. In these two regions, the target was only aligned to the potato tuber ADP-Glc PPase. The ligands Mg^{2+} and dATP were inherited from the 3PKP and glucose-1-P was inherited from the phospo-glucose moiety of the ADP-Glc bound to the subunit B of the potato tuber ADP-Glc PPase. The final model was validated with the DOPE score of Modeller (Shen, Sali 2006) and the program Verify3D (Luthy, Bowie et al. 1992).

Conservation of Lys42

An amino acid sequence alignment of *E.coli* ADP-Glc PPase and twenty representative species of bacterial ADP-Glc PPases taken from diverse branches of the phylogenetic tree (Machtey, Kuhn et al. 2012a), along with *S. tuberosum* (potato tuber, small subunit) (Jin, Ballicora et al. 2005a), *E. coli* GlmU (N-acetylglucosamine 1-phosphate uridylyltransferase) (Brown, Pompeo et al. 1999) and *E. coli* RmlA (glucose-1-phosphate thymidylyltransferase) (Sivaraman, Sauve et al. 2002) was created to highlight the conserved residues in the N-terminal region (Table S1). The first 80 residues of the *E. coli* ADP-Glc PPase were aligned with the twenty-three homologues and the consensus was outlined in black. It has been previously noted that residues located in the N-terminus of the ADP-Glc PPases have pertinent structural implications in the matters of allosteric regulation and substrate binding, and this structure-function characteristic has been studied in *E. coli* and *A. tumefaciens* ADP-Glc PPase (Bejar, Ballicora et al. 2006, Gomez-Casati, Igarashi et al. 2001).

Lys42 with an additional consensus of Gly28, Gly30, and Arg32 is conserved in bacteria, plants, and other members of the superfamily (RmlA and GlmU) (Figure 10).

Modeling of Lys42 Interactions

The structure of a bacterial ADP-Glc PPase and a plant subunit are available, but unfortunately, one is in absence of substrates (Cupp-Vickery, Igarashi et al. 2008) and the other has ATP bound in a non-productive conformation (Jin, Ballicora et al. 2005a). For that reason, we built models using information available from others enzymes of the superfamily as described in Materials and Methods. Modeling of the *E. coli* ADP-Glc PPase with a nucleotide triphosphate (dATP), Glc-1P, and Mg^{2+} ligands revealed the possible interactions of Lys42. After running 100 different models with Modeller 9.11 we obtained an "ensemble" of conformations that surveyed the mobility the side chain provides. The clearest pattern extracted from the analysis was that Lys42 is in direct contact with Asp142. In 70% of the models, the distance between the ε-amino group of Lys and one of the oxygen atoms from the carboxylate was less than 3.5 Å. This is of significant importance because Asp142 is a catalytic residue proposed to chelate Mg^{2+}. In 45% of the models one oxygen atom of Asp142 is less than 3.5 Å from the Mg^{2+} cation. The only other possible interaction that Lys42 has is with the nucleotide triphosphate substrate. In 10% of the models the ε-amino group is less 3.5 Å from the oxygen bridging the α- and β-phosphorous groups, which is the leaving atom in the reaction. Figure 12 depicts the residues that may participate in a network of with Lys42. The importance of these interactions raises the hypothesis that Lys42 is critical for catalysis.

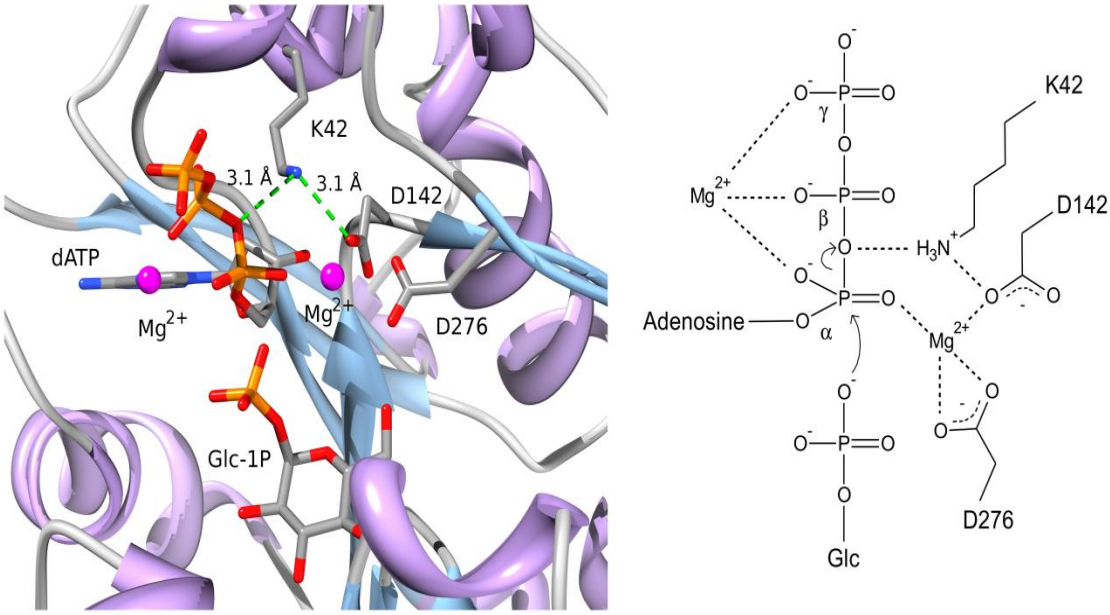

Figure 12. Homology model of the *E. coli* ADP-Glc PPase with substrates bound. Model was built as described in Materials and Methods. Side chains of Lys42 and previously described catalytic residues are shown. The network of interactions (Lys42/Asp142/Mg^{2+}/Asp276) is depicted above.

Effect of Lys42 Mutations on k_{cat}

To explore the role of Lys42 we mutated it to several other amino acids with different characteristics. The most striking effects on the kinetic properties were on the k_{cat} values. Replacing Lys42 by any other residue decreased k_{cat} at least three orders of magnitude compared to the wild type (Figure 13 and Table 4). The mutants K42E and K42T had the lowest turnover with a dramatic ~3300- and ~4000-fold decrease, respectively (Figure 13). Interestingly, replacing Lys42 to another positively charged side chain (K42R) did not preserve the activity and also had a dramatic decrease in turnover number. This indicated that charge, at this position, is not the only factor needed for an effective catalysis. All the other residues, whether polar, hydrophobic, small, or bulky had an even lower activity (Figures 11 and Table 4). Some of the other kinetic parameters were affected by the mutations, but they were not as dramatic as the effects observed on k_{cat}.

Effect of Lys42 Mutations on Apparent Affinity of Substrates

Apparent affinities for the *E. coli* ADP Glc PPase substrates were determined from saturation curves. Four mutants (K42Q, K42R, K42C and K42E) appeared to have similar affinities for the ATP substrate as the wild type (Table 1). On the other hand, K42T and K42L mutants exhibited a 2-fold decrease in $S_{0.5}$ for ATP. The alanine mutant displayed a nearly 2.5-fold decrease. Hill values for all mutants were within range of the wild type (n = 1.5), which indicates that the mutations did not significantly affect the homotropic cooperativity in ATP binding. Glc-1P apparent binding affinity was only slightly affected by different side chains at position 42. There was a nearly 2-3 fold increase in $S_{0.5}$ for Glc-1P for all mutants, with the

exception of K42T which displayed the highest increase (~4-fold) of $S_{0.5}$ for Glc-1P (Table 1, Figures 14 and 15).

Effect of Lys42 Mutations on Mg^{2+} Cofactor Kinetics

ADP-Glc PPase enzymes need the presence of the divalent magnesium cation as a cofactor. Saturation curves of this metal are generally sigmoidal implying a strong cooperativity. Here, we observed that the cooperativity of cofactor binding decreased in all mutants, which was evident from a decreased in the Hill coefficients (Table 1 and Figure 16). All mutations produced enzymes with a similar $S_{0.5}$ for Mg^{2+}, except K42A (0.30 mM) and K42T (0.90 mM) (Table 1). The affected cooperativity could be an indirect response to the Lys42 mutation, as it has been noted above that Lys42 interacts with Asp142, a residue that has been proposed to chelate the cofactor in ADP-Glc PPase enzymes (Figure 12) (Frueauf, Ballicora et al. 2001) .

Effect of Lys42 Mutations on Fructose-1,6-bisphosphate Activation

Kinetic analysis revealed that the Lys42 mutants have a lower apparent affinity for FBP activator in comparison with the wild type ($A_{0.5}$ = 0.049 mM) (Table 2 and Figure 16). The apparent affinities for the Lys42 mutants decreased 1.6 to 8-fold, with the exception of K42A ($S_{0.5}$ = 0.037 mM). Almost one order of magnitude decrease in activator affinity was noted for the K42E mutant ($S_{0.5}$ = 0.397 mM). There was a certain degree of variability on the activation fold (V_m/V_o), which is the activity in presence of saturating concentrations of activator compared to the activity in its absence. This may reflect an effect on the ratio of activated/non-activated forms, or R/T forms according to the MWC model of allosterism (Fersht 1999)

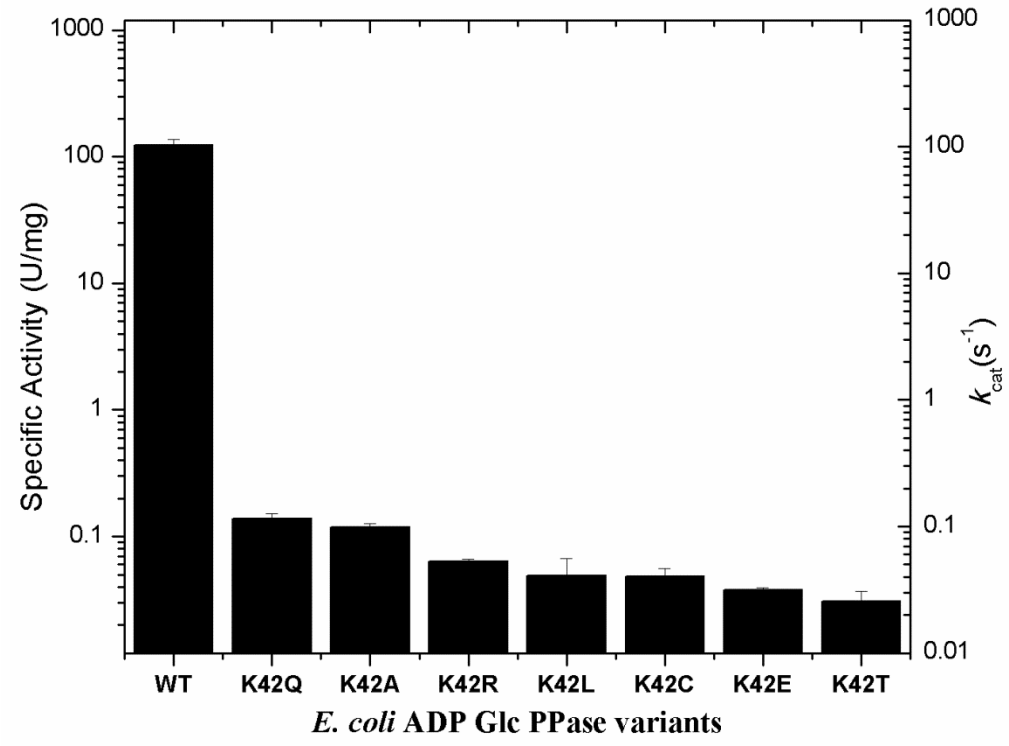

Figure 13. Specific activity and k_{cat} of *E.coli* ADP-Glc PPase variants in the synthesis direction. Specific Activity (U/mg) and k_{cat} (s^{-1}) values were determined in the presence of saturated conditions of substrates (ATP and Glc-1P) and activator (FBP) as described in Materials and Methods. A mean value calculated from three independent experiments.

Table 1. Kinetic parameters in the synthesis direction for the wild-type *E.coli* ADP-Glc PPase and Lys42 mutants.

Enzyme[a]	**$S_{0.5}$ Glc-1-P**[b]	**n_H**	**$S_{0.5}$ ATP**[b]	**n_H**	**$S_{0.5}$ Mg^{2+}**[b]	**n_H**
	mM		*mM*		*mM*	
WT	0.027 ± 0.008	0.9	0.20 ± 0.02	1.5	1.88 ± 0.05	4.3
K42Q	0.058 ± 0.004	1.4	0.20 ± 0.02	1.3	2.31 ± 0.39	1.6
K42A	0.054 ± 0.004	1.1	0.56 ± 0.04	1.5	0.30 ± 0.05	1.2
K42R	0.059 ± 0.004	1.4	0.26 ± 0.02	1.2	1.39 ± 0.59	1.1
K42L	0.070 ± 0.007	1.1	0.08 ± 0.01	1.1	2.19 ± 0.24	1.6
K42C	0.070 ± 0.005	1.1	0.14 ± 0.01	1.1	1.78 ± 0.26	1.4
K42E	0.048 ± 0.005	1.1	0.12 ± 0.01	1.3	1.72 ± 0.17	2.7
K42T	0.102 ± 0.008	1.2	0.09 ± 0.01	1.0	0.90 ± 0.08	1.8

[a]Enzymes were purified to homogeneity and saturation kinetics for Glc-1P, ATP and Mg^{2+} were performed at 37°C using a Malachite Green colorimetric assay as described under "Experimental Procedures".

[b]$S_{0.5}$ and Hill coefficient numbers (n_H) of Glc-1P, ATP and Mg^{2+} for the WT (*wildtype*) and Lys42 mutant enzymes were determined in the presence of activator (1mM FBP).

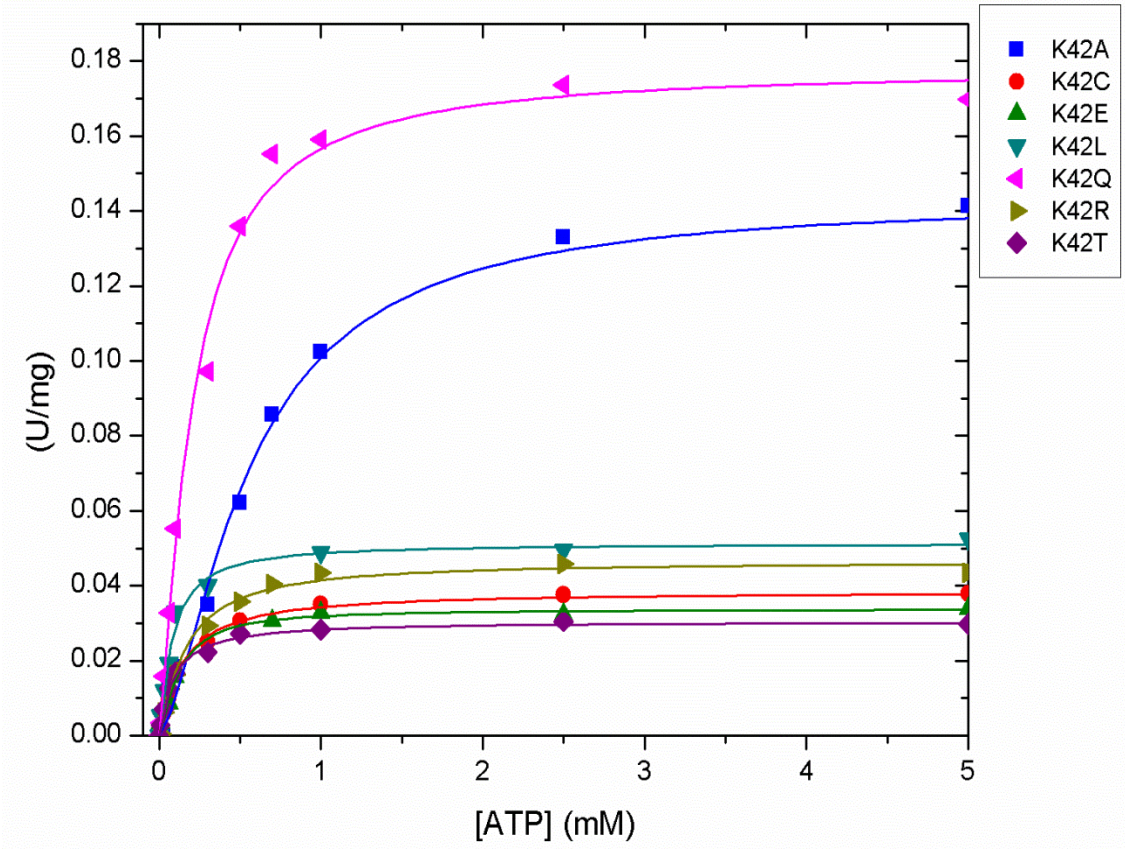

Figure 14. ATP Saturation Curves for Lys42 mutants of *E. coli* ADP-Glc PPase in the synthesis direction. Specific Activity (U/mg) and ATP substrate concentration (mM). All enzymes were assayed at varying dilutions for optimal kinetic analysis.

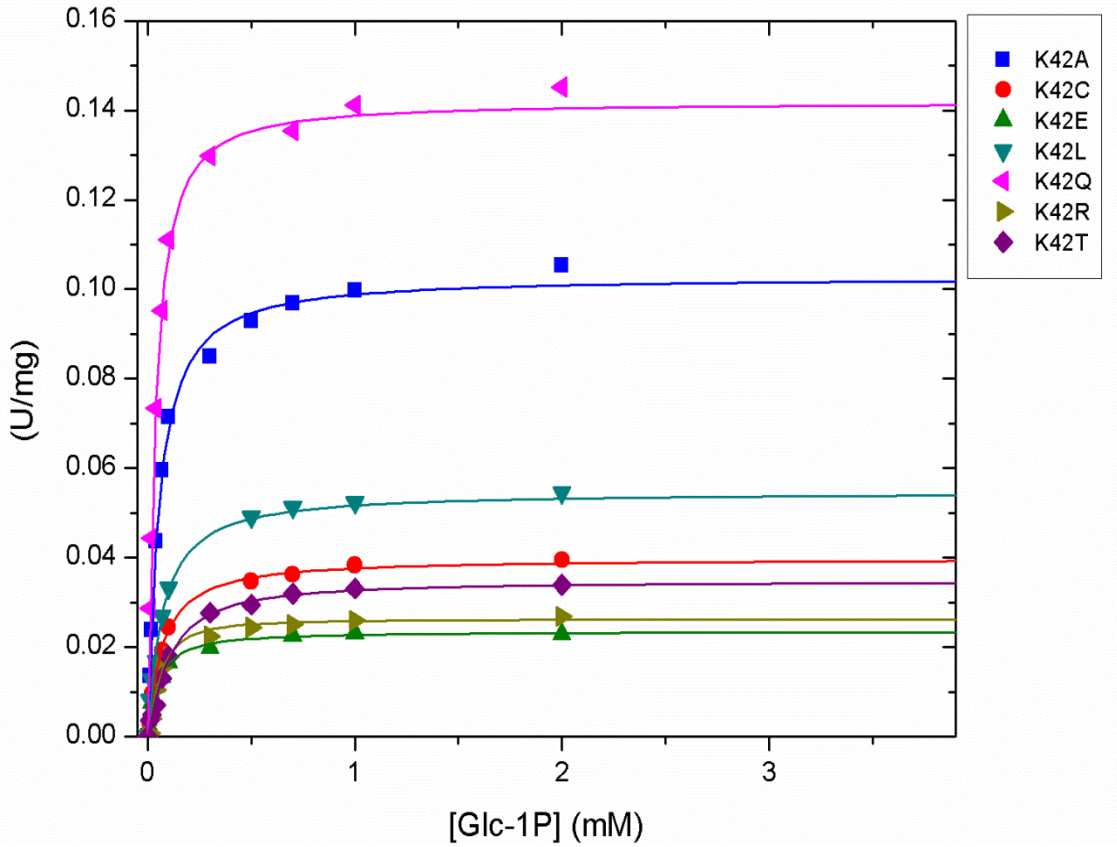

Figure 15. Glc-1P Saturation Curves for Lys42 mutants of *E. coli* ADP-Glc PPase in the synthesis direction. Specific Activity (U/mg) and Glc-1P substrate concentration (mM). All enzymes were assayed at varying dilutions for optimal kinetic analysis.

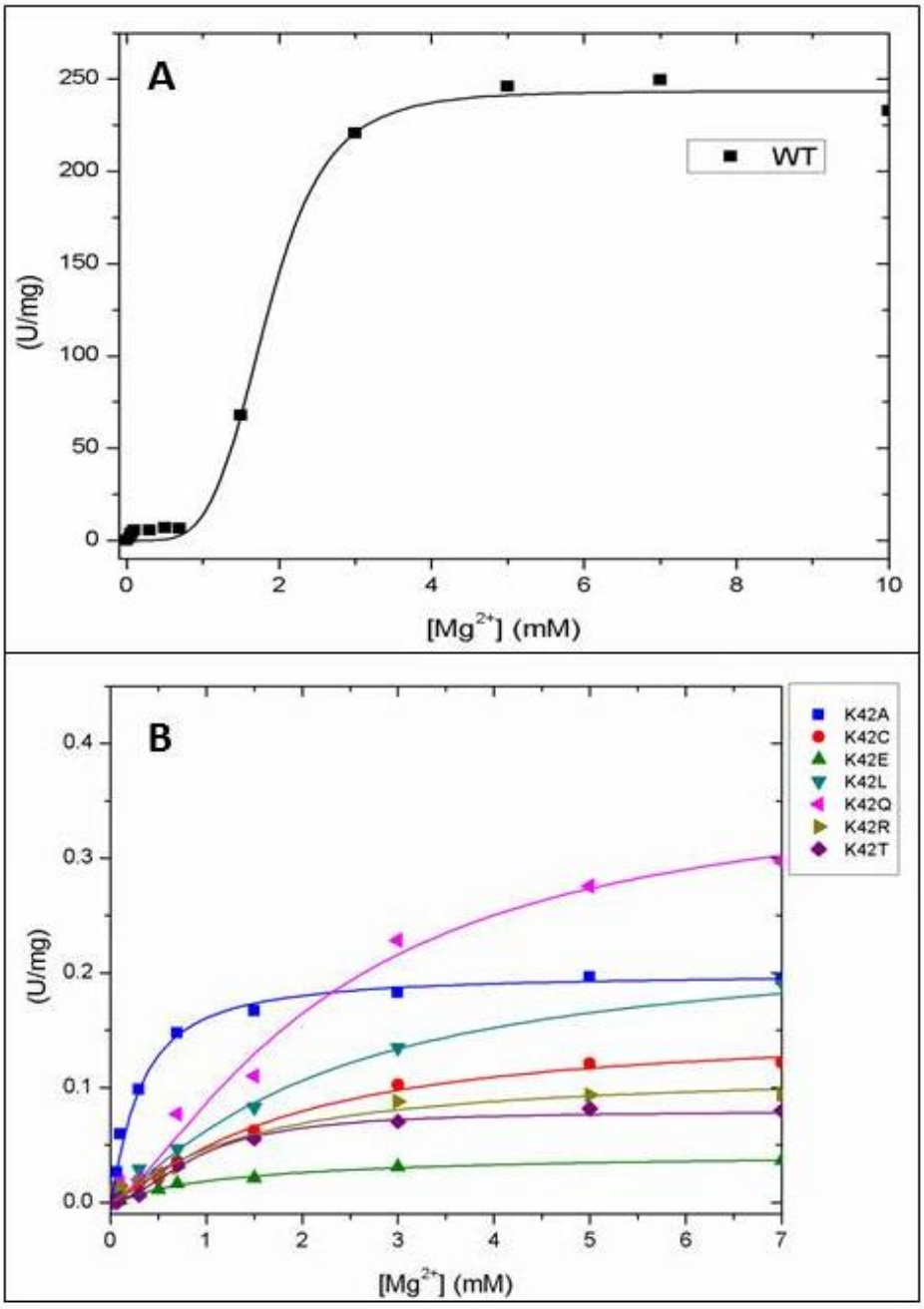

Figure 16. Mg^{2+} Saturation Curves for WT and Lys42 mutants of *E. coli* ADP-Glc PPase in the synthesis direction. Specific Activity (U/mg) and Mg^{2+} (cofactor) concentration (mM); (A) WT and (B) Lys42 Mutants. All enzymes were assayed at varying dilutions for optimal kinetic analysis.

Table 2. Activation and inhibition parameters of *E. coli* ADP-Glc PPase Lys42 variants in the ADP-Glc synthesis direction.

Enzyme [a]	FBP			AMP		
	$A_{0.5}$	n_H	Activation [b] (V_m/V_o)	$I_{0.5}$	n_H	Remaining Act. [c] 100 x (V_∞/V_o)
	mM		-fold	mM		(%)
WT	0.049 ± 0.008	1.1	27.0	0.080 ± 0.006	1.3	8.9
K42Q	0.110 ± 0.040	0.7	2.6	0.272 ± 0.070	0.9	8.3
K42A	0.037 ± 0.010	1.1	3.6	0.121 ± 0.028	0.8	40.6
K42R	0.078 ± 0.004	1.1	18.0	0.026 ± 0.004	1.1	14.2
K42L	0.068 ± 0.010	1.5	2.0	0.079 ± 0.011	1.0	16.4
K42C	0.180 ± 0.049	0.7	6.5	0.323 ± 0.068	0.8	26.8
K42E	0.397 ± 0.077	1.2	8.4	0.188 ± 0.083	1.5	48.4
K42T	0.192 ± 0.038	1.4	3.1	N/A[d]	N/A	N/A

[a] Assays were performed as described in Materials and Methods.

[b] V_o is the activity in absence of activator

[c] Remaining activity is the ratio between the activity in absence (V_o) and saturating concentrations of inhibitor (V_∞), respectively.

[d] No inhibition detected up to 7 mM AMP

A lower activation fold means a lower maximum response to the activator, which could be caused by a higher proportion of active forms in solution or that the activated form is less effective. K42R mutant have a similar activation fold (V_m/V_o) than the wild type (18-fold), with Leu having the lowest (2-fold) (Figure 17 and Table 2). In all cases, the ability of the enzymes to respond to FBP was preserved. But clearly, if a positive charge was no present at this site, the overall effect was altered, at least in part.

Effect of Lys42 Mutations on Adenosine Monophosphate Inhibition

All mutants preserved the sensitivity to AMP inhibition with the only exception of K42T. K42R exhibited a slightly higher apparent affinity to AMP inhibition ($I_{0.5}$ = 0.026 mM), but within the range of the wild type ($I_{0.5}$ = 0.080 mM). The rest of the mutants displayed only an increase in $I_{0.5}$ from 3- to 5-fold. None of the Lys42 mutants were completely inhibited by AMP at saturating concentrations ($V_\infty/V_o > 0$), which is a well-known behavior of the wild-type enzyme (Bejar, Ballicora et al. 2006) (Figure 18 and Table 2).

Effect of Lys42 Mutations on the Pyrophosphorolysis (Reverse) Direction

As the ADP-Glc PPase reaction is reversible *in vitro*, we explored whether the mutations affected the kinetic parameters in the (non-physiological) pyrophosphorolysis direction for ADP-Glc and PP_i (substrates in the reverse direction). As it was observed in the synthesis direction, the most dramatic effect was on k_{cat} (V_m). For the wild type, the V_m was 42 or 60 s^{-1} for the saturation with PPi or ADP-Glc, respectively. Mutations decreased V_m 3 to 4 orders of magnitude, but the apparent affinity for either substrate was not significantly changed. Some mutant enzymes displayed a slightly higher or lower K_m (Table 3). Overall, mutating the Lys42

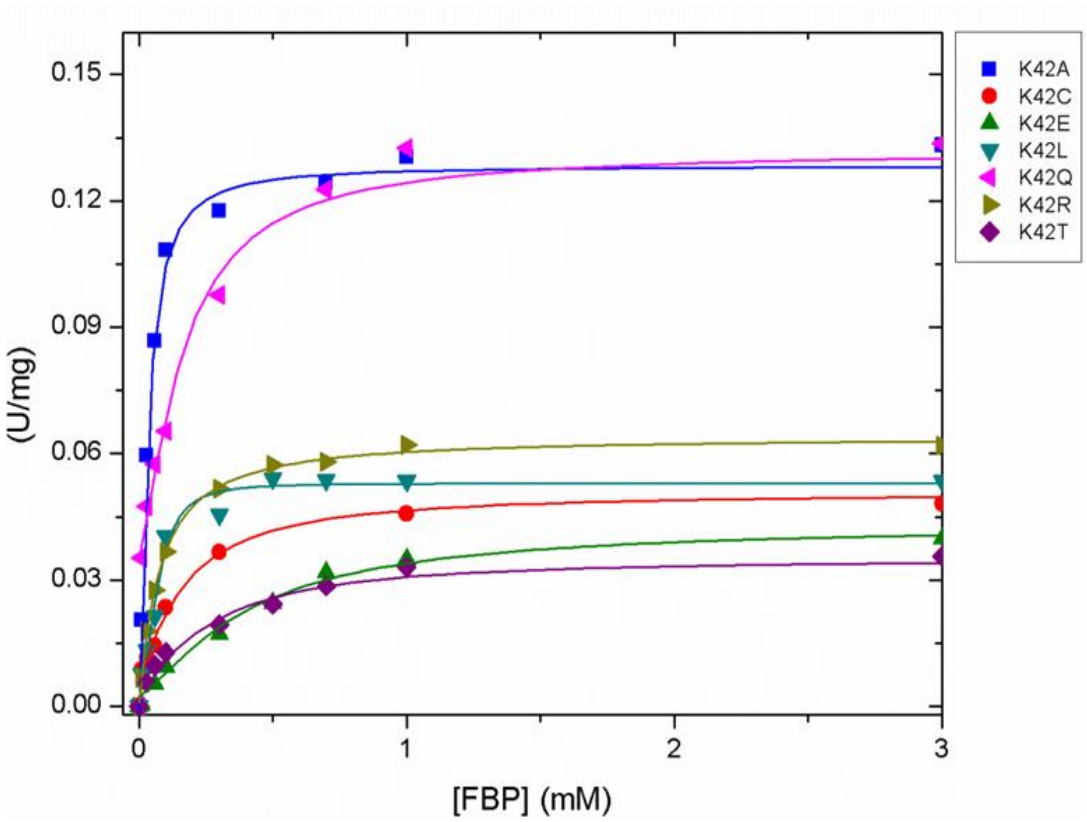

Figure 17. FBP Activation Curves Lys42 Mutants *E.coli* ADP-Glc PPase. All enzymes were assayed at varying dilutions for optimal kinetic analysis.

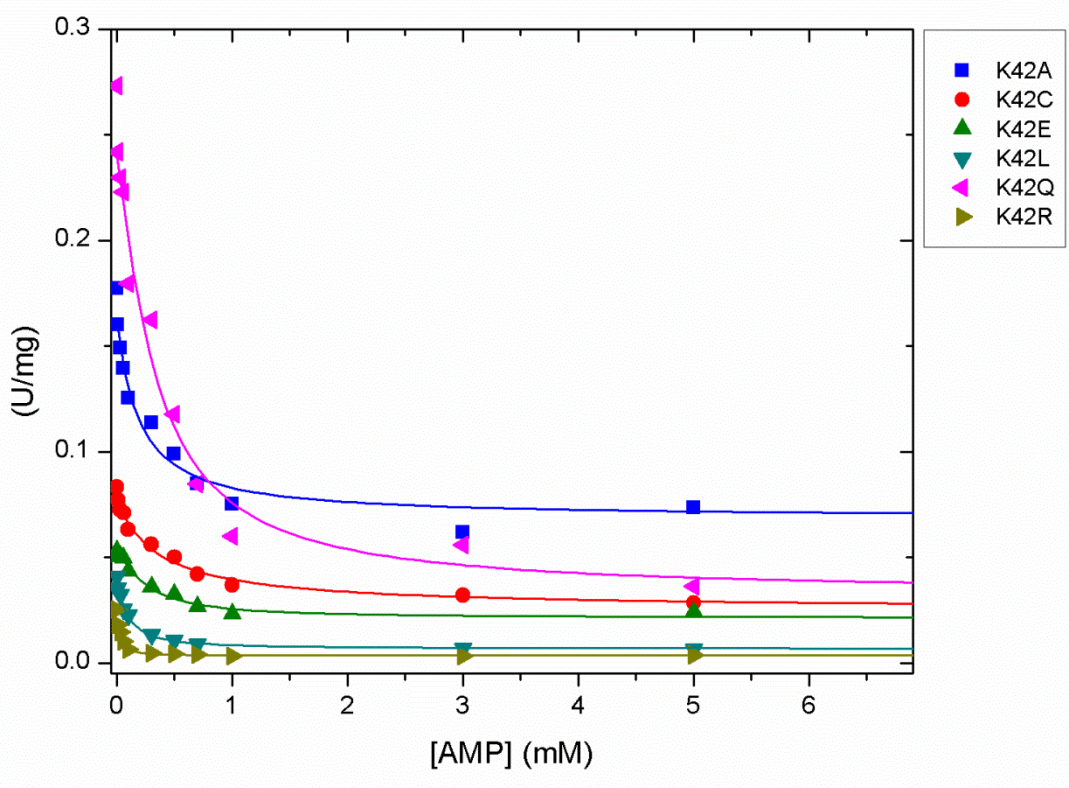

Figure 18. AMP Inhibition Curves Lys42 Mutants *E.coli* ADP-Glc PPase. All enzymes were assayed at varying dilutions for optimal kinetic analysis.

Table 3. Kinetic parameters of *E. coli* ADP-Glc PPase Lys42 variants in the pyrophosphorolysis direction.

Enzyme [a]	PP_i		ADP-Glc		
	K_m	V_m	$S_{0.5}$	V_m	n_H
	mM	s^{-1}	mM	s^{-1}	
WT	0.20 ± 0.02	60 ± 2	0.22 ± 0.08	42 ± 6	1.1
K42Q	0.28 ± 0.05	0.059 ± 0.003	0.11 ± 0.01	0.051 ± 0.002	1.9
K42A	0.13 ± 0.02	0.029 ± 0.001	0.11 ± 0.02	0.035 ± 0.002	1.3
K42R	0.17 ± 0.03	0.027 ± 0.001	0.42 ± 0.02	0.029 ± 0.004	1.3
K42L	0.12 ± 0.03	0.007 ± 0.001	0.11 ± 0.03	0.007 ± 0.001	1.0
K42C	0.30 ± 0.05	0.012 ± 0.001	0.045 ± 0.003	0.011 ± 0.001	2.2
K42E	0.13 ± 0.02	0.018 ± 0.001	0.054 ± 0.008	0.018 ± 0.001	1.8
K42T	0.36 ± 0.12	0.006 ± 0.001	0.072 ± 0.006	0.005 ± 0.001	2.0

[a] Assays were performed as described in Materials and Methods in presence of activator FBP (1 mM).

residue yielded is a decrease in activity in the reverse direction, which also highlights the significant role of this residue in catalysis in both directions (Figures 19 and 20).

Characterization and Catalytic Properties of Lys42 Residue of *E.coli* ADP-Glc PPase

Homology modeling predicted Lys42 interacts with the oxygen bridging the α- and β-phosphorous groups of the ATP substrate, as it is also observed in the crystal structure in other members of the superfamily (RffH and RmlA). That interaction would make PPi a better leaving group by stabilizing a developing negative charge in the transition state. This implies a critical role for Lys42 in agreement with computational studies on the UDP-Glc PPase from *Leishmania major* (Führing, Cramer et al. 2013). That distant eukaryotic homologue (12 % identity) catalyzes the same chemistry, has a relatively similar fold, and it shares few conserved residues in the active site (though some critical ones are different). In the simulations of that study, the interaction of Lys95 with the nucleotide β-phosphorous was important to direct the PPi to its exit channel (Führing, Cramer et al. 2013). In addition, a single K95A mutant had a remaining activity of 0.5% in standard conditions; but unfortunately, no other characterization was performed (Steiner, Lamerz et al. 2007). In the crystal structure of *L. major* UDP-Glc PPase bound to an analog of UTP, the distance between the nitrogen of the ε-amino group of Lys95 and any atom of the β-phosphorous is longer than 6.3 Å (PDB code 4M28). However, during the simulations those atoms got closer.

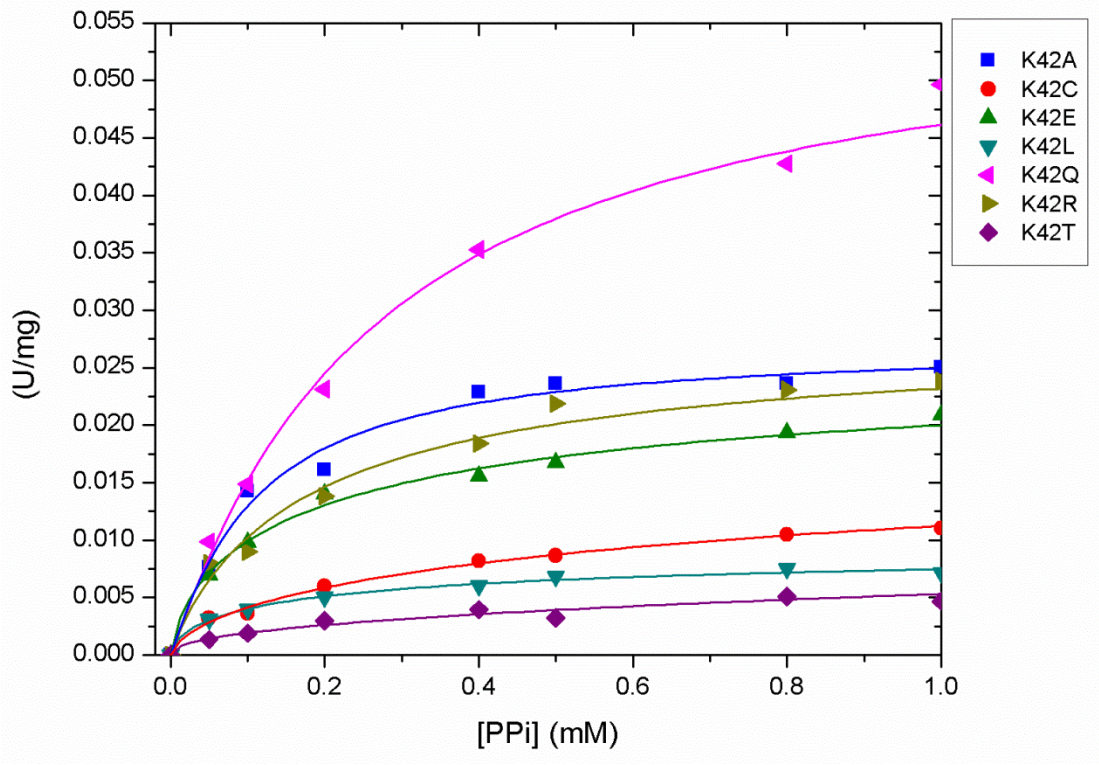

Figure 19. PP_i Substrate Saturation Curves Lys42 Mutants in the pyrophosphorolysis direction.

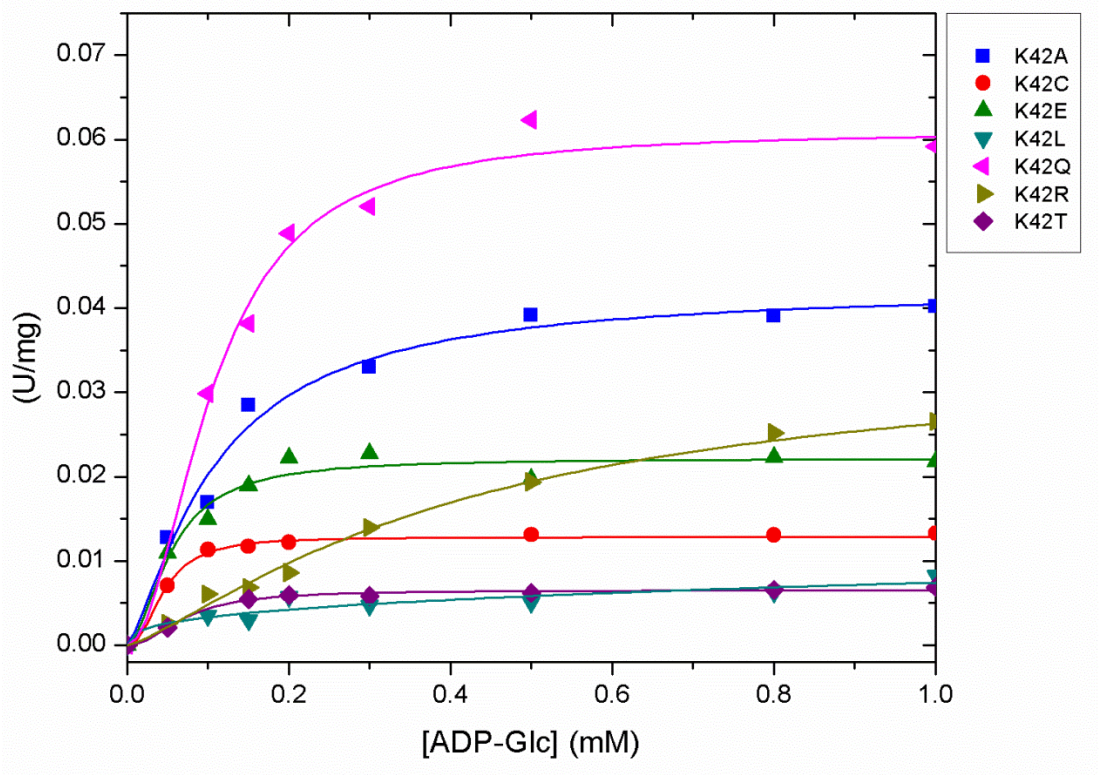

Figure 20. ADP-Glc Substrate Saturation Curves Lys42 Mutants in the pyrophosphorolysis direction.

The position of Lys42 in our *E. coli* ADP-Glc PPase models is compatible with a catalytic role as it was postulated for Lys95 from *L. major* UDP-Glc PPase.

Site directed mutagenesis and kinetic characterization confirmed the critical role of Lys42. We observed a dramatic decrease of more than three orders of magnitude in k_{cat} and k_{cat}/Km (or the analogous $k_{cat}/S0.5$) for all substrates in all mutants in both the forward (Table 4) and reverse direction (Figures 13-19, Tables 1-3). The effects on the apparent affinities for all substrates were relatively minor. However, there was a noticeable change on the cooperativity for the cofactor. This is explained by an interaction between Lys42 and Asp142, which would indirectly affect the chelation of Mg^{2+}. The effects of some mutations on the allosteric regulators deserve further analysis, but the effects were not 16 comparable to the impact the mutations had on catalysis. With the exception of K42A, all mutations decreased the apparent affinity for FBP, but less than one order of magnitude (Table 2). Interestingly, previous studies showed that there were some secondary effects on FBP affinity when Asp142 and Asp276 were mutated. For instance, there was a 12.8- and 16-fold increase in *A*0.5 for the D276N and D142E mutants, respectively (Frueauf, Ballicora et al. 2001, Bejar, Ballicora et al. 2006). Still, the effect of those site-mutations were mainly on catalysis (up to three to four orders of magnitude) (Frueauf, Ballicora et al. 2001, Bejar, Ballicora et al. 2006). Lys42 is located near Lys39, which is involved in the binding of the activator FBP (Gardiol, Preiss 1990). It is possible that changes at Lys42 site may cause a slight perturbation in the neighboring Lys site, or that Lys42 is at least partially involved in the communication between the

Table 4. k_{cat} and $k_{cat}/S_{0.5}$ for ATP and Glc-1P (substrates) of WT and Lys42 mutant *E.coli* ADP-Glc PPase enzymes, in the synthesis direction.

Enzyme[a]	k_{cat} [b]		**ATP**	**Glc-1P**
		-fold decrease[c]	$k_{cat}/S_{0.5}$	$k_{cat}/S_{0.5}$
	s^{-1}		$s^{-1}mM^{-1}$	$s^{-1}mM^{-1}$
WT	103 ± 11	1	515	3814
K42Q	0.140 ± 0.006	736	0.7	2
K42A	0.098 ± 0.002	1051	0.2	2
K42R	0.053 ± 0.001	1932	0.2	0.9
K42L	0.041 ± 0.002	2512	0.5	0.6
K42C	0.040 ± 0.002	2575	0.3	0.6
K42E	0.032 ± 0.002	3312	0.3	0.7
K42T	0.026 ± 0.002	3962	0.3	0.2

[a] Enzymes were purified to homogeneity and assays were performed at 37 °C as described under "Experimental Procedures."

[b] k_{cat} values were calculated from curves via assays performed in the presence of saturated substrates (ATP and Glc-1P) and activator (FBP). Assays were averaged from three independent experiments.

[c] Fold decrease was calculated using wildtype enzyme activity as a reference.

regulatory and the active site. It has been shown that a major effect of the activator is to affect the affinity for the nucleotide, and that residues involved in that allosteric signal are in the loop Pro103-Arg115. However, we cannot discard a secondary allosteric effect on k_{cat} in which the network of interactions Lys42/Asp142/Mg^{2+}/Asp276 participate (Figure 12).

There are some alternatives about the mechanism by which Lys42 exerts its role. According to previous definitions of potential catalytic roles (Holliday, Mitchell et al. 2009), Lys42 may be either 1) a "stabilizer" that electrostatically stabilizes the formation of negative charge in the products, 2) a "proton shuffler" donating a proton to PPi making it a better leaving group, 3) an "activator" by positioning Asp142 to chelate Mg^{2+}, or a combination of those three. It is clear that the main role of Lys42 is not related to substrate binding, and considering the low k_{cat} of the mutants, it seems to be a catalytic residue falling under any of the above categories (Holliday, Almonacid et al. 2007). Lys42 must be selectively stabilizing the transition state based on the fact that all mutations selectively decreased k_{cat} compared to any other parameters for the substrates in any direction. Comparison with nucleic acid polymerases may provide interesting insights into the specific role of Lys42. It seems there are certain mechanistic similarities between bacterial NDP-sugar PPases and 17 nucleic acid polymerases in spite of their structural differences. In nucleic acid polymerases, a nucleophile (-OH group from a ribose, rather than a phosphorous) attacks the α-phosphorous of a nucleotide triphosphate to release PPi as a product. In addition, NDP-sugar PPases seem to bind two metals as

well (Moretti, Chang et al. 2011), and at least the one that interacts with the α-phosphorous is also surrounded by two critical Asp residues. Recently, it was postulated that a Lys residue in several nucleic acid polymerases serves as a general acid to stabilize the β-phosphorous of NTP to make the product (PPi) a better leaving group (Castro, Smidansky et al. 2009). In agreement, the pH curve for those enzymes shows a sharp decrease around pH ~10. In the *E. coli* ADP-Glc PPase the activity falls around ~9.5 (Preiss, Shen et al. 1966), which is also compatible with a Lys residue with a slightly altered p*K*a. Due to the environment of Lys42, this p*K*a could be different from the expected value in solution (Isom D.G., Castañeda C.A., Cannon BR and García-Moreno B. 2011). Lys42 is surrounded by several non-polar side chains (Leu33, Thr37, Val45, Ile53, and Val277) that would lower the p*K*a of the ε-amino group and enhance the putative acid catalysis. On the other hand, the interaction with Asp142 would have the opposite effect; but, since Asp142 most likely chelates Mg^{2+}, its influence may be dampened (Figure 15). More experiments are needed to confirm whether the catalytic role of Lys42 is a general acid. However, it may not be simple to dissect an individual role for Lys42 since it may be part of a network of interactions that stabilize the transition state. Computational simulations on the *E. coli* ADP-Glc PPase may provide more insights into the specific role of Lys42 in catalysis.

CHAPTER THREE

THE IMPORTANT ROLE OF THE ARG32 RESIDUE AND ANALYSIS OF THE ARG32/LYS42 DOUBLE MUTANTS IN *E.COLI* ADP-GLUCOSE PYROPHOSPHORYLASE

ADP-glucose pyrophosphorylase (ADP-Glc PPase) is the regulatory enzyme of the starch biosynthesis pathway in plants and glycogen in bacteria. It catalyzes the synthesis of the glucosyl donor ADP-glucose. Some of the residues are conserved in the bacterial ADP-Glc PPases, but are not in some plant forms. One of them is Arg32 in the *Escherichia coli* ADP-Glc PPase. To explore the overall role of this residue, we performed site-directed mutagenesis, kinetic, and computational analysis (Molecular Dynamic Simulations). There are notably two conserved residues present in the bacterial ADP-Glc PPase that are not located in all heterotetrameric plant ADP-Glc PPase that may have important roles (Arg32 and Lys42 in *E. coli*) (Ballicora, Iglesias et al. 2003, Ballicora, Iglesias et al. 2004, Ballicora, Erben et al. 2007). Several important residues for substrate binding and catalysis of the bacterial ADP-Glc PPase have been characterized (Ballicora, Iglesias et al. 2003, Ballicora, Iglesias et al. 2004, Gomez-Casati, Igarashi et al. 2001, Bejar, Jin et al. 2006, Frueauf, Ballicora et al. 2001). The specific role of Arg32 has not been investigated despite the evidence of its importance. This residue is highly conserved in the family with the exception of some plant L subunits (some of those may be catalytic deficient (Ballicora, Dubay et al. 2005, Crevillen, Ballicora et al. 2003, Ventriglia, Kuhn et al. 2008)). Arg32 belongs the motif

GXG[T/S]R., which is conserved in the superfamily of sugar-phosphate nucleotidylyl transferases (Blankenfeldt, Asuncion et al. 2000, Brown, Pompeo et al. 1999, Jin, Ballicora et al. 2005, Sivaraman, Sauve et al. 2002, Koropatkin, Cleland et al. 2005, Pelissier, Lesley et al. 2010). On the other hand, Arg32 is not present in the eukaryotic UDP-Glc PPase (Steiner, Lamerz et al. 2007). Previously, replacement of Arg25 (Arg32 in *E. coli*) by Ala in the *Agrobacterium tumefaciens* enzyme highlighted the importance of this residue (Gomez-Casati, Igarashi et al. 2001). However, a systematic study about the role of this residue has not been performed.

Here, our mutagenesis and kinetic studies, modeling, and molecular dynamics explored the crucial role of the Arg32 in *E. coli* ADP-Glc PPase interactions with the ATP and Glc-1P substrates. Results highlight the importance, not only of the charge, but also of the guanidinium group of the Arg32 residue in *E. coli* ADP-Glc PPase. Molecular Dynamics further detail the role of the Arg32 side chain length and guanidinium moiety as it outlines substrate positioning in the WT and mutant *E. coli* ADP-Glc PPase. The previous illustrates the significance of this particular residue in the catalysis of the ADP-Glc PPase from *E. coli*.

Materials

Strataclone™ Blunt PCR cloning kit was purchased from Agilent Technologies, Inc. (Clara, CA). BL21 (DE3) cells were obtained from Novagen. Glc-1P, ATP, AMP, FBP, $MgCl_2$ and inorganic pyrophosphatase were from Sigma. NEB Turbo® Cells, Restriction enzymes, Phusion® DNA polymerase were purchased from New England Bio Labs (Ipswich, MA). The Source 15Q 4.6/100 column was acquired from GE Healthcare Life Sciences.

Site-Directed Mutagenesis

The pETEC plasmid was the template used for site-directed mutagenesis of *E. coli* wild type and mutants. This plasmid is a derivative of pET-24a from Novagen with the coding region of *E .coli* ADP-Glc PPase. Site directed mutagenesis was performed by PCR overlap extension as described before (Kuhn, Figueroa et al. 2010). Oligonucleotides for both Arg32 and Arg32/Lys42 mutants were designed using BioEdit® software (Hall 1999) and purchased from Integrated DNA Technologies (IDT, San Diego) (Tables S3 and S4). Verification of coding regions of the mutated plasmids was confirmed via automated cycle sequencing reactions at the University of Chicago Cancer Research Center.

Expression and Purification of WT and Arg32 Mutant Enzymes

Plasmids were transformed into BL21(DE3) cells for expression. Transformed cells were induced at an OD_{600} of 0.6-0.8 with 0.5 mM isopropyl-β-D-thiogalactoside, followed by an incubation period of 16 hrs at 25ºC. The culture was harvested, centrifuged at 10,000 g for 20 min at 4 °C, and the precipitate was resuspended in *Buffer A* (50 mM Hepes, pH 8.0, 5 mM $MgCl_2$, 0.1 mM EDTA, 10% sucrose). The re-suspended samples were sonicated on ice three times for 30 s, centrifuged at 15,000 g for two 15-min intervals at 4ºC, and the supernatants were collected as crude extracts. Proteins were purified via FPLC using DEAE-Sepharose and Source15Q 4.6/100 PE columns (Figure 23) to homogeneity and verified via SDS-PAGE as described before (Kuhn, Falaschetti et al. 2009) . Next, 1L of a transformed BL21(DE3) cell culture yielded 2–12 mg of desalted purified protein, respectively (Figures 21-22).

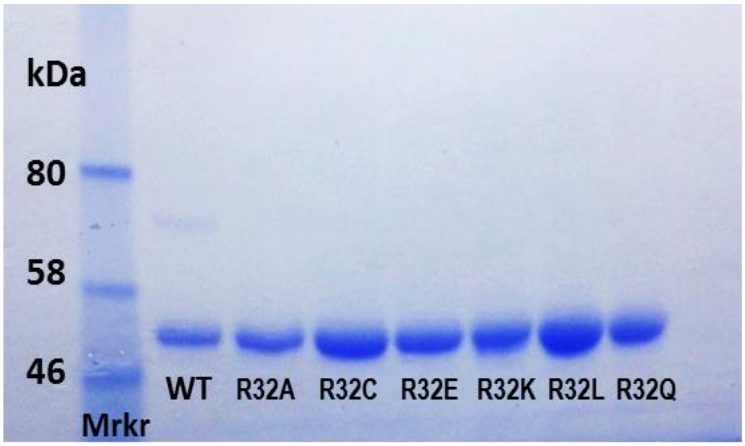

Figure 21. SDS PAGE Verification: WT vs. Arg32 mutants. SDS-PAGE was loaded with 10µL of 1mg/mL for WT, R32A, R32C, R32E, R32K, R32L, and R32Q, respectively, to verify protein purification and samples (50kDa per subunit of the homotetrameric enzyme) for the *E.coli* ADP-Glc PPase WT and mutants with New England Biolabs® protein marker #7708S.

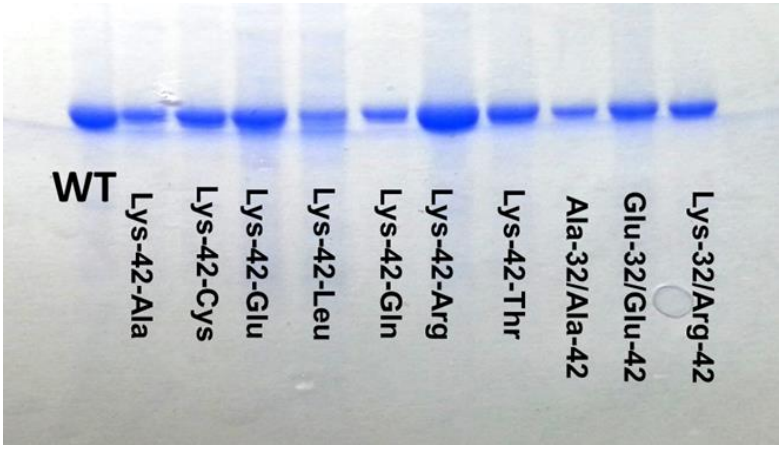

Figures 22. SDS PAGE Verification: WT vs. Arg^{32}/Lys^{42} mutants. All proteins were purified as described in "Methods and Materials".

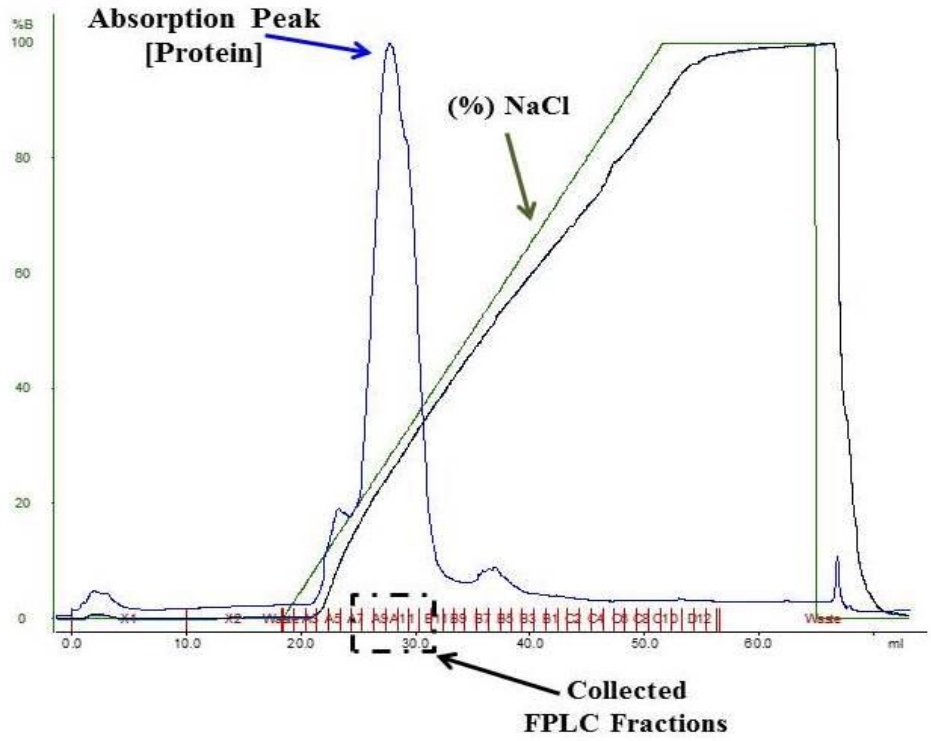

Figure 23. FPLC Purification of WT enzyme via (SourceQ) column. Source15Q (quaternary ammonium; strong anion exchange column) FPLC chromatograph of WT *E.coli* ADP-Glc PPase. All protein samples were eluted from column with Buffer B (1M NaCl elution gradient). Malachite-Green colorimetric assay screening verified collected protein fractions.

Arg32 Mutants Enzyme Assay – Synthesis Direction

To measure the specific activity, as well as other enzyme kinetics, a colorimetric assay was utilized: Malachite Green Assay (Fusari, Demonte et al. 2006). Each kinetic reaction tube contained 50mM HEPES buffer (pH 8.0), 7mM $MgCl_2$, 1mM Glucose-1-Phosphate, 1.5mM ATP, 1mM Fructose-1,6-BisPhosphate, 0.0005 U/µl Pyrophosphatase, 0.2 mg/ml of Bovine Serum Albumin (BSA), and millipore water to 40µl. The reaction tubes (with "premix" reagents) were placed in a 37ºC water bath and reaction begin with the addition of 10µl diluted enzyme. After 10min, the kinetic reaction was stopped with the addition of 400 µl Malachite Green-Ammonium Molybdate-Tween20 solution and MG-Phosphate complex (in reaction tube) stabilized with 34% Sodium Citrate. Measurements of 250µl aliquots (in 96-well microplate) were taken at a λ of 595nm, using the BioTek EL808 microplate reader (Winooski, VT). Absorbance were converted to Activity (nmol/min) and Specific Activity (U/mg) respectively and $S_{0.5}$, $A_{0.5}$ and $I_{0.5}$ (substrate, activator and inhibitor at 50% of maximal velocity) values were calculated after fitting in the Origin versions 7.5 and 8.0 with Hill equations for Glc-1P and ATP ($S_{0.5}$) ($y=Vmax (X^n /K^n +X^n)$ and FBP and AMP Activation and Inhibition curves ($y = Start+ (End – Start) * (X^n /K^n +X^n)$ (Frueauf, Ballicora et al. 2001, Fusari, Demonte et al. 2006).

Enzyme Assay – Pyrophosphorolysis Direction

Kinetic affinity in the reverse direction for both ADP-Glc and PPi substrates was determined using a coupled spectrophotometric assay. The reaction was carried out in 15s intervals for a total of 20min. The reaction mixture consisted of 80 mM HEPPS buffer (pH 8.0), 5 mM $MgCl_2$, 1mM Fructose-1,6-bisphosphate, 1 mM ADP-Glc, 0.6mM NAD^+, 10mM NaF, 0.01 mM Glucose 1,6-bisphosphate, 2 units/ml Phosphoglucomutase, 2 units/ml Glucose-6-phosphate Dehydrogenase, 0.2 mg/ml BSA (bovine serum albumin), and enzyme in a total volume of 0.14 ml. For both the ADP-Glc and PP_i varying assays, the reactions were initiated with the addition of 10µL of $NaPP_i$ (at varying final concentrations from 0-1.4mM $NaPP_i$ in the PPi kinetics; 1.4mM $NaPP_i$ for ADP-Glc kinetics), for a final volume of 0.15mL per reaction well. All Pyrophosphorolysis reactions were performed at 37ºC in a 96-well plate and read at 340nm using a the BioTek EL808 microplate reader (Winooski, VT), which measured the nmols of NADH produced (with 1nmol NADH being the standard as the NAD^+ reactant is reduced to NADH in the presence of the pyrophosphorolysis reaction that forms Glc-1P) via the coupled assay (Frueauf, Ballicora et al. 2001, Kuhn, Falaschetti et al. 2009, Bejar, Ballicora et al. 2004).

Methods for Circular Dichroism Spectra Analysis

Circular Dichroism analysis on wild type and mutant *E. coli* ADP-Glc PPases enzymes (0.33mg/mL) was performed using OLIS DSM 20 Hummingbird (Olis, Inc.) to determine whether a disturbance of the secondary structure of the *E. coli* ADP-Glc PPase

enzyme occurred as a result of PCR site-directed mutagenesis on site-32. A solution containing 5mM $MgCl_2$, 0.1mM EDTA (ethylenediaminetetraaceticacid) and water was utilized to store enzyme during CD analysis. Using a 1cm path length CD spectra data points were measured from 260nm to 200nm at 20ºC and adjusted for any buffer effect. The molar ellipticity (θ) of the samples were calculated using the following equation:

$$\theta = \text{mdeg}*\text{MRW}/ (10*L*C)$$

Where mdeg is the measurement of spectra data points in millidegrees, MRW is the measure of 200kDa over 432 residues for the average molecular weight (g/mol) of each residue of the *E. coli* ADP-Glc PPase protein, C is the concentration of protein (mg/mL) in CD analysis sample measured and L is the 1cm path length of the cell. (Greenfield 2006, Hwang, Hamada et al. 2007, Kelly, Price 2000)

CD Analysis of the *E. coli* ADP-Glc PPase WT and Arg32 Mutant Enzymes

Examination of CD Spectra Data Analysis revealed no marked disturbance in the secondary protein structure for the ADP-Glc PPase mutants (versus that of the WT) were noted.

Computational Methods

Using the crystal structure of the small subunit of the *Solanum tuberosum* ADP-Glc PPase complex with ATP (1YP3) (Jin, Ballicora et al. 2005) and *Agrobacterium tumefaciens* ADP-Glc PPase (3BRK) (Cupp-Vickery, Igarashi et al. 2008) as templates, the first *E. coli* homotetramer model was generated using Modeller (Figures 24a-d) (Sali, Blundell 1993) as described before (Figueroa, Esper et al. 2011). Of the four subunits, only two had ATP,

subunit A and subunit C. Arg32 and corresponding residues in all of the subunits was changed to the following residues: Lys, Ala and Glu. Four structures were generated (WT and mutants) and two Mg^{2+} ions were placed in the active site for all four subunits. The protein, substrates and ions were placed in a TIP3 water box that extended at least 10 Å beyond the protein in all directions and 0.1 M NaCl adjusted to neutralize the charge in the water box. Placement of the substrates, residue mutations, and the generation of the water box were all assembled using the molecular graphics program VMD (Humphrey, Dalke et al. 1996).

Each molecule was brought to equilibrium using the molecular dynamics program NAMD (Phillips, Braun et al. 2005). The equilibration procedure involved energy minimization with and without restraints on the protein coordinates (3000 steps each), slow heating from 10 to 310 K (30,000 steps), pressure and temperate equilibration using a Langevin piston (10,000 steps) and unrestrained dynamics for 100,000 steps before data was acquired. Periodic boundary conditions were used. The cutoffs for non-bonding (van der Waals and electrostatic) interactions were 12 Å. The switch distance was 10 Å, and 1.0 1-4 scaling factor was used. All calculations were done using CHARMM 27 parameters (Mackerell, Feig et al. 2004). Molecular dynamic simulations (10 ns) were created using NAMD for the wild type and the three mutants of each subunit.

A second model of the *E. coli* ADP-Glc PPase was generated by using the crystal structure of the small subunit of the potato tuber ADP-Glc PPase complex with ADP-glucose, 1YP4 (Jin, Ballicora et al. 2005) and 3BRK (Cupp-Vickery, Igarashi et al. 2008) as templates. In this model, one of the four subunits, B, had ADP-Glucose, which was replaced by ATP and

Glc-1 Phosphate. Two other subunits, A and C, contained ADP, which remained in the MD simulations. As earlier, residue 32 and corresponding residues were changed to Lys, Ala, and Glu. The structure was enclosed in a water box and was brought to equilibrium and 10 ns of molecular dynamics were generated. The root mean square deviation (RMSD) plots and root mean square fluctuations were generated using a standard script in VMD (Humphrey, Dalke et al. 1996) .

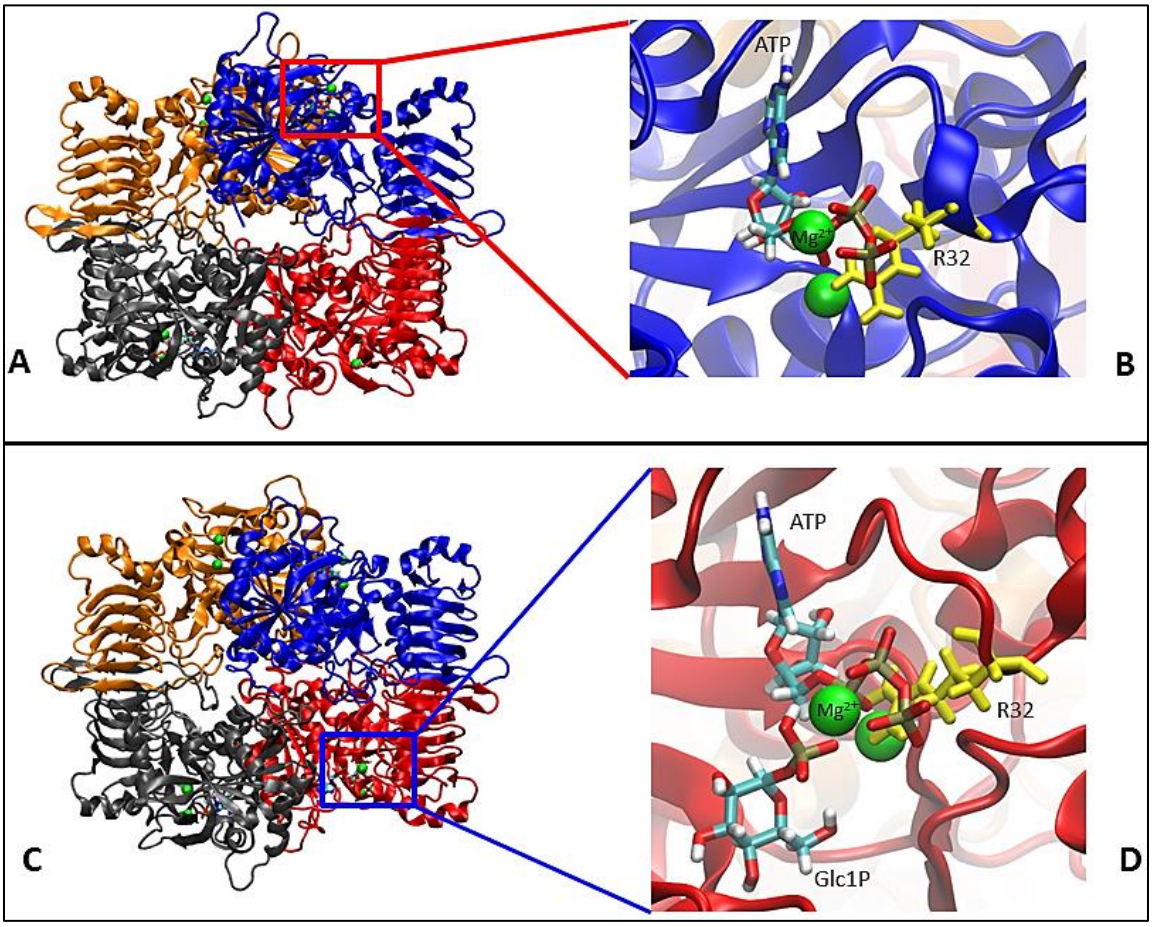

Figure 24. Homology Models of the ADP-Glucose Pyrophosphorylase homotetramer with ATP via VMD simulation. A) Model 1 of the "open" conformation of the *E. coli* ADP-Glucose Pyrophosphorylase homotetramer with ATP. ATP molecules are shown in Subunit A (blue) and C (gray) and two Mg^{2+} ions in each subunit (green). B) Detailed view of the putative active site in subunit A (one of the two subunits that has ATP substrate placed in the predicted active site) of model 1 of ADP-Glucose Pyrophosphorylase with two Mg^{2+} ions (green) and the Arginine residue under investigation highlighted in yellow. C) Model 2 of the ADP-Glucose Pyrophosphorylase homotetramer in the "closed" conformation with ATP and Glc1P substrates in complex. ATP and Glc1P substrates are shown placed in Subunit B (red), ATP molecules in Subunit A (blue) and C (gray) and two Mg^{2+} ions in each subunit (green). D) Detailed view of the putative active site in subunit B of model 2 of ADP-Glucose Pyrophosphorylase with ATP, Glc1P, and two Mg^{2+} ions (green) in complex. The arginine under investigation is highlighted.

Effect of Arg32 and Arg32/Lys42 Mutations on k_{cat} of *E. coli* ADP-Glc PPase

To explore the overall role of Arg32 and evaluate the importance of the guanidinium group, we replaced it with Lysine (R32K, -amino group), Alanine (R32A, - methyl group), Cysteine (R32C, -sulfide group), Glutamate (R32E, - carboxylate group), Glutamine (R32Q, - amide group; neutral; polar) and Leucine (R32L, -hydrophobic side chain) via site directed mutagenesis, and the specific activity was measured. The wild type *E. coli* ADP-Glc PPase had a maximum velocity of 124 (U/mg), whereas the alanine mutant (R32A) lacking the electrostatic capabilities of the guanidinium group displayed a specific activity of 1.56 (U/mg) – an apparent 79-fold decrease in activity. The leucine mutant which contains a bulkier 3-carbon side chain decreased the V_m to 0.65 (U/mg), which was 191-fold lower. The glutamine (R32Q) and glutamate (R32E) mutants provided information about the importance of polarity, being both of similar size but with neutral or opposite charge (negative), respectively. The R32Q mutant displayed a V_m of 1.58 (U/mg), a 78 fold decrease in activity where the R32E mutant had a V_m of 0.038 (U/mg), with the highest decrease in specific activity (3263-fold). The R32C mutant was at the same level of R32A exhibiting a specific activity of 2.14 (U/mg), a 58 fold decrease in activity. The mutant R32K had the highest of activity among the mutants at 10.6 (U/mg) – only a 12-fold decrease – illustrating the importance of the positively charged side chain at residue 32 of the *E. coli* WT ADP-Glc PPase (Figure 25 and Table 6). Lower k_{cat} values were observed for Arg32/Lys42 mutants, with the lowest as R32K/K42R (Figure 26 and Table 13).

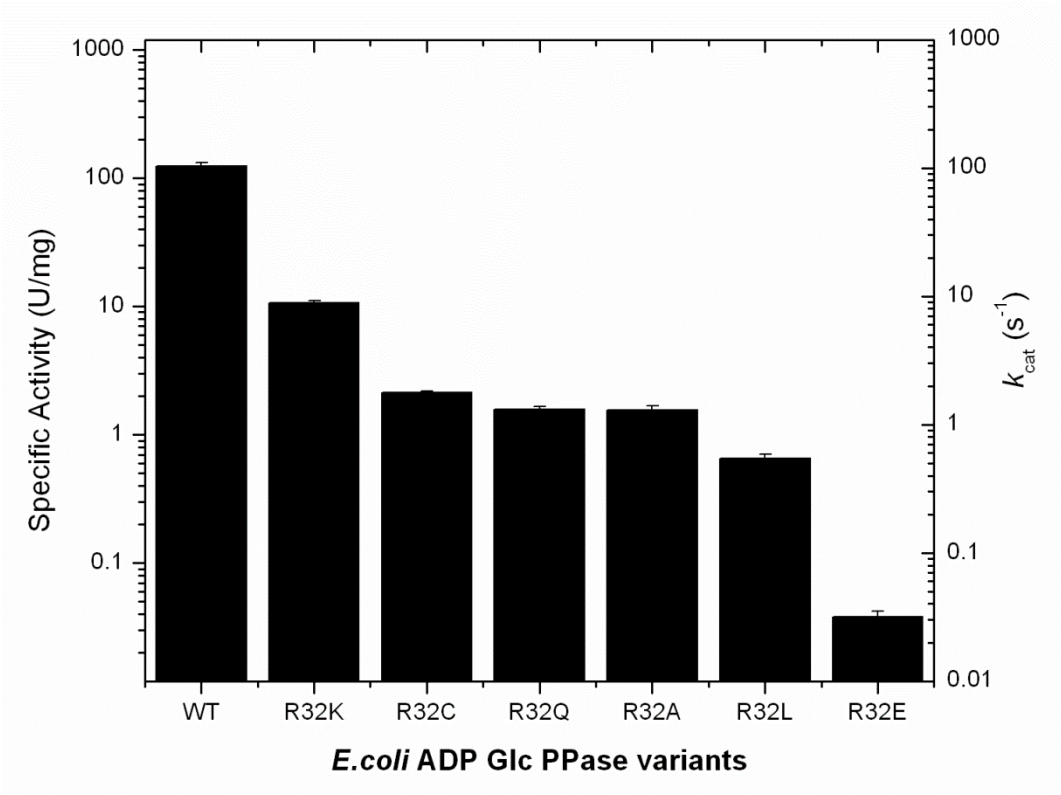

Figure 25. k_{cat} and Specific Activity of *E.coli* WT and mutant ADP-Glc PPases in the synthesis direction.

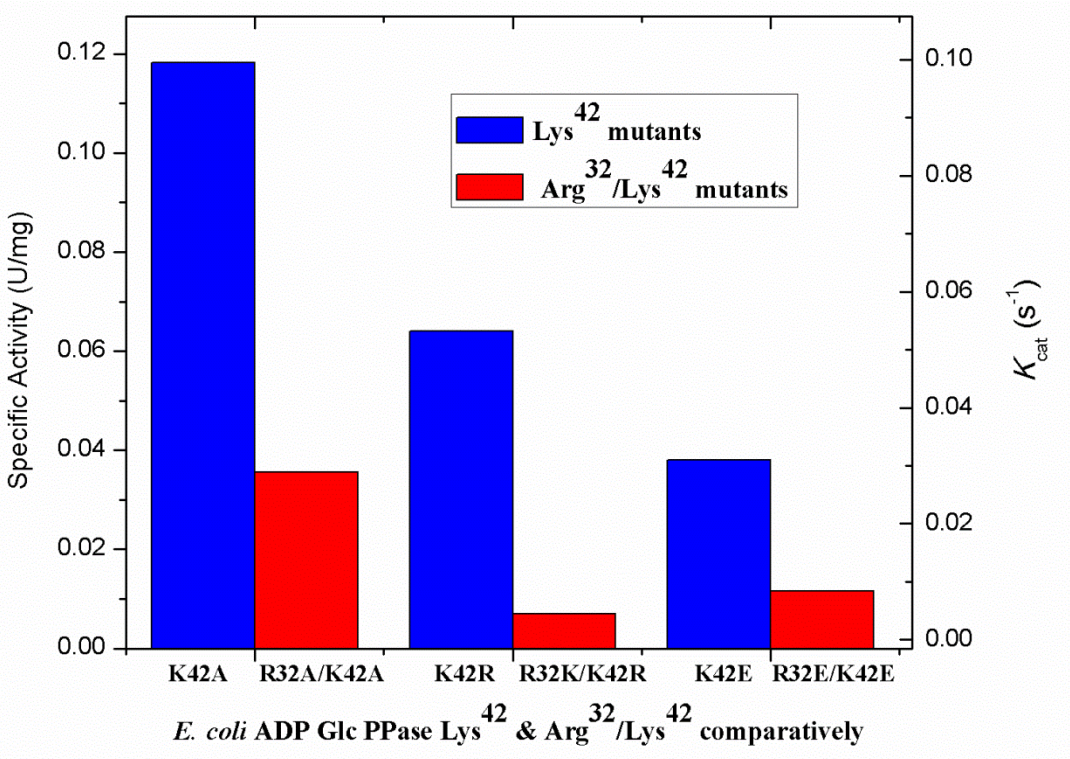

Figure 26. Comparison: Specific Activity and k_{cat} of Lys^{42} and Arg^{32}/Lys^{42} mutant *E.coli* ADP-Glc PPase enzymes. All Arg^{32}/Lys^{42} enzymes were purified to homogeneity and assayed as the WT and Lys^{42} mutants, as described under "Experimental Procedures." Similarly, the Specific Activity (U/mg) and k_{cat} (s^{-1}) values were determined in the presence of saturated conditions of substrates (ATP and Glc-1P) and activator (FBP), and a mean value calculated from three independent experiments. The Arg^{32}/Lys^{42} mutants were five orders of magnitude lower than the WT and 3 to 10-fold lower activity than their Lys^{42} counterparts (i.e. K42A; 0.118 (U/mg) and R32A/K42A; 0.014 (U/mg), K42R; 0.064 (U/mg) and R32K/K42R; 0.007 (U/mg), K32E; 0.038 (U/mg) and R32E/K42E; 0.012 (U/mg)).

Effect of Arg32 and Arg32/Lys42 Mutations on ATP Kinetics

In the crystal structure of the potato tuber S subunit ADP-Glc PPase, Arg33 (homologous to Arg32 in the *E. coli* enzyme) does not contact ATP (Figure 27) (Sivaraman, Sauve et al. 2002) . However, in the homologous *E. coli* glucose-1-phosphate thymidylyltransferase (Sivaraman, Sauve et al. 2002), the γ-phosphorous of the nucleotide dTTP interacts with Arg13 (Figure 24). In the S subunit potato tuber ADP-Glc PPase, a sulfate ion, is in place of the γ-phosphorous. Consequently, the phosphates of ATP are pointing away from Arg33 and interacting with the backbone of Phe254 and Gly255 near the Glc1P binding site (Phe240 in the *E. coli* enzyme (Bejar, Jin et al. 2006)). Thus, by comparison with structures of other sugar-phosphate nucleotidylyl transferase homologues, it is expected that the ATP γ-phosphorous interacts with Arg32 in the active form of the *E. coli* ADP-Glc PPase. For that reason, to determine the effects of the positively charged Arg32 residue and their interactions with ATP, we performed saturation kinetics on all Arg32 mutants. Fitting the data to a Hill equation we found that the wild type enzyme exhibited an $S_{0.5}$ for ATP of 0.20 mM. We noted that the neutral side chains, R32A and R32L, displayed a $S_{0.5}$ (ATP) of 0.25 mM and 0.23mM, respectively. Despite a slightly higher concentration of ATP substrate was required to reach V_m for the neutral mutants, the difference with the wild type was not significant. In addition, in the sulfide (R32C), the polar amino acids R32Q, and the negatively charged carboxylate R32E mutants, the $S_{0.5}$ (ATP) was 0.38 mM, 0.23 mM and 0.32 mM, respectively. Interestingly, the positively charged mutant, R32K ("amino group" side chain) displayed a $S_{0.5}$ (ATP) of 0.49 mM. Taken all this together, all mutants have only a slightly

lower apparent affinity for the ATP substrate. This suggests that the Arg32 may minimally affect the binding of the enzyme with ATP. A comparative analysis of the Arg32, Lys42 and Arg32/Lys42 mutants in ATP substrate binding illustrates the importance of the residues-32 and -42 in regard to *E. coli* ADP-Glc PPase ATP affinity (Figures 28-30, Figure 31 and Tables 5 and 7).

Effect of Arg32 and Arg32/Lys42 Mutations on the Apparent Affinity for Glc-1P

As Glc-1P is the other substrate that binds second (Haugen, Preiss 1979) after ATP, it is also needed to see the effect of the mutations on this ligand. The WT $S_{0.5}$ (Glc-1P) was 0.027 mM (n_H of 0.86) (Table 5), in good agreement with previous reported data (Hill, Wong et al. 2015). Some of the mutations did not affect significantly the apparent affinity for Glc-1P. For instance, R32K, R32L, and R32E had an $S_{0.5}$ (Glc-1P) of 0.016, 0.051, and 0.025 mM, respectively. On the other hand, R32A, R32C, and R32Q had an $S_{0.5}$ (Glc-1P) of 0.101, 0.292 and 0.370 mM, respectively, which means that the apparent affinity was decreased 3- to 14-fold for these mutants. However, the distance between this Arg32 and the putative Glc-1P site is too long to have a direct effect (Bejar, Jin et al. 2006) . Most likely, since Glc-1P binds after ATP, this is a secondary effect on the interaction with the first substrate (Haugen, Preiss 1979). A comparative analysis (kinetics) of the Arg32 and Arg32/Lys42 mutants in Glc-1P substrate binding was performed. The Arg32/Lys42 mutants had lower activity in the presence of saturated Glc-1P compared to the wild-type enzyme (Figure 32, Tables 5 and 7). Catalytic efficiencies for the ATP and Glc-1P substrates for the Arg32 and Arg32/Lys42 mutants were much lower than that of the wild-type enzyme (Tables 6, 8 and Equation S5).

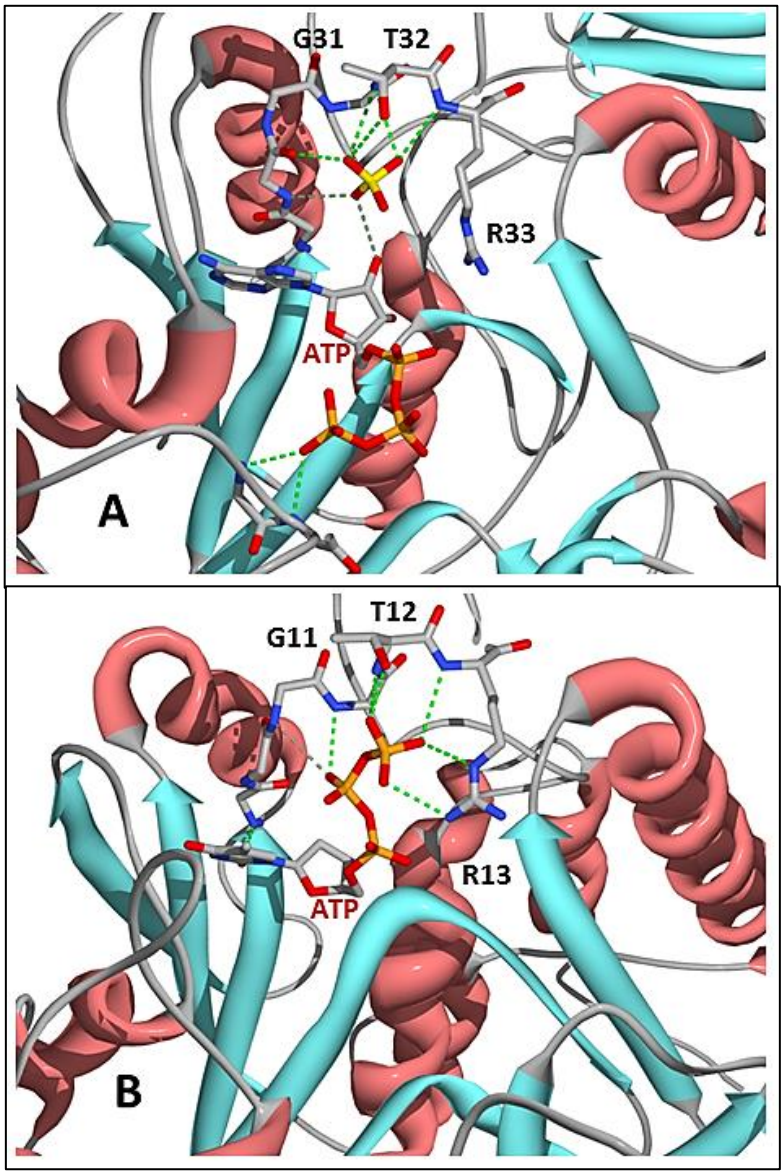

Figure 27. Stu and TDP Homology Models. (A) Subunit A of the potato tuber ADP-Glc PPase crystal structure (PDB code 1YP3). Detailed view of the Arg^{33} residue's (and neighboring residues: Thr^{32} and Gly^{31}) interaction with a sulfate moiety, and not ATP – as sulfate was in abundance during the crystallization process. (B) Subunit A of the E. coli glucose-1-phosphate thymidylyltransferase (RffH). View of the Arg^{13} residue (and the neighboring Thr^{12} and Gly^{11}) as the Arg^{13} interacts with the γ-phosphorous of the ATP substrate in the *E. coli glucose-1-phosphate* thymidylyltransferase. Dashed green lines indicate electrostatic interactions between the atoms of the residues and substrate/sulfate moiety, of both enzymes displayed.

Table 5. Kinetic parameters of wild-type *E.coli* and Arg32 mutant ADP-Glc PPases in the synthesis direction.

	$S_{0.5}$ Glc-1P[b]	n_H	$S_{0.5}$ ATP[b]	n_H	$S_{0.5}$ Mg^{2+}[b]	n_H
Enzyme[a]	*mM*		*mM*		*mM*	
WT	0.027 ± 0.008	0.9	0.20 ± 0.02	1.5	1.88 ± 0.05	4.3
R32K	0.016 ± 0.003	0.5	0.49 ± 0.03	1.7	2.94 ± 0.08	4.1
R32C	0.292 ± 0.047	1.0	0.38 ± 0.09	0.8	2.49 ± 0.13	2.8
R32Q	0.370 ± 0.037	1.5	0.23 ± 0.03	1.1	3.16 ± 0.07	3.3
R32A	0.101 ± 0.028	0.9	0.25 ± 0.02	1.1	2.93 ± 0.09	3.2
R32L	0.051 ± 0.026	0.8	0.23 ± 0.05	0.9	3.37 ± 0.09	3.6
R32E	0.025 ± 0.007	0.7	0.32 ± 0.28	1.0	5.88 ± 0.29	3.6

[a]Enzymes were purified to homogeneity and saturation kinetics for Glc-1P, ATP and Mg^{2+} were performed at 37°C using a Malachite Green colorimetric assay as described under "Experimental Procedures".

[b]$S_{0.5}$ and Hill coefficient numbers (n_H) of Glc-1P, ATP and Mg^{2+} for the WT (*wildtype*) and Arg32 mutant enzymes were determined in the presence of activator (1mM FBP).

Table 6. k_{cat}, $k_{cat}/ S_{0.5}$ for ATP and Glc-1P (substrates) of wild-type *E.coli* WT and Arg32 mutant ADP-Glc PPases in the synthesis direction.

Enzyme[a]	k_{cat}[b]		**ATP**	**Glc-1P**
		-fold decrease[c]	$k_{cat}/ S_{0.5}$	$k_{cat}/ S_{0.5}$
	s^{-1}		$s^{-1}mM^{-1}$	$s^{-1}mM^{-1}$
WT	103 ± 11	1	515	3814
R32K	8.86 ± 0.68	12	18	554
R32C	1.78 ± 0.05	58	5	6
R32Q	1.32 ± 0.09	78	6	4
R32A	1.30 ± 0.16	79	5	13
R32L	0.54 ± 0.10	191	2	10
R32E	0.032 ± 0.003	3219	0.1	1

[a] Enzymes were purified to homogeneity and assays were performed at 37 °C as described under "Experimental Procedures."
[b] k_{cat} values were calculated from curves via assays performed in the presence of saturated substrates (ATP and Glc-1P) and activator (FBP). Assays were averaged from three independent experiments.
[c] Fold decrease was calculated using wildtype enzyme activity as a reference.

Table 7. Kinetic parameters in the synthesis direction for *E.coli* WT and Arg32/Lys42 mutant ADP-Glc PPase enzymes.

Enzyme[a]	**$S_{0.5}$ Glc-1-P**[b]	**n_H**	**$S_{0.5}$ ATP**[b]	**n_H**	**$S_{0.5}$ Mg^{2+}**[b]	**n_H**
	mM		*mM*		*mM*	
wild-type	0.027 ± 0.008	0.9	0.20 ± 0.02	1.5	1.88 ± 0.05	4.3
R32A/K42A	0.080 ± 0.002	2.1	0.10 ± 0.01	1.3	-----	--
R32E/K42E	0.092 ± 0.010	1.2	0.12 ± 0.01	1.2	0.10 ± 0.02	1.0
R32K/K42R	0.042 ± 0.002	1.5	0.12 ± 0.01	1.3	0.18 ± 0.02	2.2

[a]Enzymes were purified to homogeneity and saturation kinetics for Glc-1P, ATP and Mg^{2+} were performed at 37°C using a Malachite Green colorimetric assay as described under "Experimental Procedures".

[b]$S_{0.5}$ and Hill coefficient numbers (n_H) of Glc-1P, ATP and Mg^{2+} for the WT (*wildtype*) and Arg32/Lys42 mutant enzymes, were determined, in the presence of activator (1mM FBP).

Table 8. k_{cat}, k_{cat}/K_m for ATP and Glc-1P (substrates) of WT and Arg32/Lys42 mutant *E. coli* ADP-Glc PPase enzymes, in the synthesis direction.

Enzyme[a]	**K_{cat}**[b]		**ATP**	**Glc-1P**
		-fold decrease[c]	**$k_{cat}/S_{0.5}$**	**$k_{cat}/S_{0.5}$**
	s^{-1}		$s^{-1}mM^{-1}$	$s^{-1}mM^{-1}$
wild-type	103 ± 11	1	515	3814
R32A/K42A	0.030 ± 0.002	3433	0.3	0.4
R32E/K42E	0.0096 ± 0.0003	10729	0.08	0.1
R32K/K42R	0.0058 ± 0.0004	17759	0.05	0.1

[a] Enzymes were purified to homogeneity and assays were performed at 37 °C as described under "Experimental Procedures."
[b] K_{cat} values were calculated from curves via assays performed in the presence of saturated substrates (ATP and Glc-1P) and activator (FBP). In addition, assays were averaged from three independent experiments.
[c] Fold decrease was calculated using WT (***wild-type***) as a reference (with a value of 1).

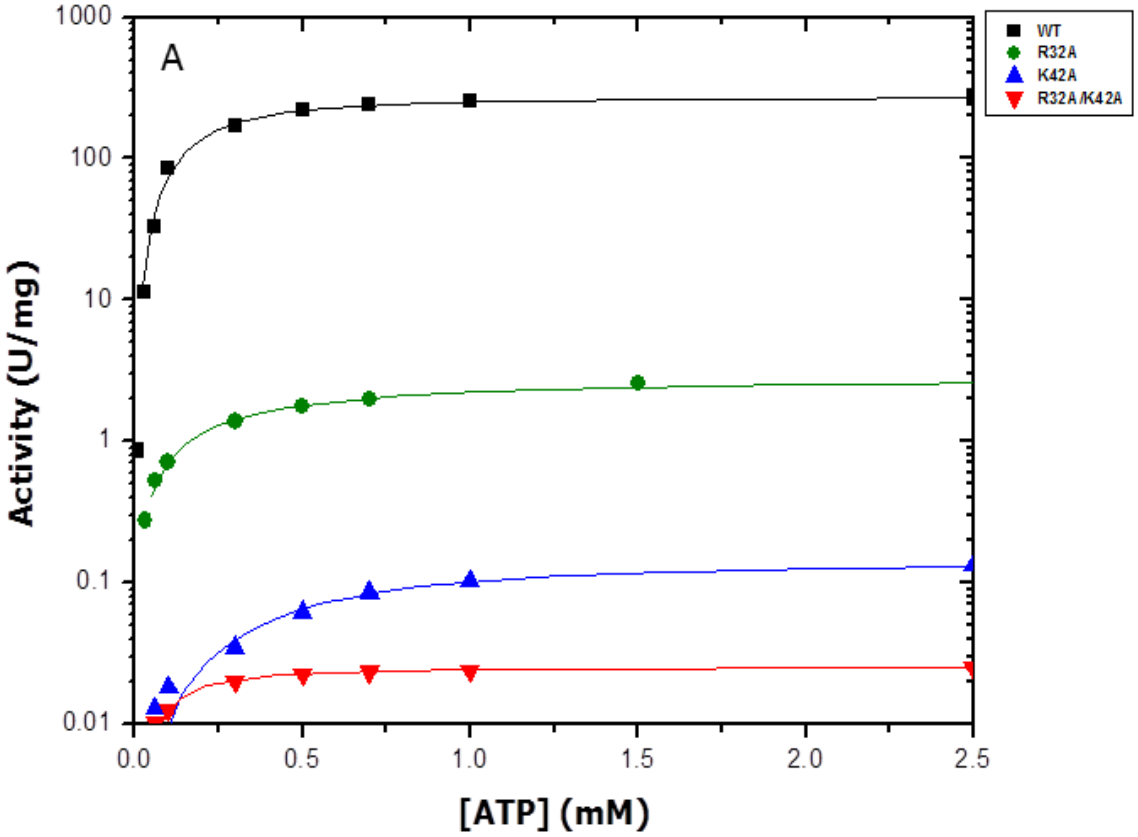

Figure 28. ATP Saturation Curves WT, Arg32, Lys42 and Arg32/Lys42 alanine mutants. Kinetics performed in the presence of 1mM FBP.

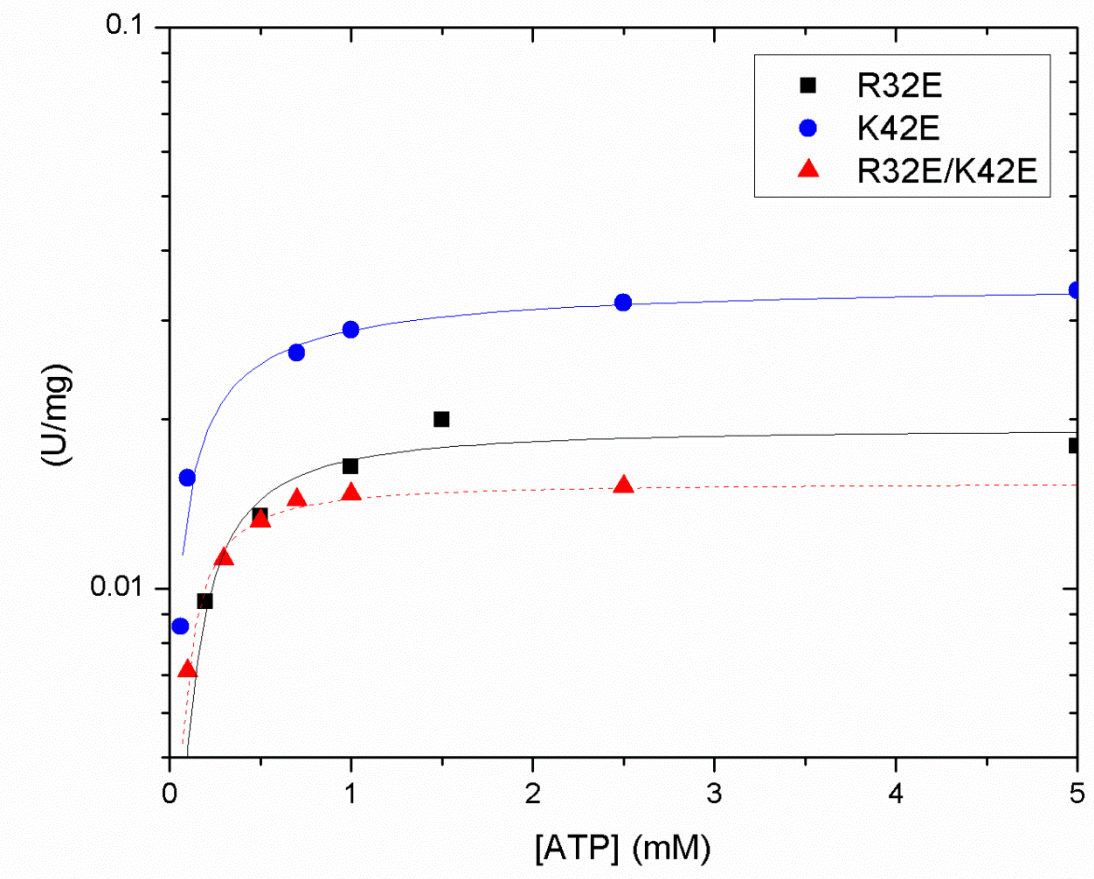

Figure 29. ATP Saturation Curves WT, Arg32, Lys42 and Arg32/Lys42 glutamate mutants. Kinetics performed in the presence of 1mM FBP.

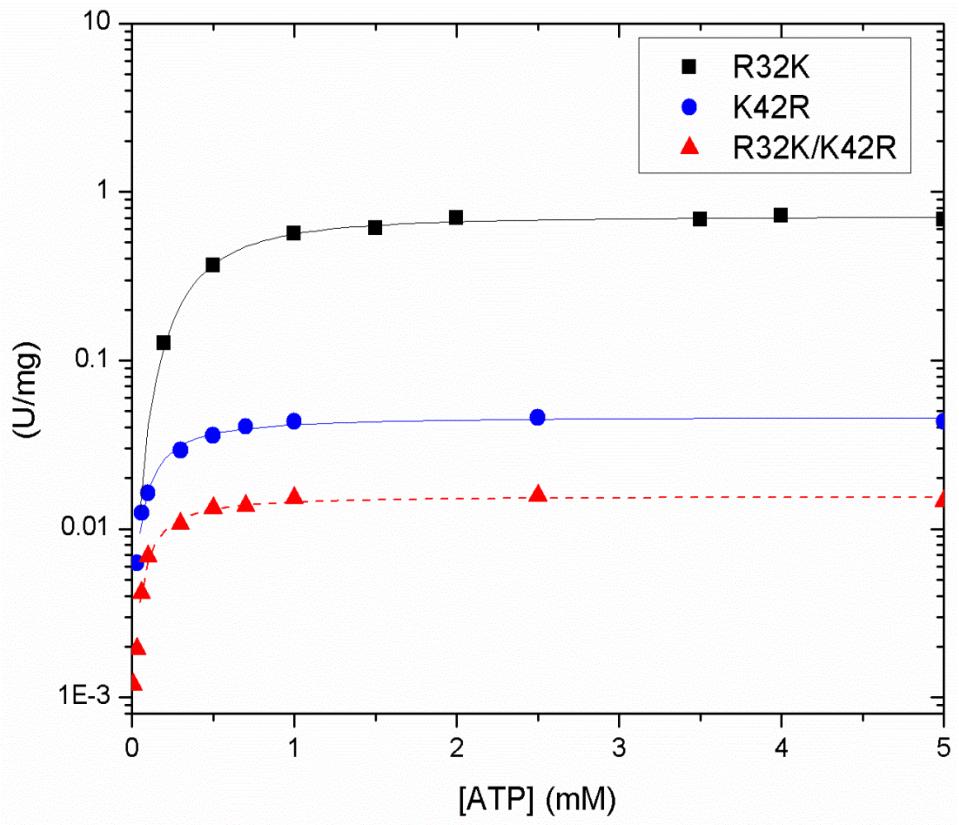

Figure 30. ATP Saturation Curves WT, Arg32, Lys42 and Arg32/Lys42 mutants. Kinetics performed in the presence of 1mM FBP.

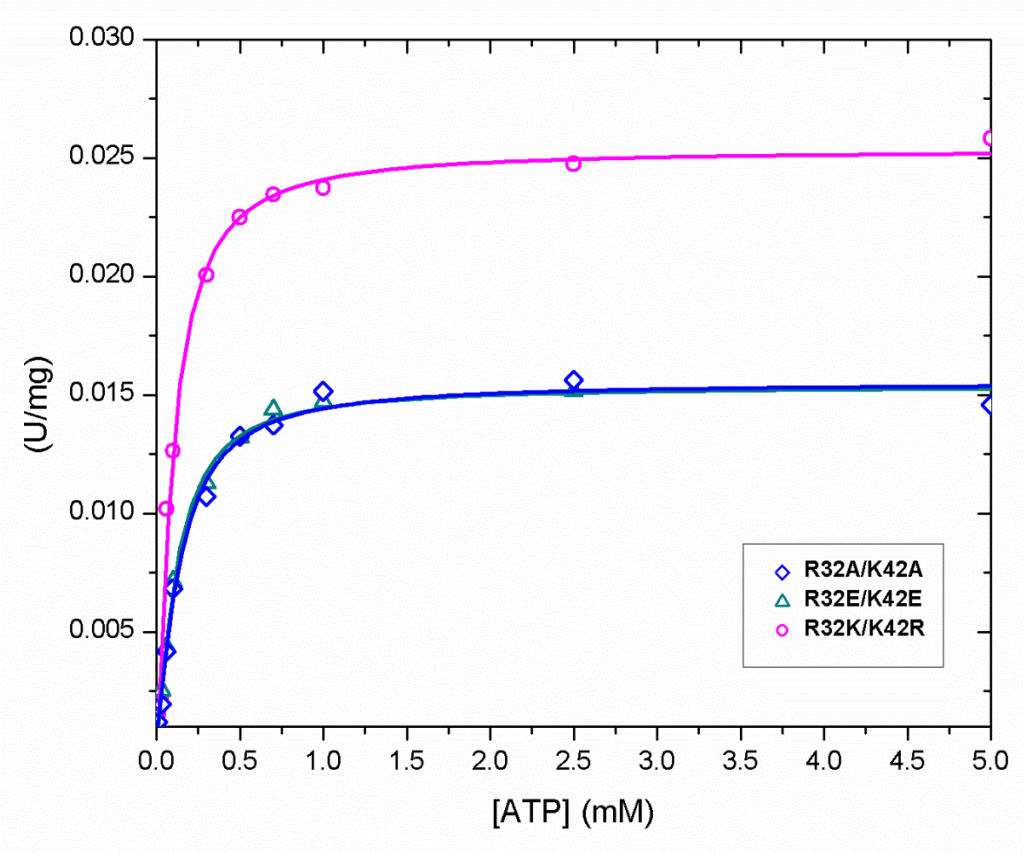

Figure 31. ATP substrate saturated curves for Arg^{32}/Lys^{42} mutant *E.coli* ADP-Glc PPase enzymes. ATP curves were determined at saturated conditions of ATP in the presence of 1mM Glc-1P (substrate) and 1mM FBP (activator). Assays were performed at 37 °C as described under "Experimental Procedures." R32A/K42A (magenta, ○), R32K/K42R (blue, ◇) and R32E/K42E (cyan, △).

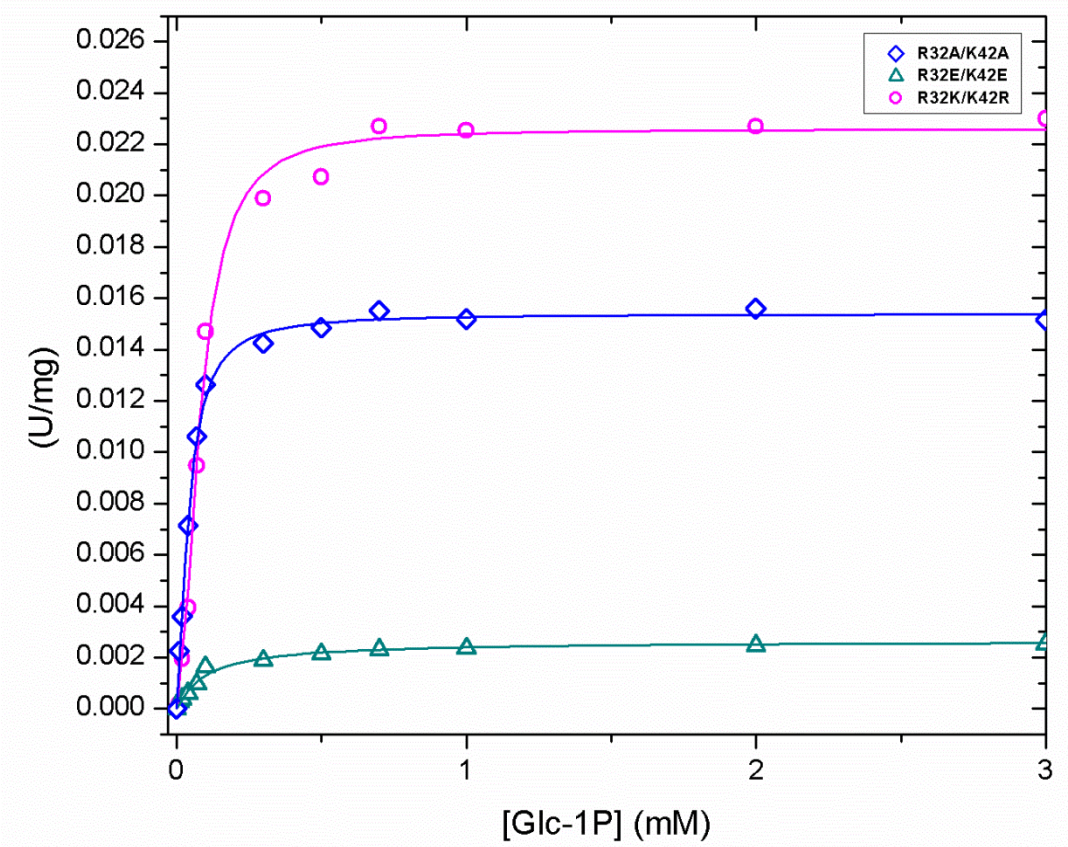

Figure 32. Glc-1P substrate saturated curves for Arg^{32}/Lys^{42} mutant *E.coli* ADP-Glc PPase enzymes. Glc-1P curves were determined at saturated conditions of Glc-1P in the presence of 1.5mM ATP (substrate) and 1mM FBP (activator). Assays were performed at 37 °C as described under "Experimental Procedures." R32A/K42A (magenta,○), R32K/K42R (blue,◇) and R32E/K42E (cyan,△).

Effect of Arg32 and Arg32/Lys42 Mutations on Mg^{2+} Curves

As the *E. coli* ADP-Glc PPase enzyme functions in presence of Mg^{2+} ions, we also explored the effect mutating the Arg32 on this cofactor kinetics. A very slight diversity in the $S_{0.5}$ of the divalent Mg^{2+} was observed for the mutants versus that of the WT ($S_{0.5}$ of 1.88 mM, n_H of 4.3). The effect of site-directed mutagenesis at residue-32 on the apparent affinity of the *E. coli* ADP-Glc PPase enzyme for the divalent ion (Mg^{2+}) was noted as follows (in decreasing affinity, increasing $S_{0.5}$) from the WT (1.88 mM) to the mutants R32C (2.49 mM), R32A (2.93 mM), R32K (2.94 mM), R32Q (3.16 mM), R32L (3.37 mM) and R32E (5.88 mM), respectively. Here also, we see a comparative analysis (kinetics) of the Arg32 and Arg32/Lys42 mutants in Mg^{2+} cofactor binding was performed. Once again here we observe significant change in the Arg32/Lys42 mutants – lower cooperativity (hill coefficients) for the Arg32/Lys42 mutants compared to the wild-type likely due to the Lys42 mutated sites (Tables 5 and 7).

Effect of Arg32 and Arg32/Lys42 Mutations on Enzyme FBP Activation

Considering the low k_{cat} obtained for the mutants, it was needed to check whether the activation of the enzyme was disrupted (Table 6). Saturation kinetics showed that WT and mutant *E. coli* ADP-Glc PPase enzymes were all activated by FBP with a high apparent affinity (Table 9). WT exhibited a 27-fold activation by FBP with an $A_{0.5}$ of 0.049 mM. The alanine (R32A), cysteine (R32C), glutamine (R32Q) and glutamate (R32E) and mutants were observed to have varying rates of activation with FBP at 4, 17, 25, 40-fold activation, respectively. Additionally, these mutants exhibited an $A_{0.5}$ of 0.077 mM (R32A), 0.084 mM

(R32E), 0.118 mM (R32Q), and 0.125 mM (R32C), respectively, in decreasing order of affinity for the FBP activator. The R32K mutant exhibited a slightly higher $A_{0.5}$ for FBP (0.074 mM) and R32L a slightly lower (0.023 mM). The similarities of FBP activation in all mutants compared to WT gives credence to the integrity of the structural complex of the mutants. In addition, this also means that Arg32 may not participate in the allosteric activation by FBP. Similar kinetic responses were also seen for the Arg32/Lys42 mutants for FBP affinity, with a lower Vmax values at saturated FBP (Figure 33 and Table10).

Effect of Arg32 and Arg32/Lys42 Mutations on AMP Enzyme Inhibition

The apparent affinity for AMP of all the mutants were within range of 3-fold to 8-fold (R32E) higher than that of the WT (excluding the R32Q mutant). WT displayed a 15-fold inhibition by AMP with an $I_{0.5}$ of 0.072 mM. (Table 11). To note, R32K exhibited a similar inhibition in the presence of AMP ($I_{0.5}$ of 0.027mM) – but one of the highest rate of inhibition at 26-fold inhibition – with R32E exhibiting an $I_{0.5}$ of 0.009 mM at 30-fold inhibition. As with R32K, the R32E displays a higher fold inhibition at less than 1% remaining activity in the presence of saturated AMP ($I_{0.5}$ of 0.022 mM). Other mutants were inhibited on the same order of magnitude as WT – and very similarly - by AMP: R32L ($I_{0.5}$ of 0.019 mM; 6-fold inhibition), R32A with an affinity for AMP close to that of the lysine mutant exhibited a $I_{0.5}$ of 0.025mM (with 3-fold inhibition) and R32C ($I_{0.5}$ of 0.022 mM; 5-fold inhibition). Arg32/Lys42 mutants, although exhibiting very little to no activity, were all inhibited by AMP (Table 12) – residues-32 and -42 do not affect FBP and AMP binding.

Table 9. Kinetic parameters of *E. coli* WT and mutant ADP-Glc PPases Activator ($A_{0.5}$).

	$A_{0.5}$ FBP[b]	**n_H**	**V_m**[c]	**Activation* (V_m/V_o)**
Enzyme[a]	*mM*		*s^{-1}*	*-fold*
WT	0.049 ± 0.008	1.1	192 ± 8	27
R32K	0.074 ± 0.032	0.9	10.1 ± 0.52	5
R32C	0.125 ± 0.009	1.7	2.45 ± 0.06	17
R32Q	0.118 ± 0.080	0.7	1.55 ± 0.23	25
R32A	0.077 ± 0.046	0.9	1.53 ± 0.11	4
R32L	0.023 ± 0.006	1.8	0.57 ± 0.02	> 49
R32E	0.084 ± 0.023	1.0	0.032 ± 0.002	> 40

[a]Enzyme activation assays were performed as described under "Experimental Procedures", for the WT (*wildtype*) and Arg32 mutants."
[b]The average $A_{0.5}$ values for the FBP activator were determined from quadruplicates then averaged with ± standard deviation and are shown for wild-type *E. coli* ADP-Glc PPase and Arg32 mutants.
[c]Wild-type and mutant *E. coli* ADP-Glc PPase WT and mutant enzymes *V*max (k_{cat}) was determined in the presence of saturated conditions of activator (FBP).

*V_0 is the activity of the enzyme in absence of the activator (FBP).

Table 10. Apparent affinity for the FBP activator in the synthesis direction for the wild type and Arg32/Lys42 mutant ADP-Glc PPase enzymes – Activator ($A_{0.5}$).

Enzyme[a]	**$A_{0.5}$ FBP**[b]	**n_H**	**V_m**[c]	**Activation* (V_m/V_o)**
	mM		*s^{-1}*	*-fold*
wild-type	0.049 ± 0.008	1.1	192 ± 8	27
R32A/K42A	0.106 ± 0.044	1.2	0.0081 ± 0.0007	5
R32E/K42E	0.069 ± 0.019	1.0	0.0085 ± 0.0003	>102
R32K/K42R	0.110 ± 0.043	1.1	0.0062 ± 0.0004	6

[a]Enzyme activation assays were performed as described under "Experimental Procedures", for the WT (*wildtype*) and Arg32/Lys42 mutants."
[b]The average $A_{0.5}$ values for the FBP activator were determined from quadruplicates then averaged with ± standard deviation and are shown for wild-type *E. coli* ADP-Glc PPase and Arg32/Lys42 mutants.
[c]Wild-type and mutant *E. coli* ADP-Glc PPase WT and mutant enzymes *V*max (k_{cat}) was determined in the presence of saturated conditions of activator (FBP).

*V_0 is the activity of the enzyme in absence of the activator (FBP).

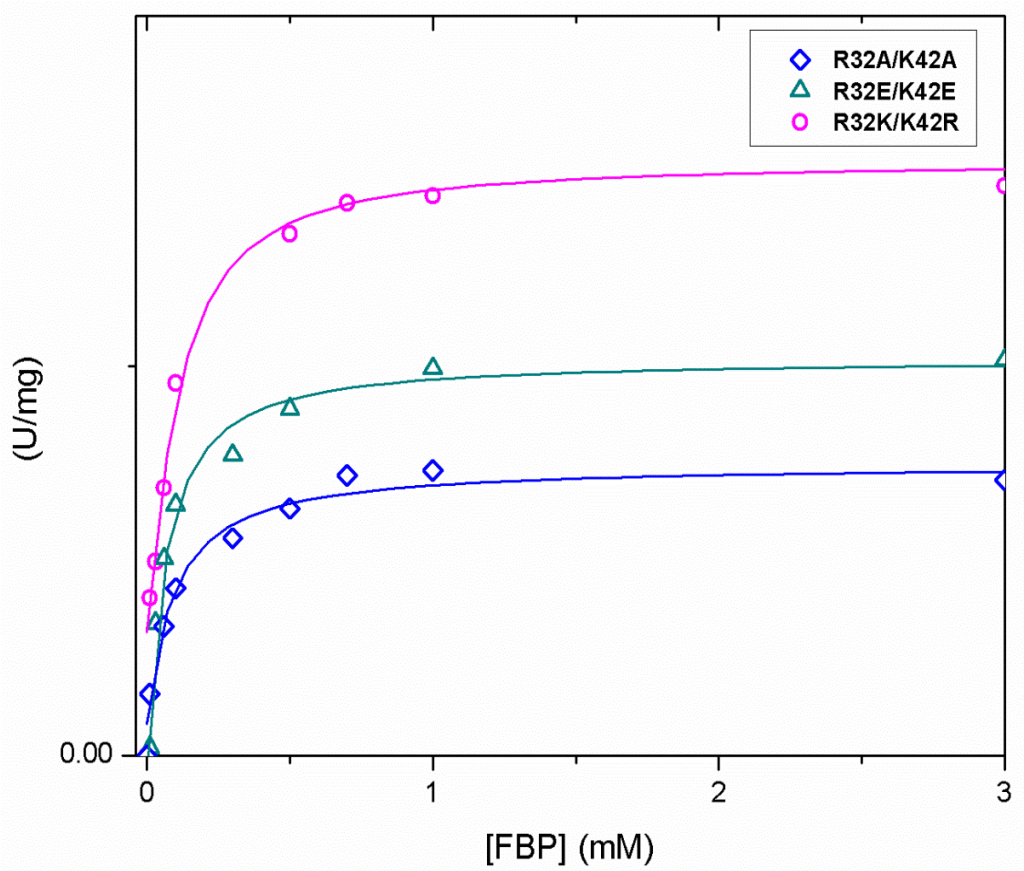

Figure 33. FBP substrate saturated curves Lys^{42} and Arg^{32}/Lys^{42} mutant *E.coli* ADP-Glc PPase enzymes. FBP curves were determined at saturated conditions of Fructose-1,6-bisphosphate in the presence of 1.5mM ATP and 1mM Glc-1P substrates. Assays were performed at 37 °C as described under "Experimental Procedures." R32A/K42A (magenta, ○), R32K/K42R (blue, ◇) and R32E/K42E (cyan, △).

Table 11. Kinetic parameters of *E.coli* WT and mutant ADP-Glc PPases Inhibitor ($I_{0.5}$).

	$I_{0.5}$ AMP[b]	**n_H**	**Remaining activity**[c] **(V_∞/V_o)**
Enzyme[a]	*mM*		
WT	0.072 ± 0.014	1.1	0.07
R32K	0.027 ± 0.008	0.7	0.04
R32C	0.022 ± 0.003	1.2	0.20
R32Q	0.100 ± 0.009	1.8	<0.01
R32A	0.025 ± 0.007	1.2	0.33
R32L	0.019 ± 0.006	0.6	0.17
R32E	0.009 ± 0.0005	1.8	0.03

[a]Enzyme inhibition assays were performed in the presence of 1mM FBP (allosteric activator), and as detailed in "Experimental Procedures", for both WT (*wildtype*) and Arg32 mutants."

[b]The average $I_{0.5}$ values for AMP were determined from a series of four independent experiments performed in quadruplicate trials.

[c]Remaining Activity was the ratio between the activity at saturating and zero concentrations of inhibition, respectively (V_∞ and V_o). V_∞ is deduced from the non-linear regression fitting of the data.

Table 12. Kinetic parameters of wild-type *E.coli* and Arg32/Lys42 mutant ADP-Glc PPases Inhibitor ($I_{0.5}$).

Enzyme[a]	**$I_{0.5}$ AMP**[b]	**n_H**	**Remaining activity**[c] **(V_∞/V_o)**
	mM		
wild-type	0.072 ± 0.014	1.1	0.07
R32A/K42A	0.301 ± 0.083	1.3	0.21
R32E/K42E	0.339 ± 0.025	1.8	0.29
R32K/K42R	0.045 ± 0.008	1.8	0.38

[a]Enzyme inhibition assays were performed in the presence of 1mM FBP (allosteric activator), and as detailed in "Experimental Procedures", for both WT (*wildtype*) and Arg32/Lys42 mutants."

[b]The average $I_{0.5}$ values for AMP were determined from a series of four independent experiments performed in quadruplicate trials.

[c]Remaining Activity was the ratio between the activity at saturating and zero concentrations of inhibition, respectively (V_∞ and V_o). V_∞ is deduced from the non-linear regression fitting of the data.

Pyrophosphorolysis of *E. coli* ADP-Glc PPase WT vs. Arg32 Mutant Enzymes

The ADP-Glc PPase reaction has been noted to be reversible *in vitro*. We measured the apparent affinities for the pyrophosphorolysis substrates (ADP-Glc and PP_i). R32K (amine), R32A (methyl), and R32E (carboxylate) mutants were chosen to explore the critical role in Arg32 plays in catalytic efficiency and activity of the wild-type *E.coli* ADP-Glc PPase enzyme. The calculated catalytic efficiency (k_{cat}/K_m) of the WT was 302 mM^{-1} s^{-1}. We noted a 142, 774 and 1776 fold decrease for the selected mutants (R32K, R32A and R32E) at 2.12, 0.39, and 0.17 mM^{-1} s^{-1}, respectively. There was a disparity in the apparent affinities for the PP_i substrate for both the mutants and wild type with R32K and R32A having a 4- to 9-fold decrease in comparison to that of the WT (0.20 mM) (Table 13). Similar affinities were noted for the ADP-Glc assay (in the presence of 1.4 mM PP_i) for the R32K (0.23 mM) and R32E (0.19 mM) mutants to that of the wild-type enzyme (0.16 mM) (Figure 34 and Table 13). However, the R32A mutant displayed a 2 fold decrease in affinity for the ADP-Glc substrate at 0.40 mM. Overall, a 2 to 3 order of magnitude decrease in maximum velocity (s^{-1}) for R32K, R32A and R32E mutants were observed in the ADP-Glc substrate pyrophosphorolysis kinetics (Figure 34 and Table 15). Here we notice that in mutating the Arg32 residue there is a decrease in activity in the reverse direction, which highlights the importance of the conserved Arg32 residue in the pyrophosphorolysis direction of the *E. coli* ADP-Glc PPase enzyme. Investigation into the roles of Arg32 and Lys42 in the reverse direction was performed for R32K/K42R; and although substrate affinities did not vary markedly from that of the wildtype, lower Vmax and catalytic efficiency values were observed (Tables 14 and 16).

Table 13. Apparent Affinity of wild-type *E.coli* and mutant ADP-Glc PPases in Pyrophosphorolysis Direction, for PP_i (substrate).

Enzyme[a]	**PP_i (substrate)**		
	K_m	**k_{cat}/K_m** [b]	**Fold Decrease (k_{cat}/K_m [b] WT/ k_{cat}/K_m [b] mutant)**
	mM	s^{-1}/mM^{-1}	*-fold*
WT	0.20 ± 0.02	302 ± 22	1
R32K	1.80 ± 0.72	2.12 ± 0.28	142
R32A	0.77 ± 0.29	0.39 ± 0.07	774
R32E	0.07 ± 0.01	0.17 ± 0.02	1776

[a]WT (*wildtype*) and Arg32 mutant enzymes were purified to homogeneity and pyrophosphorolysis assays were performed in the presence of 1mM ADP-Glc (substrate) and 1mM FBP (activator) at 37 °C and measured at 340nm (to detect NADH produce), as described under "Experimental Procedures."

[b] Catalytic Efficiency was defined by calculating the k_{cat} per K_m (s^{-1}/mM^{-1}) values in the pyrophosphorolysis direction, as recorded in the "Experimental Procedures".

Table 14. Affinity of wild-type *E.coli* and Arg32 mutant ADP-Glc PPases in Pyrophosphorolysis Direction, for PP_i (substrate).

Enzyme[a]	PP_i (substrate)		
	$S_{0.5}$	k_{cat}/K_m [b]	Fold Decrease (k_{cat}/K_m [b] WT/ k_{cat}/K_m [b] mutant)
	mM	s^{-1}/mM^{-1}	*-fold*
wild-type	0.20 ± 0.02	302 ± 22	1
R32K/K42R	0.14 ± 0.01	0.097 ± 0.007	3113

[a]WT (*wildtype*) and R32K/K42R mutant enzymes were purified to homogeneity and pyrophosphorolysis assays were performed in the presence of 1mM ADP-Glc (substrate) and 1mM FBP (activator) at 37 °C and measured at 340nm (to detect NADH produce), as described under "Experimental Procedures."

[b] Catalytic Efficiency was defined by calculating the k_{cat} per K_m (s^{-1}/mM^{-1}) values in the pyrophosphorolysis direction, as recorded in the "Experimental Procedures".

Table 15. Apparent Affinity of wild-type *E.coli* and Arg32 mutant ADP-Glc PPases in Pyrophosphorolysis Direction for ADP-Glc (substrate).

Enzyme [a]	ADP-Glc (substrate)			
	$S_{0.5}$	V_m	Fold Decrease	n_H
	mM	s^{-1}	*-fold*	
WT	0.16 ± 0.02	33 ± 2.3	1	1.6
R32K	0.23 ± 0.05	1.40 ± 0.17	24	1.8
R32A	0.40 ± 0.12	0.18 ± 0.03	183	1.5
R32E	0.19 ± 0.02	0.017 ± 0.008	1941	1.4

[a] WT (*wildtype*) and Arg32 mutant enzymes were purified to homogeneity and pyrophosphorlysis assays were performed in the presence of varying substrate (PP_i) at 37 °C using a spectrophotometric wavelength of 340nm (to detect NADH product synthesized from reduction assay), as described under "Experimental Procedures."

*Concentration of PP_i was held constant at 1.4mM and FBP (activator) at 1mM.

Table 16. Affinity of *E.coli* WT and R32K/K42R mutant ADP-Glc PPases in Pyrophosphorolysis Direction for ADP-Glc (substrate).

Enzyme	ADP-Glc (substrate)			
	$S_{0.5}$	V_m	Fold Decrease	n_H
	mM	s^{-1}	*-fold*	
wild-type	0.16 ± 0.02	33 ± 2.3	1	1.6
R32K/K42R	0.27 ± 0.06	0.018 ± 0.002	1833	1.3

[a] WT (*wildtype*) and Arg32 mutant enzymes were purified to homogeneity and pyrophosphorlysis assays were performed in the presence of varying substrate (PP_i) at 37 °C using a spectrophotometric wavelength of 340nm (to detect NADH product synthesized from reduction assay), as described under "Experimental Procedures."

*Concentration of PP_i was held constant at 1.4mM and FBP (activator) at 1mM.

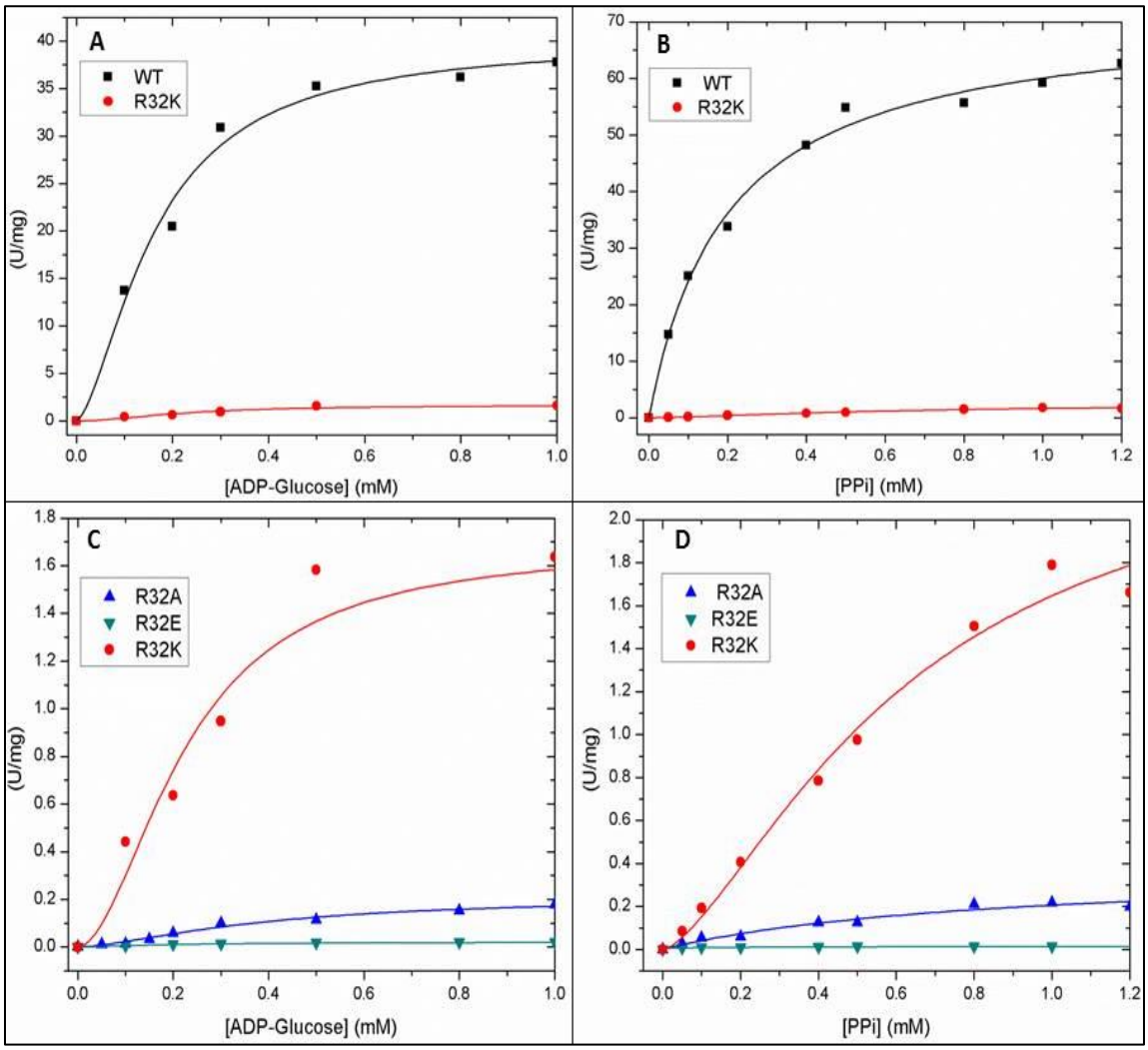

Figure 34. Kinetic Analysis of Arg32 mutants in the Pyrophosphorolysis Direction. (A) Comparative analysis of WT (black ■) and R32K (red ●) for ADP-Glucose substrate affinity. (B) Comparative analysis of WT (black ■) and R32K (red ●) for PP_i substrate affinity. (C) Comparative analysis of R32K (red ●) mutant to R32A (blue ▲) and R32E (cyan ▼) mutants for ADP-Glucose substrate affinity. (D) Comparative analysis of R32K (red ●) mutant to R32A (blue ▲) and R32E (cyan ▼) mutants for PP_i substrate affinity.

Computational Results: MDS (Arg32 Mutants)

RMSD plots of the protein and individual substrates were generated for both models and all mutants after alignment of the proteins to their respective initial position (frame 0). RMSD measures the average distances between the atoms that are time specific; we can therefore visualize the level of flexibility in the molecule selected with greater values indicating a higher degree of variation between the structures at that time point and the initial structure. Figures 35a-d and Figures 36-37 show the 10ns RMSD plots for the ATP structures in model 1. Figure 38 shows the ATP located in subunit A of model 1 where the Arg32 was mutated. The ATP in the wild type structure stayed consistent with RMSD ranges of 0.2-0.4Å. After 2 ns, the ATP from R32A shows a 1.0Å RMSD difference.

Although this drastic of a change is not seen in the R32K and R32E mutations, around the completion of 5ns, R32K and R32E ATP begin to deviate from the wild type ATP with an RMSD difference of approximately 0.4Å. Figures 33a-b and Figure 35 look at the ATP in subunit C where homologous mutations of the Arg32 were made. The ATP of the wild type structure in subunit C also stayed uniform with RMSD ranges around 0.5Å, but the mutated structures showed an increase in ATP flexibility with RMSD values of 0.8 Å or higher after 4ns. The consistency of the wild type ATP structures in subunit A (Figures 33a-b and Figure 34) and C of model 1 shows that ATP is constrained due to the critical arginine (Figures 33c-d and Figure 35). Replacement of Arg32 allows for an increase in mobility and flexibility of the ATP substrate. The same trend is not evidence in Model 2 that contains both ATP and Glc-1P in the assumed active site.

RMSD plots over time showed the that wild type increased the most in movement and does so in shorter amount of time than the other three mutants. As shown by Figures 33a-d and Table 11, by the end of the 10 ns production however, the wild type and mutant RMSD values of the ATP substrate converge. There is greater mobility in the ATP from the wild type enzyme than the other mutants which is contrary to what was observed in model 1 (Figures 33-35 and Table 11). A similar trend was also observed in the RMSD plot of Glc-1P from model 2 (Figure 33).

The Critical Role of the Arg32 Residue

To supplement these kinetic findings, we see that Molecular Dynamics illustrates the orientation of the ATP substrate bound to the mutants R32A, R32E and R32K (Figures 32 – 35). Figures 39-40, shows the distribution of ATP (in binding) for WT versus mutants with Lys42 incorporated to display the dihedral angles of substrate movement. These interactions vary in accordance with k_{cat} displayed by the WT and mutants in the ATP substrate assays (Figure 26). The change in the site-32 residue and corresponding side chain dictates a more liberal movement in the ATP substrate as it enters the substrate interaction site of the mutated ADP-Glc PPase; thereby, creating a difficulty for the neighboring Glc-1P substrate to interact with the now displaced ATP substrate to complete the ADP-Glc synthesis reaction (Figure 32). Some Arg32 Mutants (R32A, R32C and R32Q) displayed a 3- to 14-fold lower apparent affinity for the Glc-1P substrate than the WT.

Table 17. RMSF values of ATP substrate in Models 1A and 1C and Model 2.

RMSF Values of ATP (per MDS Model)			
Enzyme[a]	Model 1 (Subunit A)	Model 1 (Subunit C)	Model 2
	Average (Å)[b]	Average (Å)[b]	Average (Å)[b]
WT	0.741 ± 0.121	0.899 ± 0.174	1.032 ± 0.133
R32K	0.890 ± 0.201	1.154 ± 0.268	1.102 ± 0.220
R32A	0.991 ± 0.226	1.484 ± 0.251	0.820 ± 0.146
R32E	1.411 ± 0.247	1.642 ± 0.497	1.048 ± 0.227

[a]The RMSF values, of ATP, are shown for WT and select Arg32 mutant enzymes (R32K, R32A and R32E) for all Models.
[b]An apparent increase in the average RMSF values is observed as the residue 32 is mutated.

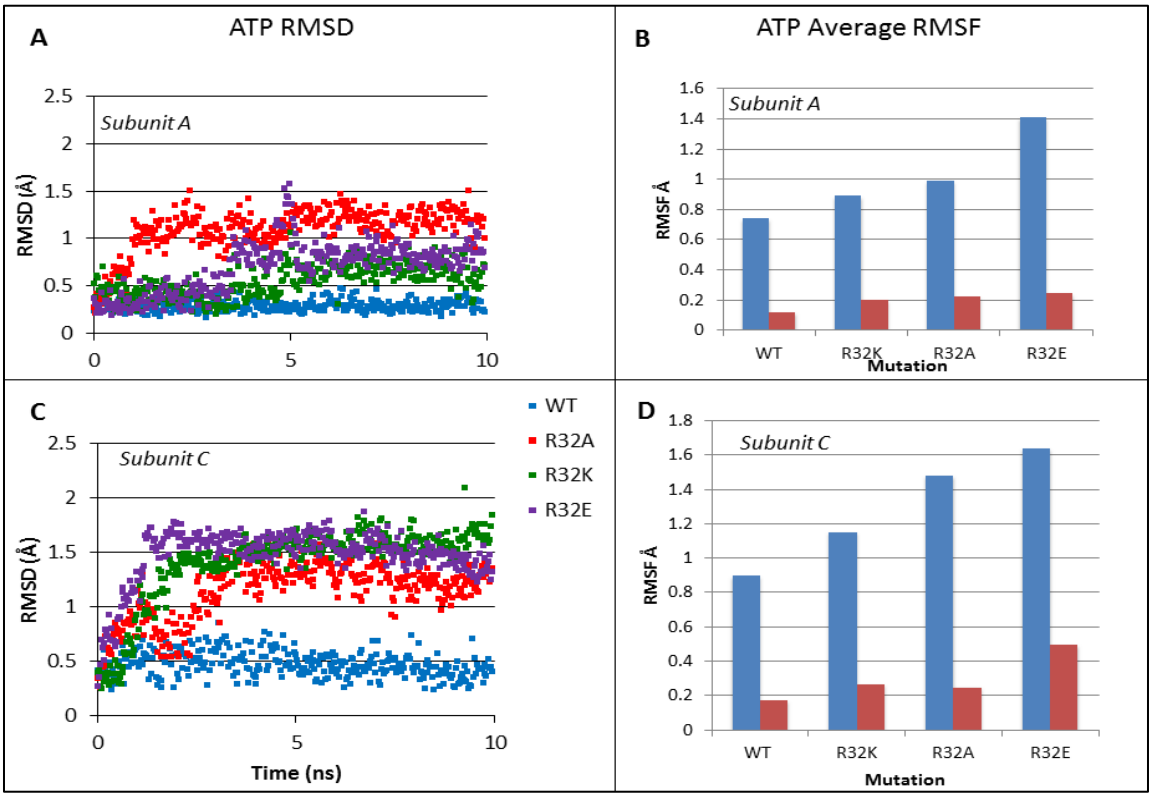

Figure 35. MDS Analysis of Arg32 mutants: ATP (substrate) RMSD and RMSF values. (A) The graph plots the RMSD values of the ATP molecule located in subunit A of the homotetramer of model 1 over the course of the 10ns. The ATP substrate from the native ADP-Glucose Pyrophosphorylase with an arginine at residue 32 stays consistent throughout the simulation. Meanwhile, the mutant enzymes result in a higher root mean square deviation values for the ATP substrate. (B) RMSF values were calculated for the ATP substrate also in subunit A from Model 1. Note the increase in the average RMSF values when residue 32 is mutated. Each nanosecond was condensed to produce 34 frames for a total of 340 frames of the 10ns simulation. (C) The graph plots the RMSD values of the ATP molecule located in subunit C of the homotetramer of Model 1 over the course of the 10ns. The ATP substrate from the native ADP-Glc-Pyrophosphorylase with an arginine at residue 32 stays consistent throughout the simulation. Meanwhile, the mutant enzymes result in a higher root mean square deviation values for the ATP substrate. (D) RMSF values were calculated for the ATP substrate also in subunit C from Model 1. Again note the increase in the average RMSF values when residue 32 is mutated.

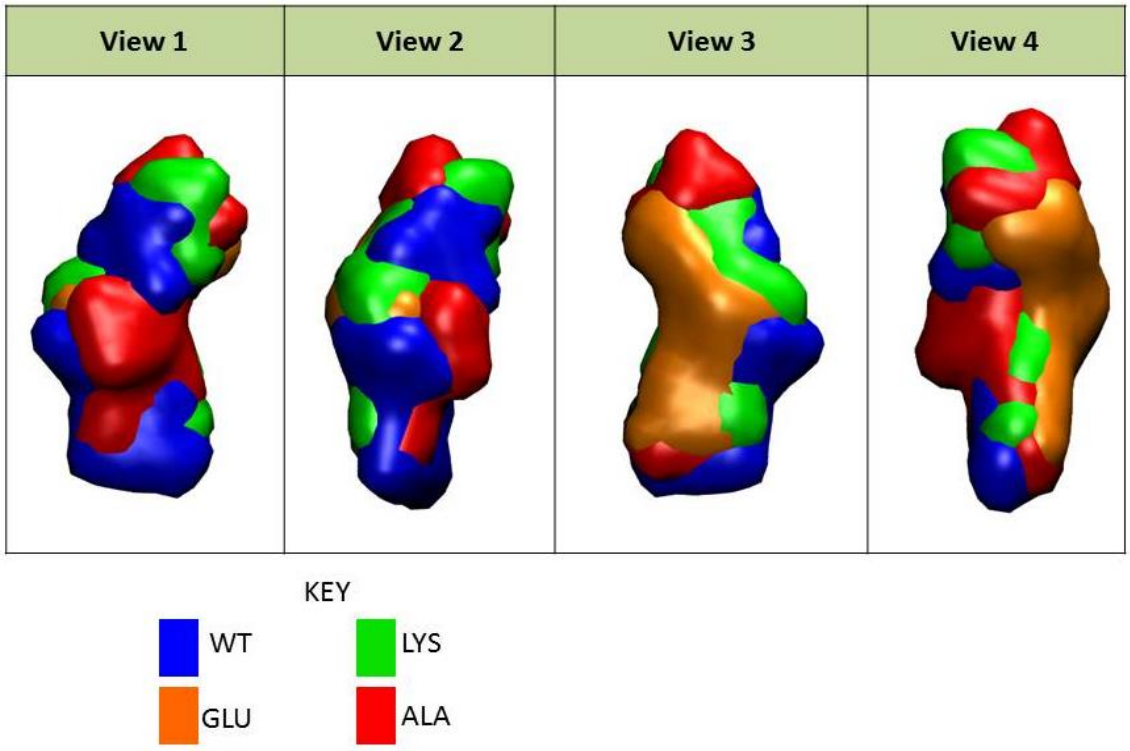

Figure 36. MDS Analysis of Arg32 mutants: Volumetric map of ATP (substrate) in subunit A. After alignment of the protein, the volumetric mapping algorithm was initiated. The blue figure is the total space the ATP in subunit A of the wild type fills over the 10ns.

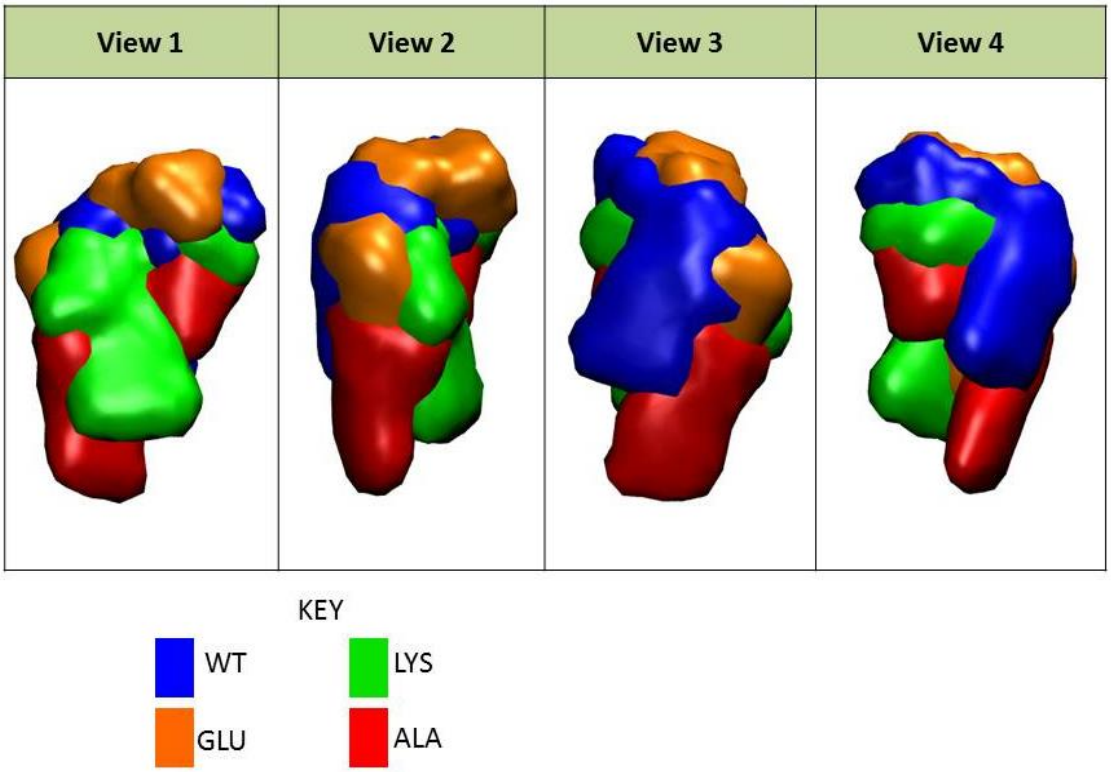

Figure 37. MDS Analysis of Arg32 mutants: Volumetric map of ATP (substrate) in subunit C. After alignment of the protein, the volumetric mapping algorithm was initiated. The blue figure is the total space the ATP in subunit C of the wild type fills over the 10ns.

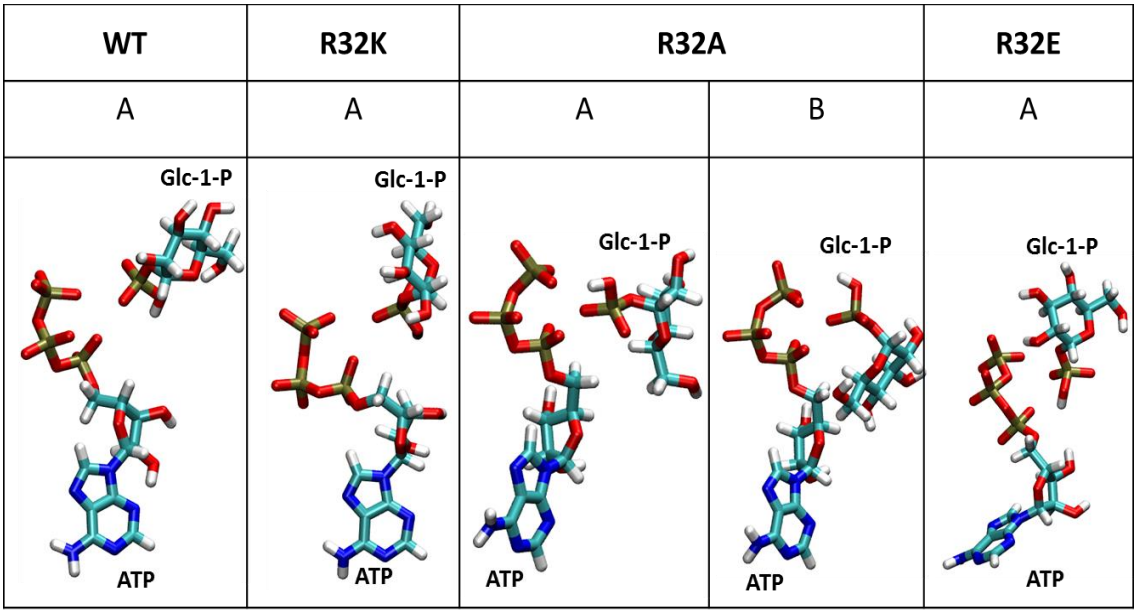

Figure 38. MDS Comparative Analysis of ATP and Glc-1-P substrate orientations: WT to Lysine (Lys), Alanine (Ala) and Glutamate (Glu) Arg32 mutants. A single representation from each of the WT and mutant simulations were pulled and are shown below. (a) Representatives from the ATP from subunit A in Model 1 (b) Representatives from the ATP from subunit C in Model 1. Note the shift in orientation of the γ-phosphorous group of the ATP substrates (black arrows) in reaction with the sidechain of the WT (Arginine-32 residue; guanidinium side chain) versus the mutants. (c) Conformations of the ATP and Glc1P in subunit B of model 2. The R32A mutation resulted in two predominant conformations of the substrates. Each nanosecond was condensed to produce 34 frames for a total of 340 frames of the 10ns simulation.

To elaborate, MDS outlines the function of the Arg32 residue in as the adenosine nucleoside and α-phosphorous group of ATP molecule complexes with the Glc-1P and pulls the terminal γ-phosphorous groups of the ATP making the PP_i a better leaving group. As suspected in kinetics, the Molecular Dynamics further elucidate the disparities in the orientation of the ATP substrate in the catalytic site of the R32A mutant, in the presence of Glc-1P versus that of the WT (Figure 38). Moreover, we find that an intriguing interaction between the R32E mutant and the two Mg^{2+} ions are present, as illustrated during the MDS computation experiments.

The previous data indicates that the mutation at site-32 may indirectly affect the ADP-Glc PPase-Mg^{2+} complex in the presence of the ATP and Glc-1P substrates. Hence, adding a negative charge (R32E) to the active site may slightly disrupt binding of the Mg^{2+}. Here, we find that the Mg^{2+} kinetics further elucidate the vital role of the nitrogen atoms of the guanidinium group of the conserved Arg32 residue and more importantly the critical location of this residue at site-32 in the *E. coli* ADP-Glc PPase. We suspected that the Arg32 residue plays a critical role in the catalysis of the *E. coli* ADP-Glc PPase in ADP-glucose (Ballicora, Iglesias et al. 2003, Ballicora, Iglesias et al. 2004, Ballicora, Erben et al. 2007, Gardiol, Preiss 1990, Preiss 1984). There are conserved two residues present (Arg32 and Lys42, respectively) within the bacterial ADP-Glc PPase enzymes, but not in the Large subunits of the heterotetrameric plant homologues.

Consequently, it has been theorized that due to the presence of these conserved residues (Arg32 and Lys42) the homotetrameric bacterial ADP-Glc PPase enzymes exhibit a more

catalytic role unlike the Large subunit of the heterotetrameric plant ADP-Glc PPase homologues which exhibit a non-catalytic - modulatory – role. To further elaborate, in the Large subunit of the Monocot (cereal) ADP-Glc PPase enzymes the respective residues -32 and -42 are Glu32 and Thr42. In the Large subunit of the Dicot ADP-Glc PPase enzymes the respective residues are Lys32/ His32/Glu32 and Thr42 (Ballicora, Dubay et al. 2005).
To explore this idea, we found that the specific activities of the WT and six (6) *E. coli* ADP-Glc PPase mutants illustrate the key role the positively charged nitrogen atoms in the Arginine guanidinium group of the "slightly branched" side-chain of the EcR32WT ADP-Glc PPase plays in stabilizing the inorganic pyrophosphate (negatively charged) product created from the γ-phosphorous of the ATP substrate, as ADP-Glc is formed. Substitution of this Arg32 residue with negatively charge, hydrophobic, sulfide or non-polar groups significantly affects the activity of the *E. coli* ADP-Glc PPase enzyme. Our results indicate that the guanidinium group of the Arg32 residue may not participate solely in binding or catalysis. Moreover, the results indicate that a positive charge alone from a lysine mutant (k_{cat} 8.86 s^{-1}) is not enough for maximum activity of the enzyme - and indicates the importance of the dual positive charges of the guanidinium group.

Now, we are able to outline a scheme for Arg32 ATP substrate interaction in the production of α-ADP-glucose by making the inorganic pyrophosphate group (of the ATP substrate) a more "suitable" leaving group (Figures 24 and 40). Additionally, disparities of the $S_{0.5}$ (ATP) for that of the WT versus mutants are apparent, but not significant. A higher concentration of ATP is needed in the mutant *E. coli* ADP-Glc PPases. These results illustrate

that the orientation of the ATP and Glc-1P *E. coli* ADP-Glc PPase substrates is stabilized in the WT (arginine residue) and more flexible in the mutants (Figures 34, 35 and 38). In further regard to computational analysis, modeling of the *E. coli* ADP-Glc PPase complements the findings of the ATP saturation curves that two nitrogen atoms of the guanidinium group may interact with the γ-phosphorous of the ATP, positioning the substrate and making the PP_i product a better leaving group (Figures 27, 30-32, 34, 38). Computational Analysis adds to reasoning that the overall rigidity of the molecular structure for site-32 is important in enzyme-ATP substrate interaction for catalysis of the protein. These results also explained why certain subunits in plants, which mostly play a regulatory role rather than catalytic, have this arginine substituted.

In Figure 38, we see that immediately after Glc-1P enters the active site, the ATP tries to get in the correct conformation to react with the Glc-1P. The increased mobility of the ATP in the Arg32 mutants could possibly inhibit the entrance of Glc-1P and halt the reaction. Such liberal movement of the ATP, as seen in the Model 1 for R32A and R32K mutants, illustrates the possibility for the lower activity of these mutants and the higher $S_{0.5}$ (Glc-1P) needed versus that of the WT. As for the R32E mutants, we see in Model 1 that there is a slight rigidity but on the opposing side of the RMSD. The positioning of the *E. coli* ADP-Glc PPase substrates (ATP and Glc-1P) appears to have turned out of proportion to one another, failing to complex and form the necessary ADP-glucose moiety necessary for glycogen synthesis.

This apparent disorientation of the ATP and Glc-1P substrates is also seen in the MD

simulations of the R32A and R32K mutants, at varying degrees. Specific activity kinetics show a marked increase in activity from R32A (1% of WT activity) to nearly 9% (of WT activity) for Lysine (R32K) mutant, representing the crucial role of positive side chain at site-32 in ADP-Glc PPase catalysis. There appears to be a directional "tethering" (positioning) of the γ-ATP-phosphorous to the substrate site by the Arg32 residue, allow the ATP to be properly positioned for attack by the second substrate (Glc1P) in the *E. coli* ADP- Glc PPase, which is exhibited in both the kinetic assays and molecular dynamic simulations. This "tethering" for proper positioning of the ATP substrate by residue-32 is absent in the R32A (alanine mutant) which lacks an elongated positively charged side chain (as the WT and R32K mutant), as such the ATP substrate in absent of a proper "tethering" residue has a more liberal movement - appears to roll around illustrated via MDS- in the substrate site and display a higher $S_{0.5}$ (ATP) (Table 5 and Figures 35-37, 39-40). However, as the lysine mutant (R32K) lacks an elongated side chain with two readily available terminal nitrogen groups (as in R32) to properly position the γ-ATP-phosphorous, there appears to be slightly more liberal movement of the ATP substrate versus that of the WT, and more of a "one handed tethering" than two (as seen with the Arg32 terminal nitrogen groups). R32K has a slightly higher $S_{0.5}$ (ATP) than the WT, but still the highest Specific Activity of the Arg32 mutants (Figure 24).

Furthermore, in opposition of a "tethering", a "repelling" or "pushing" of the γ-phosphorous of the ATP substrate is noted in the glutamate mutant (Figures 35-40). As there are two subunits present in the homotetrameric *E.coli* ADP-Glc PPase enzyme which function to produce the ADP-glucose donor, it is notable that both are affected when expressed with

this site-32 mutation. It was noted that the carboxylate (negative) side chain of the R32E mutant appears to "push" the ATP substrate, via repelling of the γ-ATP-phosphorous, toward the opposite side of the active site – both in Subunit A and Subunit C (Figures 35-38). R32E exhibited the lowest Specific Activity (~3300 fold decrease) and higher $S_{0.5}$ (ATP) than of the WT (Figures 25 and Table 6). Double mutants displayed an even lower interaction with the ATP substrate (Figure 26), as Arg32 interacts with the γ-ATP-phosphorous and Lys42 residue with the β-ATP-phosphorous, and by mutating both sites (two residues) we removed the ability of ATP binding for the mutants compared to that of the wildtype (Figure 40).

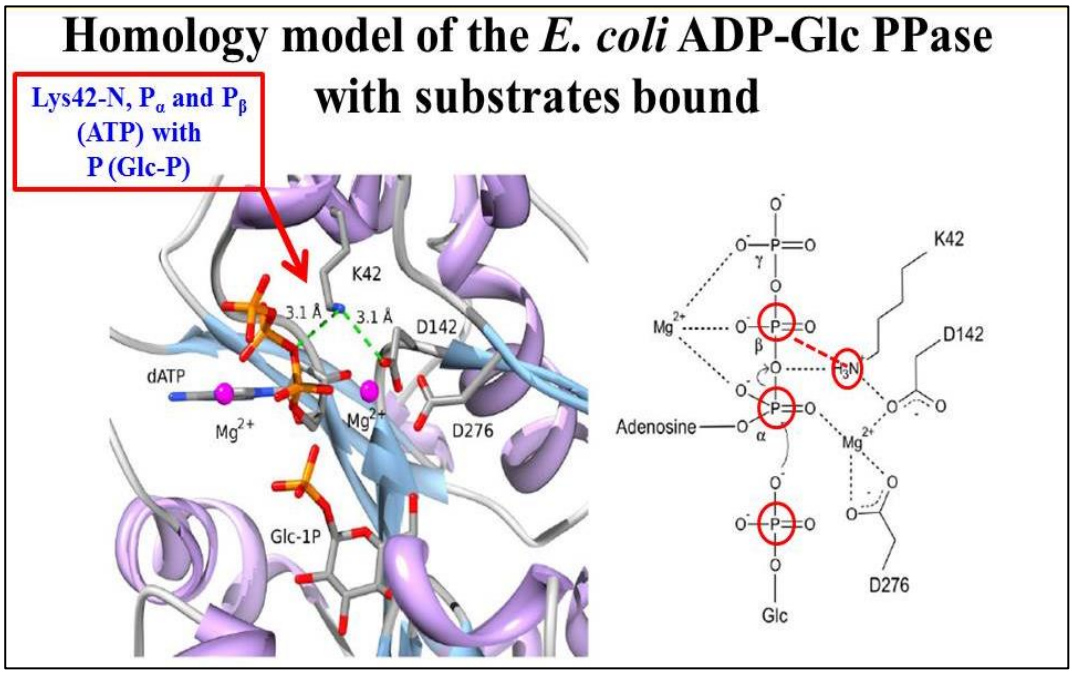

Figure 39. *E.coli* ADP-Glc PPase Lys42 Homology Model and Dihedral Angle Determination (Using 4 points): P_α and P_β (ATP), P (Glc-1P) and N (Lys42).

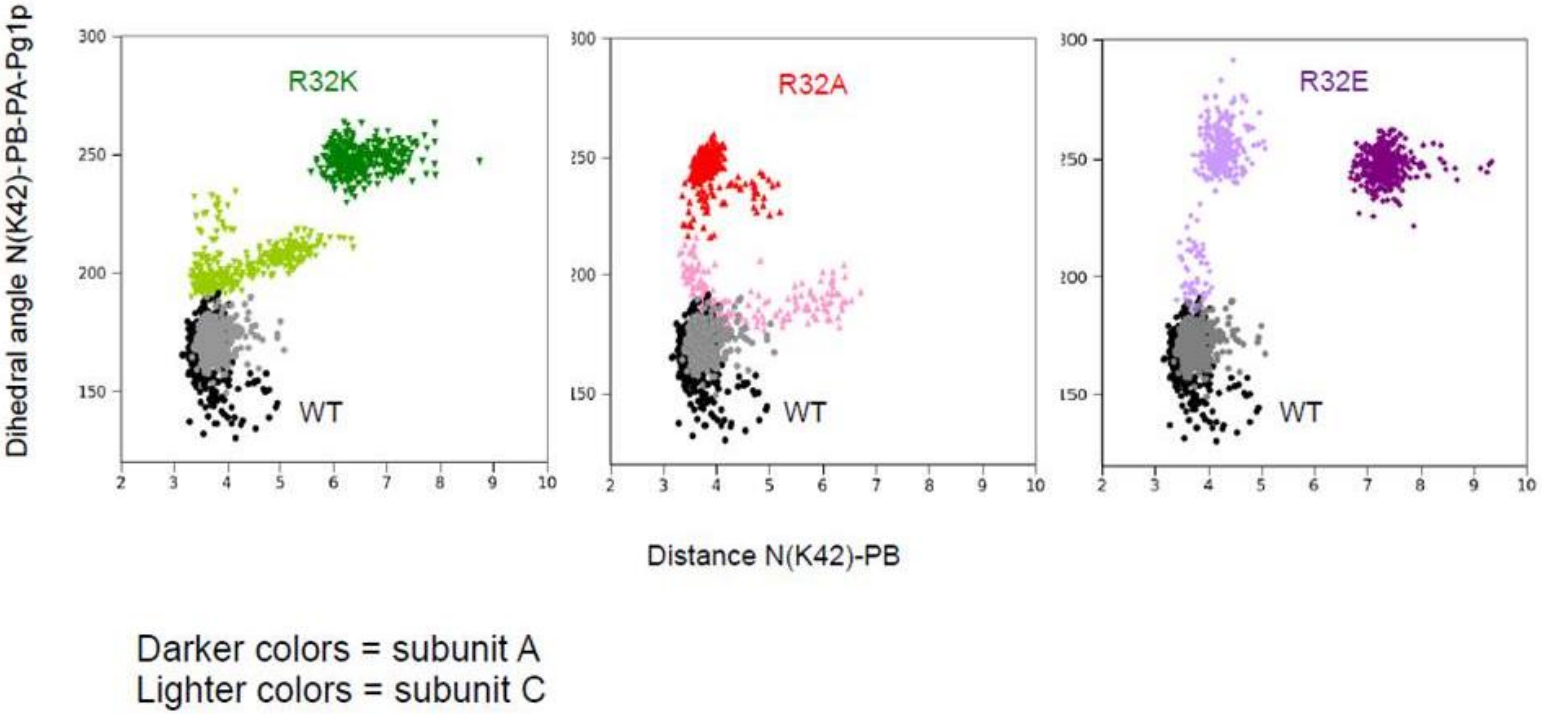

Figure 40. Distribution of different conformers (of the ATP substrate) in the Molecular Dynamic Simulation by distance ("Distance N(K42)-PB") and dihedral angle ("Dihedral angle N(K42)-PB-PA-Pg1p"). Darker colors are from subunit A and lighter colors from subunit B. WT values are included in all three panels for comparison.

As circular dichroism illustrates, the secondary structures of the Arg32 mutants have not been perturbed, in comparison to the WT, so residue side chain (electrostatic interactions and length) play a pertinent role in ATP substrate binding.

Hence, we see both kinetic analyses where the affinity for the ATP substrate dictates the positioning of ATP and molecular dynamic simulated illustration of the importance of the orientation of ATP in the substrate site, as all mutants exhibit a lower specific activity and higher $S_{0.5}$ (ATP) (Figure 26 and Tables 5 and 6). Thus, the critical role of the conserved Arg32 guanidinium side chain in stabilizing the ATP substrate for proper orientation in the substrate site, as the two positively charge nitrogen atoms of the Arg32 residue (6.22 angstroms in length) guanidinium group interacting with the γ-phosphorous of the ATP to create the PP_i leaving group for the production of ADP-glucose in *E. coli* glycogen biosynthesis, is observed.

It is important to note that all catalytic activity (Specific activity and k_{cat} values) of the Arg32 and Arg32/Lys42 mutants was not entirely lost, there is a threshold. In 2007, it was noted that during kinetic analysis the measured misreads of mutant genetic codons by tRNA in the bacterial cell led to a miniscule translation of a wild-type enzyme in mutants. This has been noted in referenced experiments and helps to explain why *E.coli* ADP-Glc PPase mutants cannot be completely inactive - any lower than an approximate 10^3 to 10^4 fold decrease. As such this explains why we did not observe a decrease of lower than 4000-fold in activity for the glutamate mutants (Kramer, Farabaugh 2007).

CHAPTER FOUR

CHEMICAL MODIFICATION APPROACH: ATTEMPTED CHEMICAL RESCUE OF ARG32CYS AND LYS42CYS MUTANTS OF *E. COLI* ADP-Glc PPASE

Previous Arginine Enzyme Residue Chemical Modification Studies

Over two decades ago (1994), the research team of Dhalla et al. regenerated the catalytic activity of the glutamine synthetase Arg339 and Arg359 mutants via chemical modification. In this experiment Dhalla and colleagues used site-directed mutagenesis to mutate the Arg339 and Arg359 residues to cysteines, which exhibited a significant decline in activity. R339C and R359C mutants reacted with 2-chloroacetamidine (CA) and 2,2'-dithiobis (acetamidine) (DTBA) to obtain arginine analogs. Lysine analogs were produced using bromopropylamine (BPA). Analogs were synthesized via "nucleophilic displacement reaction" (S_N2 reaction) in the presence of DTT to reduce disulfide bonds. Such analogs were determined to have similar (more or less) length (in angstroms) to the Arg339 and Arg359 residue sidechains: Arginine 6.22Å), R339/359C-CA (5.40 Å), R339/359C-DTBA (6.58 Å) and R339/359C-PA (7.85 Å) – and Lysine (6.33 Å). Chemically modified mutants (following DTT reduction) desalted via G-25 Sepharose columns and incubated between 0min to24hrs (Dhalla, Li et al. 1994).

Glutamine Synthetase (GS) kinetic analysis was performed and WT enzyme activity was 120 μmol $min^{-1}mg^{-1}$, R339C as 1.3 and R359C 0.6 μmol $min^{-1}mg^{-1}$. Upon

examination of the ATP affinity for WT GS and mutants, there was a decline for the R339C (89 ± 12μM) and R359C (140 ± 6μM) in comparison to the WT GS ATP affinity (1.5 ± 0.3 μM). Activity was regenerated following the chemical modification process. This was observed via kinetic analysis: R339-CA (80 μmol $min^{-1}mg^{-1}$), R339-PA (38 μmol $min^{-1}mg^{-1}$), R339C-DTBA (32 μmol $min^{-1}mg^{-1}$), R359C-CA (37 μmol $min^{-1}mg^{-1}$) and R359-DTBA (9.9 μmol $min^{-1}mg^{-1}$). An apparent increase in ATP substrate affinity was also noted for the chemically rescued cysteines: R339-CA (6.6 ± 0.4μM), R359-CA (3.2 ± 0.4μM), R339C-DTBA (28 ± 1μM), R359C-DTBA (26 ± 3μM) and R339C-BPA (46 ± 3μM). The chemical modification process worked well considering native cysteine groups were not affected by solutions in this process (Dhalla, Li et al. 1994). This experimentation process illustrated one possibility for the chemical modification approach in our empirical analysis of the Arg32 and Lys42 residues of *E. coli* ADP-Glc PPase – a candidate for arginine or lysine analogs.

Previous Lysine (γ-thia-lysine Synthesis) Chemical Rescue Studies

Synthesis of a γ-thia-lysine side chain via chemical modification has been performed for aldolase, carboxylase and aminotransferase enzymes (Planas, Kirsch 1991, Smith, Hartman 1988, Hopkins, O'Connor et al. 2002).

Lys107 of Fructose-1,6-bisphosphate Aldolase – The role of the FBP aldolase enzyme is to catalyze the reaction in which FBP is converted to dihydroxyacetone (DHAP) and glyceraldehyde-3-P (reversibly; Fru1P is converted to glyceraldehyde). In 2002, Hopkins and colleagues, via site-directed mutagenesis, changed the Lys107 residue to cysteine (K107C) to explore the possibility of "chemical rescue" of enzyme catalytic

activity via chemical modification (bromoethylamine; BrEA; aminoethylation) (Hopkins, O'Connor et al. 2002). Initially, there was a 30% decrease in native enzyme (WT) activity, in the presence of BrEA during aminoethylation process. As such, Hopkins et al. determined that "non-targeted" cysteine residues were exposed to the "solvent" and as a result affected during the chemical modification process, in the presence of 1mM DTT. As such alanine mutagenesis was performed on these "non-targeted" cysteine groups. Following the previous, the K107C mutant was then aminoethylated via an S_N2 modification reaction with BrEA. It was determined via electron spray ionization fourier transform mass spectroscopy (ESI-FTMS) that 2.5 aminoethylations occurred per aldolase subunit. Comparatively, the K107C kcat was much lower than the WT. However, following aminoethylation, the K107C-EA (noted as "tetK107C-EA" in article) mutant displayed a 40-fold increase in activity ($10.8 \pm 0.1\ s^{-1}$), which was up to 77% of the wild-type value ($14.0 \pm 0.3\ s^{-1}$). There was also a measureable increase in FBP substrate affinity for the K107C-EA ($10.7 \pm 0.2\mu M$) from $450 \pm 10\ \mu M$ (K107C), which was closer to the WT ($14 \pm 1\mu M$). Conclusively, Hopkins et al. was able to determine that the lysine (K107) was replaced by a γ-thia-lysine during the catalytic mechanism for FBP aldolase, and that the kinetic analysis of substrate affinity for the "rescued" K107C (K107C-EA) for FBP and Fru1P substrates was similar to that of the native lysine residue (K107) in the WT. Furthermore, by utilizing ESI-FTMS they were able to closely identify the residues affected and degree of protein modification for this Fructose-1,6-bisphosphate aldolase during the K107C "chemical rescue" procedure (Hopkins, O'Connor et al. 2002).

Lys258 of Aspartate Aminotransferase in E.coli – The Asp Aminotransferase enzyme is responsible for transferring an α-amino group from the L-aspartate and L-glutamate amino acids to α-ketoglutarate and oxaloacetate. An essential residue in the *E. coli* species of this enzyme is Lys258 (K258). In 1991, Planas et al. converted the K258 residue to cysteine via site-directed mutagenesis. Less than 10^{-6} activity (compared to the WT), in the presence of L-aspartate, was observed for the K258C mutant. Additionally, the alanine mutant (K258C) was noted as being incapable of catalyzing the Aspartate Aminotransferase reaction. After chemical modification (aminoethylation with BrEA, following disulfide reduction with DTT), activity of 10^5 times higher than the K258C mutant was "rescued" in the K258C-EA chemically modified mutant (with a k_{cat} value nearly 7% of the WT, at $9.86 \pm 0.6\ s^{-1}$). Similar improvements for the substrate (Km) values was also seen for the L-aspartate substrate (K258C-EA; 3.47±0.14mM and WT; 1.87 ± 0.7mM). Planas et al. identified an "acidic limb" of the K258 residue playing a role in enzyme catalysis via interaction with the Asp Aminotransferase substrate(s), and evaluated the γ-thia-lysine of the K258C-EA mutant. Here, they noted that the basicity of the K258A, K258C and K258C-EA were slightly lower than the WT K258 – with the chemically "rescued" mutant (K258C-EA) displaying the highest at only 1.3 pH units lower than that of the WT lysine. As such, they postulated that the due to mutation a lack of ε-NH_2 presence in the WT lysine may have resulted in poor dissociation constants – and Vmax values - seen in the K258C and K258A mutants. Chemical modification, in the Planas experiments displayed the important role of pH and electrostatic ability of the lysine residue, in substrate binding affinity and enzyme catalysis (Planas, Kirsch 1991).

Lys166 and Lys329 in Ribulosebisphosphate Carboxylase/Oxygenase of ***Rhodospirillum rubrum*** – The Ribulosebisphosphate Carboxylase/Oxygenase enzyme is responsible for the catalysis of the oxidative degradation of the ribulosebisphosphate molecule. In 1988, Smith et al. performed aminoethylation on the cysteine mutants of these to lysines observed to play a key role in the enzyme (K166C and K329C). The two cysteine mutants lacked catalytic activity, and thus aminoethylation ("chemical rescue") was performed – via chemical modification with BrEA for 0 to 1200min. For this aminoethylation experiment, Smith and colleagues found that the BrEA solution was highly selective and only modified one cysteine – the mutated K166C or K329C – and no the "non-targeted" native 5 cysteines in the Ribulosebisphosphate Carboxylase enzyme – so no alanine mutagenesis of native cysteines was required. The sulfur groups of the K166C and K329C mutants created a modest perturbation in the secondary structure of the protein; however, chemical modification appeared to "reverse" this issue. Furthermore, a significant decrease in catalytic activity was observed for the cysteine mutants, which elucidated the importance of the native enzyme lysyl residues (sites 166 and 329). A "rescue" of catalytic activity was observed for the K166C-EA and K329C-EA chemically modified mutants, with activity and Km values increased from the K166C and K329C mutants, closer to the wild-type values. Conclusively, oxygenase activity was "restored" for the modified cysteine mutants and chemical modification appeared to result in a "reversal" of effects on activity by the cysteine mutations (K166C and K329C) with k_{cat} values close to 20% (K166C-EA) and 60% (K329C-EA) of the WT was observed (Smith, Hartman 1988).

Chemical Rescue Attempts for R32C and K42C Mutants

Upon review of the preceding experimental approaches, we selected three compounds for chemical modification of the Arg32 and Lys42 cysteine mutants: 2-chloroacetamidine (CA; arginine analogs), 2-bromopropylamine (BPA; lysine analogs) and bromoethylamine (BrEA; lysine analogs) (Figure 41). BioEdit (Hall 1999) genetic and amino acid sequence analysis software revealed that there are nine native cysteines (C61, C163, C167, C263, C338, C360, C377, C382 and C388) present in the WT *E. coli* ADP-Glc PPase, but which were exposed to "solvent" during the chemical modification process, was unable to be determined beforehand – some suggestions were noted. To perform this task, we designed an experiment in accordance with the protocol from Dhalla et al both with and without DTT. The, initially designed EcR32C-Chloroacetamidine mutant Specific Activity assay interfered with the Malachite Green Colorimetric assay: the DTT (used to reduce the sulfide group of the EcR32C mutant) prevented the yellow -> green color shift required to determine the Malachite Green-Ammonium Molybdate-P_i complex. Thus, the reaction remained a bright yellow color. A second trial, removing DTT, using "G25" sepharose columns, yielded slightly better measureable results utilizing a spectrophotometrically measurable analyte; measurable at a wavelength of 595nm).

Lys42Cys "Chemical Rescue" Attempt – K42C mutant underwent chemical modification with BrEA and BPA generating analogs of the lysine to synthesize the γ-thia-lysine as with other lysine-to-cysteine chemically modified mutant enzymes (Planas, Kirsch 1991, Smith, Hartman 1988, Hopkins, O'Connor et al. 2002). Here, there was a

slight change from the previous R32C modified mutants, K42C-EA and PA were performed from 0 to 240min. Longer incubation time with solvents were utilized, as seen with previous experiments (Planas, Kirsch 1991, Hopkins, O'Connor et al. 2002). However, K42C-EA and K42C-PA displayed a similar k_{cat} to the K42C mutant (0.04 s^{-1}), at 0.056 s^{-1}; 0.064 s^{-1} (20min; 60min) and 0.054 s^{-1}; 0.052 s^{-1} (20min; 60min), respectively (Figure 42 and Table 18).

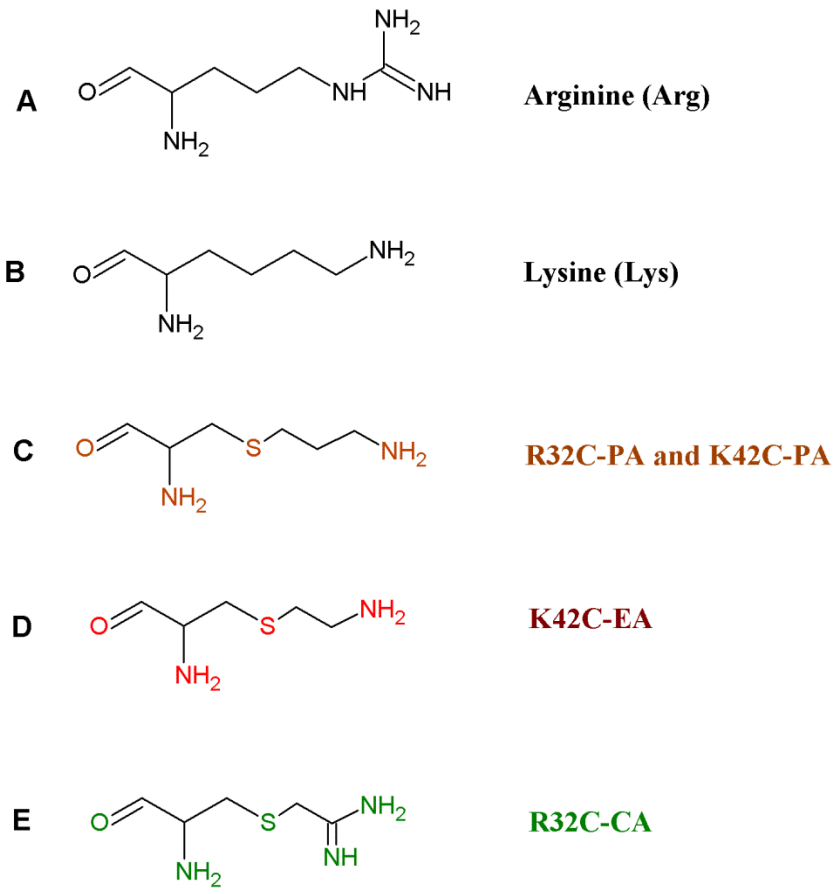

Figure 41. Sketches of Arg32 and Lys42 sidechains and Chemical Modification sidechains. (A-B) WT Arg32 and Lys42 sidechain depictions. (C-E) S_N2 reactions were performed and C-E illustrate side chain modifications with bromoethylamine, bromopropylamine and 2-chloroacetamidine.

Arg32Cys "Chemical Rescue" Attempt - As such, an attempt to rescue activity lost in the mutant R32C (1.78 s^{-1}) comparable to the original WT kinetic analysis of 103 s^{-1}. As such, an experiment was designed (with DTT using G25 sepharose columns and without DTT, with a 20min solution incubation period at 30°C). For the R32C mutant 2-chloroacetamidine and BPA were utilized. Unfortunately, both exhibited a lower – much lower – specific activity than the WT and R32C mutants (R32C-CA; 0.263 s^{-1} and R32C-BPA; 0.136 s^{-1}, with DTT). Similar results for R32C modifications without DTT were observed (Figures 43 and 44, Table 18).

WT in the presence of BrEA, BPA and CA - "Chemical rescue" was not observed for the Arg32Cys and Lys42Cys chemically modified mutants either. Investigation of the WT enzyme in the presence of the chemical rescue reagents was assessed, to elucidate whether "non-target" cysteines have been affected or exposed to "solvent" as observed in previous experiments. A new sample of WT was utilized to fully evaluate the effect of the "chemical modifier" solutions on the wild-type enzyme. This investigation displayed a significant decrease in activity for WT-EA, WT-PA and WT-CA, with WT-CA having the lowest remaining catalytic activity at 23% of the WT (Table 19). Here were discover the crux of the problem – at least one or more of the native nine *E.coli* ADP-Glc PPase cysteines are exposed to "solvent" and would require alanine mutagenesis, as performed by both Hopkins and Smith (Smith, Hartman 1988, Hopkins, O'Connor et al. 2002). However, to discover which "non-targeted" cysteines of the ADP-Glc PPase are modified in the presence of CA, BrEA and BPA is another project to be designed. Conclusively,

we were able to discover that a number of cysteines of the nine native *E.coli* ADP-Glc PPase cysteines are exposed to chemical modifications on the surface of the enzyme and that future “chemical rescue” experiments would benefit from alanine mutagenesis of these “non-target” cysteines prior to chemical modification. Also, we found that DTT may inhibit colorimetric results of the Malachite Green assay.

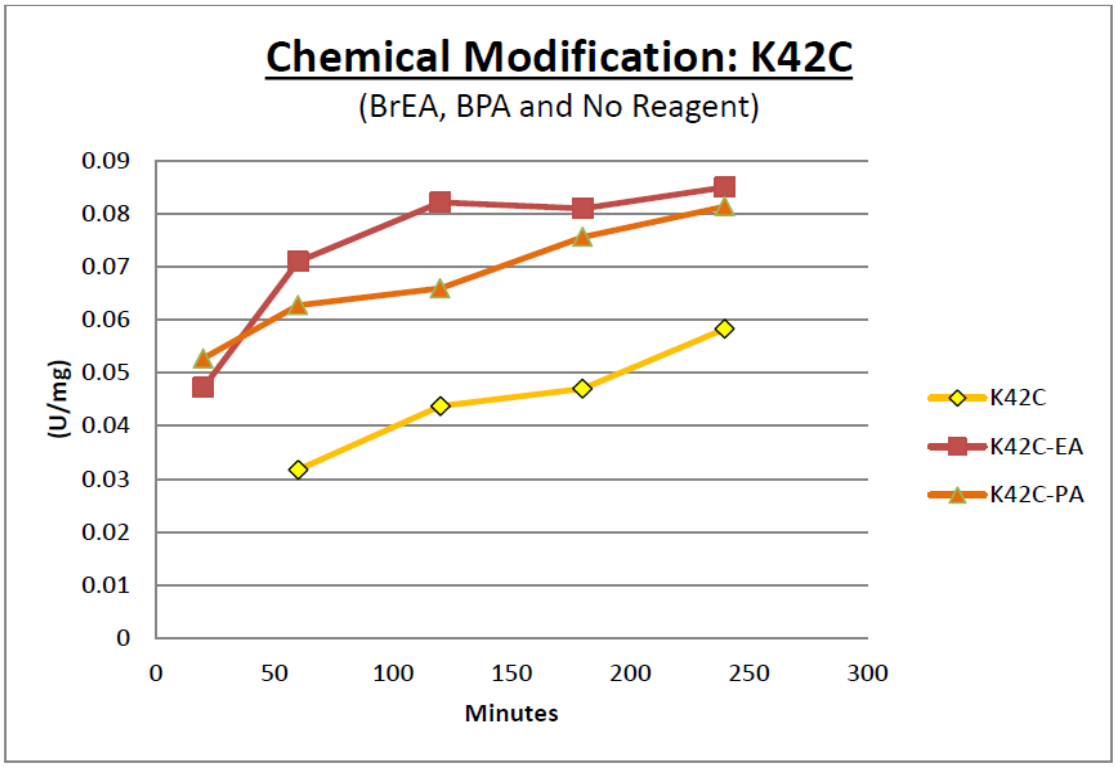

Figure 42. Lys42 Chemical Modification. Lys42Cys (K42C) with Bromopropylamine (orange), Bromoethylamine (red) and control (yellow; K42C and water).

Table 18. Arg32 and Lys42 Chemical Modification.

Enzyme[a]	**Incubation**[b] **period**	$\mathbf{V_m}$
	min	s^{-1}
R32C[c]	---	1.78 ± 0.05
R32C-Water	20	0.695 ± 0.19
R32C-CA	20	0.263 ± 0.086
R32C-PA	20	0.136 ± 0.003
K42C[c]	---	0.040 ± 0.002
K42C-EA	20	0.056 ± 0.007
K42C-EA	60	0.064 ± 0.004
K42C-PA	20	0.054 ± 0.002
K42C-PA	60	0.052 ± 0.001

[a]Enzyme activation assays were performed as described under "Experimental Procedures". Enzymes were not reduced with DTT, as it has been found to interfere with the colorimetric analysis of the Malachite Green Assay

[b]Enzymes were incubated with Water, CA, BrEA or BPA for 20min and/or 60min at 30ºC.

[c]Arg32Cys and Lys42Cys mutants were assayed under Malachite Green protocol outlined under "Materials and Methods" in chapters two and three.

*V_f is calculated k_{cat} after chemical modification and V_i for WT was a calculated from R32C and K42C *E. coli* ADP-Glc PPase samples and assayed using Malachite Green protocol described in "Materials and Methods".

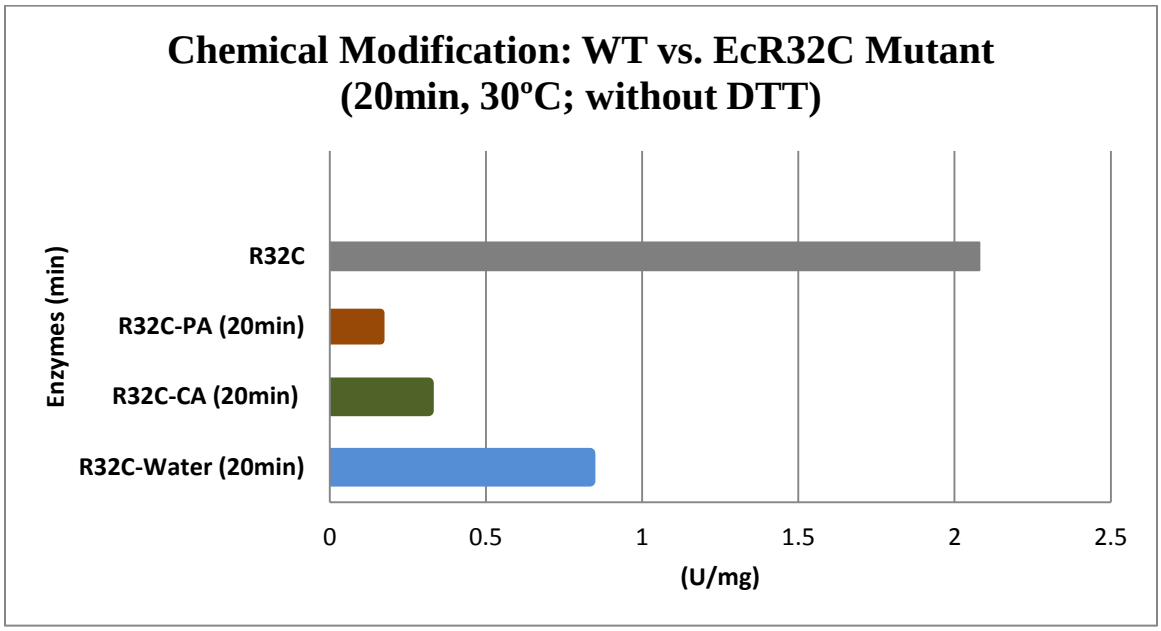

Figure 43. Arg32 Chemical Modification without DTT (dithiothreitol). Arg32Cys (R32C; grey; performed under standard Malachite Green assay protocol, as noted in "Methods and Materials" of previous chapter), Arg32Cys (R32C) with Bromopropylamine (red), 2-chloroacetamidine (green) and control (R32C and water; blue).

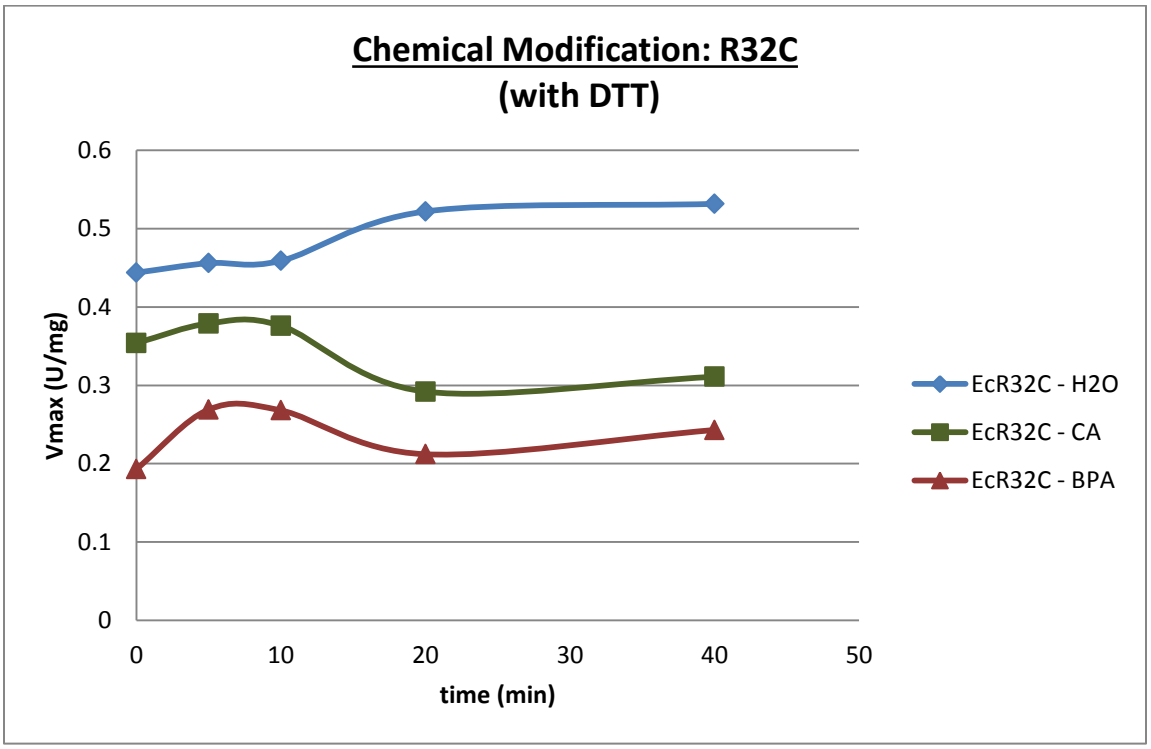

Figure 44. Arg32 Chemical Modification with DTT. Arg32Cys (R32C) with Bromopropylamine (red), 2-chloroacetamidine (green) and control (R32C and water; blue).

Table 19. WT Chemical Modification.

Enzyme[a]	**Incubation**[b] **period**	$\mathbf{V_m}$	**Remaining Act. 100 x (V_f/V_i)**
	min	s^{-1}	(%)
WT[c]	---	160 ± 7	100
WT-EA	20	112.3 ± 0.5	70.2
WT-EA	60	119 ± 6	74.4
WT-PA	20	70 ± 5	43.8
WT-PA	60	75 ± 3	46.9
WT-CA	20	37.5 ± 2.5	23.4

[a]Enzyme activation assays were performed as described under "Experimental Procedures". Enzymes were not reduced with DTT (dithiothreitol), as it has been found to interfere with the colorimetric analysis of the Malachite Green Assay
[b]Enzymes were incubated with either CA, BrEA and BPA for 20min and/or60min at 30ºC.
[c]Wild-type enzyme assay was done separately, in presence of water and no BrEA/BPA solution as control.
*V_f is calculated k_{cat} after chemical modification and V_i for WT was a calculated from a new sample of WT *E. coli* ADP-Glc PPase and assayed using Malachite Green protocol described in "Materials and Methods".

Expected Results and Conclusions of Chemical Rescue Experiments

Project (Arg32Cys and Lys42Cys) - Previous experimentations have noted a distinct disparity in the length of the mutated (R32C and K42C) and chemically modified mutant residues (R32C-CA, R32C-PA, K42C-CA and K42-EA). Recall, Dhalla et al. noted in 1994, a 0.82 Å difference between the R339/359 and R339/359C-CA modified mutants and a 1.63 Å difference between the R339/359 and R339/359C-PA modified mutants. Had the initial "R32C and K42C Chemical Modification" experimental approach been a success we would have been able to confirm or investigate the pertinent role of both the charge of the residue sidechains (Arg32 and Lys42), as well as the importance of the proximity of the sidechain(s) to the γ-phosphorous (Arg32 terminal amine; guanidium moiety) and β-phosphorous-o-linkage (Lys42 ε-amine) of the ATP substrate for *E.coli* ADP-Glc PPase. In this case, a success is define as a prominent rescue of wild-type activity for the chemically modified R32C and K42C mutants. As alanine mutagenesis and kinetic analysis of the 9 native cysteines in the wild-type enzyme would be exponentially costly – in both time and resources – and considering the possible combinations of cysteines exposed to the solvent are unknown, modelling would be the next logical suggestion for discovering these "solvent-exposed" cysteines. Thus, a key result of the present chemical modification experiment is the noted likelihood of cysteines "exposed" to the solvent.

CHAPTER FIVE

CONCLUSIONS

Experimental Approach: Success in Protein Expression and Assays

As previously noted, both mutant Arg32 and Lys42 ADP-Glc PPase were designed using the BioEdit® software and obtained (via PCR site-directed mutagenesis) prior to expression. BL21(DE3) cells carrying the mutant ADP-Glc PPase gene (pet24a vector) were induced in LB Media (kanamycin) with 0.5mM IPTG during the Log stage of the *E.coli* growth phases (OD_{600} of 0.6 - 0.8) . As such we were able to take advantage of the intracellular mechanisms of the *E.coli* BL21(DE3) cell growth process and avoid production of endogenous (WT) ADP-Glc PPase proteins. Therefore, a two-step FPLC purification was adapted (DEAE and HiPrep/SourceQ column chromatography – and Size Exclusion Chromatograpy, when empirically required) (Figures 45 - 46). The previous and analysis of the R32E and K43E mutants displaying relative "inactivity", exemplified the "absence" of any residual measured background WT activity. In this regard, we were able to determine relatively certain values for mutant ADP-Glc PPase specific activities and k_{cat}. *Kinetics*: The malachite green-ammonium molybdate complex interacts with the PPi byproduct of the ADP-Glc reaction allowing us to measure ADP-glucose production, in the synthesis direction (Figure 47). The reverse was accomplished employed a coupled assay diagramed in Figure 48. Here we quantitatively measured the production of Glc-1P via the reduction of NAD^+ to NADH.

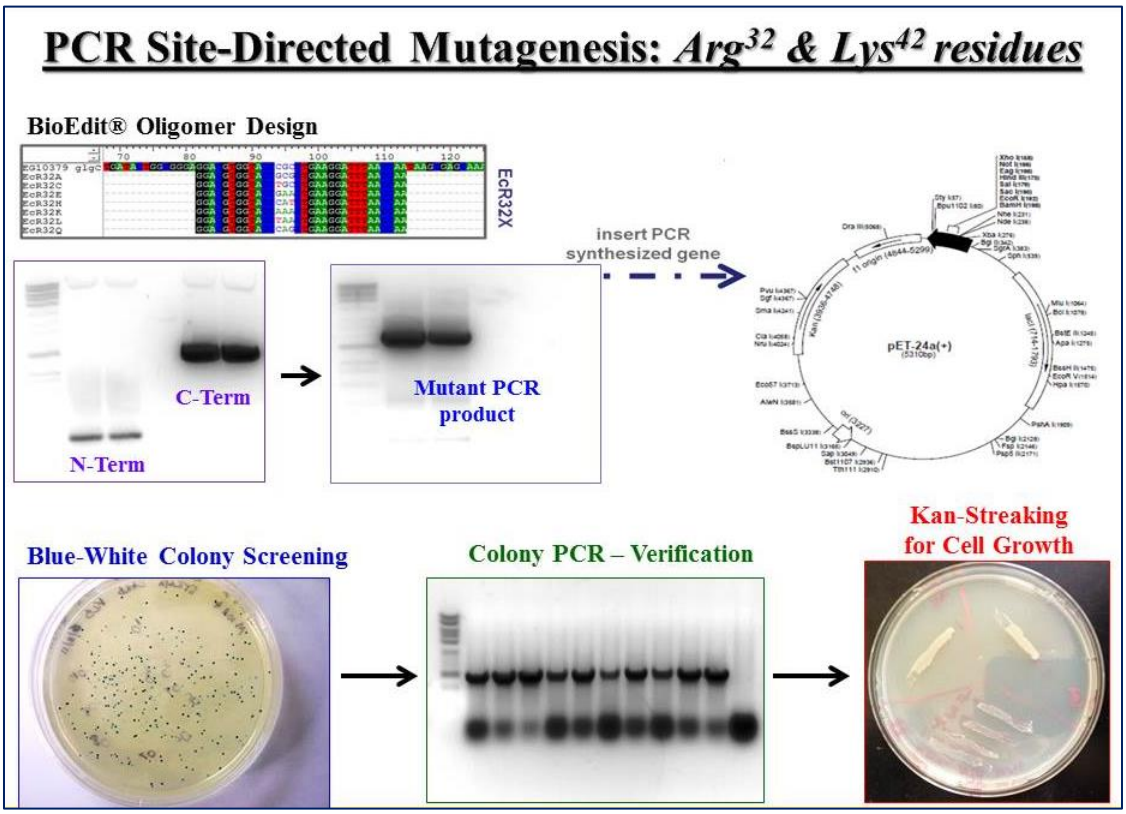

Figure 45. PCR Site-Directed Mutagenesis and Cell Transformation of Arg32/Lys42 Mutants.

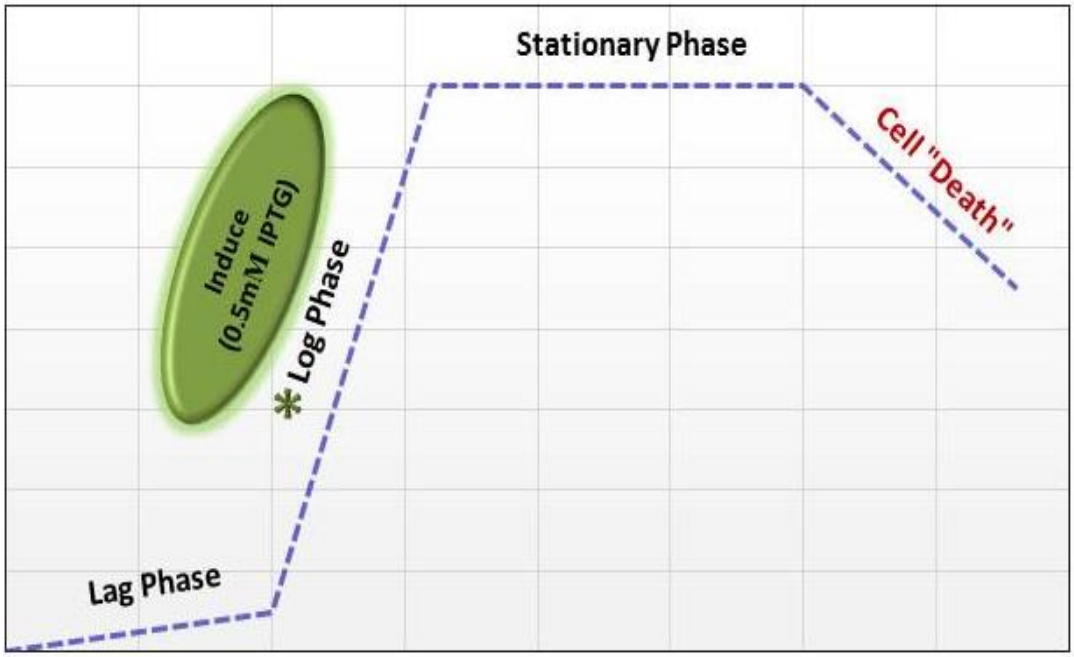

Figure 46. *E.coli* BL21(DE3) Cell Growth Curve (Laboratory). Wild type and *E.coli* ADP-Glc PPase_pETEC mutants were transformed into BL21(DE3) competent cells and induced with 0.5mM isopropyl-β-D-thiogalactoside (IPTG) then later incubated for 16hrs at 25ºC. Cultures were harvested after grown to OD_{600} between 0.6 and 0.8.

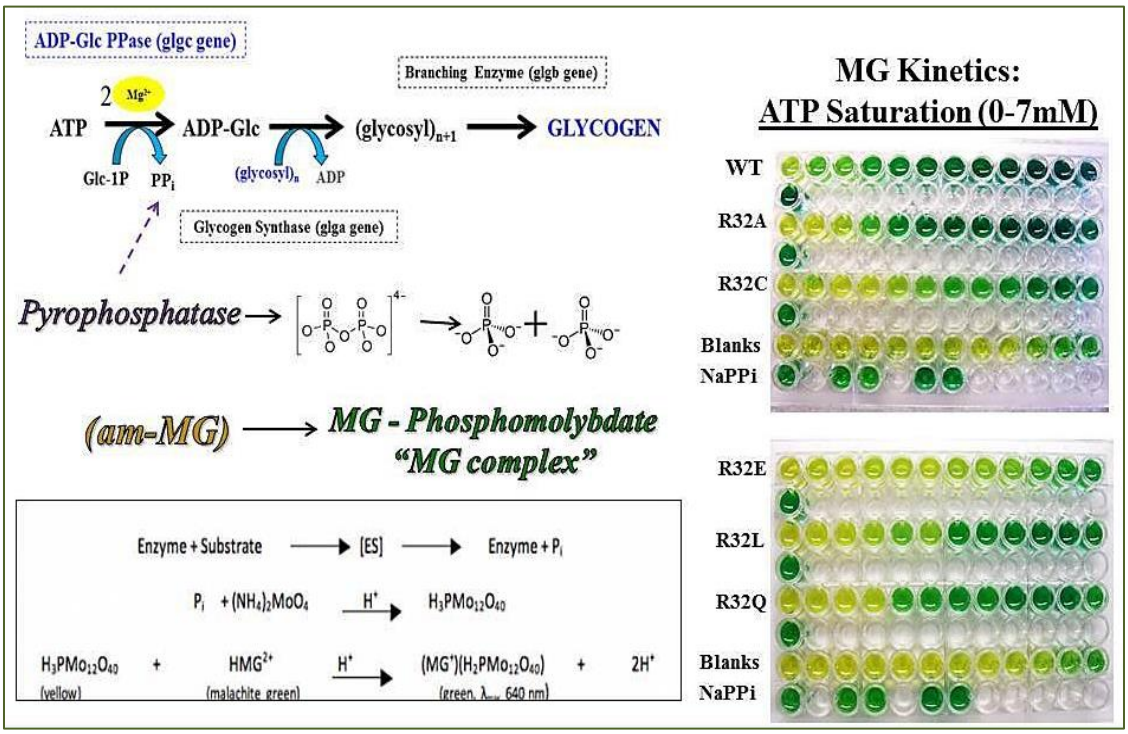

Figure 47. A Colorimetric Approach: Malachite Green Assay. (Fusari, Demonte et al. 2006).

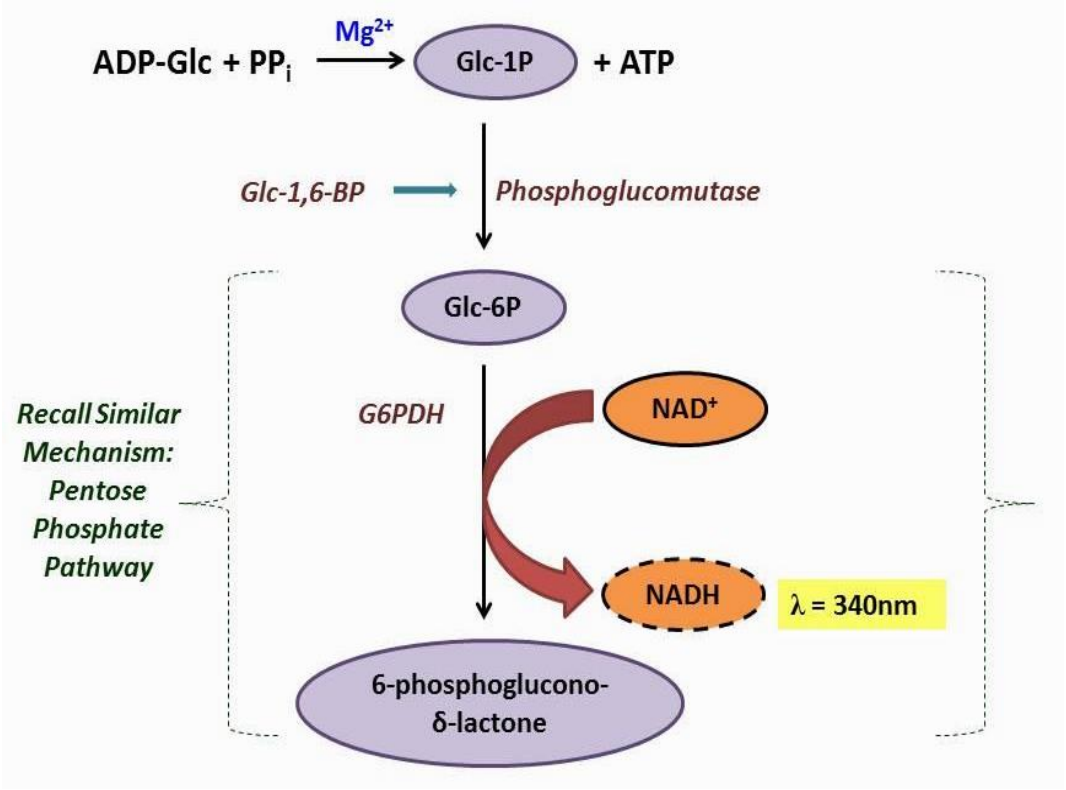

Figure 48. Pyrophosphorolysis (Coupled) Assay.

Critical Factors of the Arg32 and Lys 42 Residues in *E. coli* ADP-Glc PPase

Conclusively, this project illustrates the important role of the guanidinium group in the Arg32 residue and its significance in stabilizing the pyrophosphate product in the ADP-Glc PPase reaction. Prior exploration into the structure and orientation of the ATP substrate and the Potato Tuber ADP-Glc PPase – via crystallography - highlighted the notion that the ATP substrate can have varying degrees of orientation which can have an overall effect on ADP-glucose production by the ADP-Glc PPase enzyme. Physicochemical properties of the Arg32 residues lends two positive charges via the two guanidinium nitrogen atoms interacting with the ɤ-Phosphorous (ATP), to position (and orientate) the ATP substrate for "attack" by the secondary substrate (Glc-P) (Figure 27). As such, the Arg32 also functions in making the pyrophosphate product a better "leaving group" - as previously exemplified in review of the mutant Arg32X kinetics (variants missing the guanidinium side chain). Arg32 (WT vs Mutants) MDS highlights the disparity in the ATP substrate conformations and "freedom" of movement for ATP substrate in Arg32-mutant and WT *E.coli* ADP-Glc PPase. Here, we postulate that the lysyl (1º) amine of Lys42 interacts (as demonstrated via Homology modelling) with "o" linkage between the the α and β-Phosphorous groups (of the ATP substrate). Furthermore, Lys42 has the ability to donate proton to P_β oxygen making it a better leaving group. Lys42 is possibly selectively stabilizing the transition state based on the fact that all mutations selectively decreased k_{cat} compared to any other parameters for the substrates in any direction (Figure 49).

Lys42: Postulated "General Acid Catalysis" and Mg^{2+} Binding Network

A possible function of Lys42 is the role of "General Acid Catalysis" (as seen in previous DNA polymerase lysine studies) (Castro, Smidansky et al. 2009), which would make the residue catalytic in that it most likely donates a proton to the negatively charged pyrophosphate leaving group to stabilize it. Lys42 is surrounded by several non-polar side chains (Leu33, Thr37, Val45, Ile53, and Val277) that would lower the pKa of the ε-amino group and enhance acid catalysis. As presently enzymologists are unable to estimate the pKa of residues such as Lys42 within the active site of an enzyme, we could not estimate the exact pKa of the Lys42 nor Lys42Arg in the catalytic pocket of the *E.coli* ADP-glc PPase enzyme. However, we are aware that the approximate pKa of the sidechains differ (Figure 49). Chapter two noted that due to the presence of a Lys42/Asp142/Asp276 network the Lys42 residue plays a critical role, in Mg^{2+} cofactor binding. Altering the Lys42 side chain, also alters both Mg^{2+} cooperativity and FBP affinity in mutants – evidence of perturbed Lys42/Asp142/Asp276 network and possibly Lys39 placement in the FBP binding site (Figure 50). Within the Lys42 model highlighting the magnesium (cofactor) binding network the position of a second magnesium ion is observed - this was seen in the TDP-Glc PPase enzyme and assumed to also be localized within the ADP-Glc PPase enzyme, for the purposes of modelling (Barton, Biggins et al. 2002, Barton, Lesniak et al. 2001).

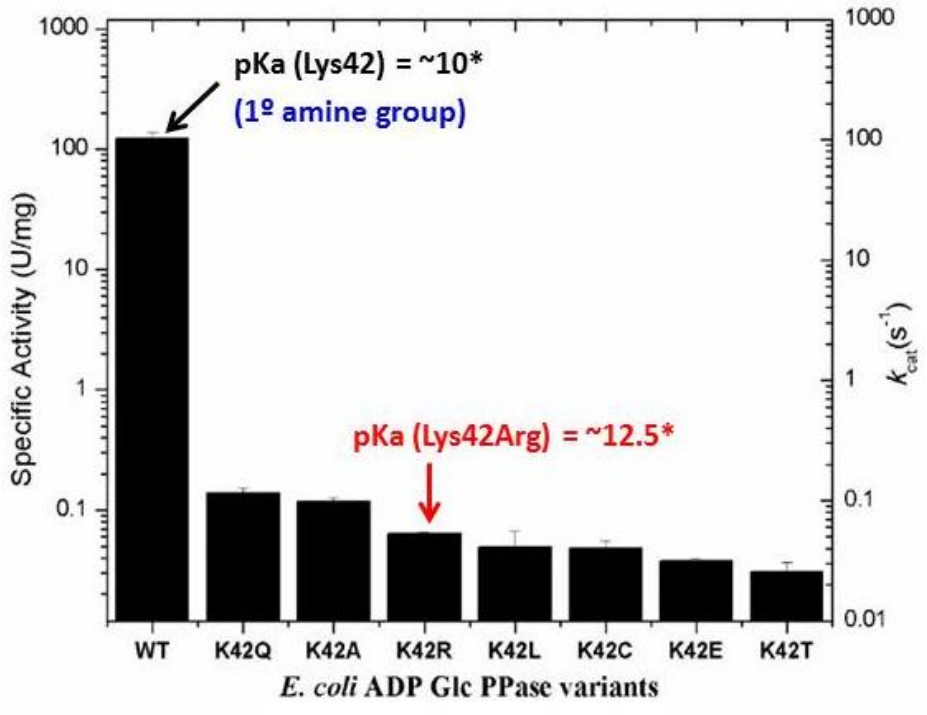

Figure 49: Lys42 Analysis (1º amine and Estimated pKa).

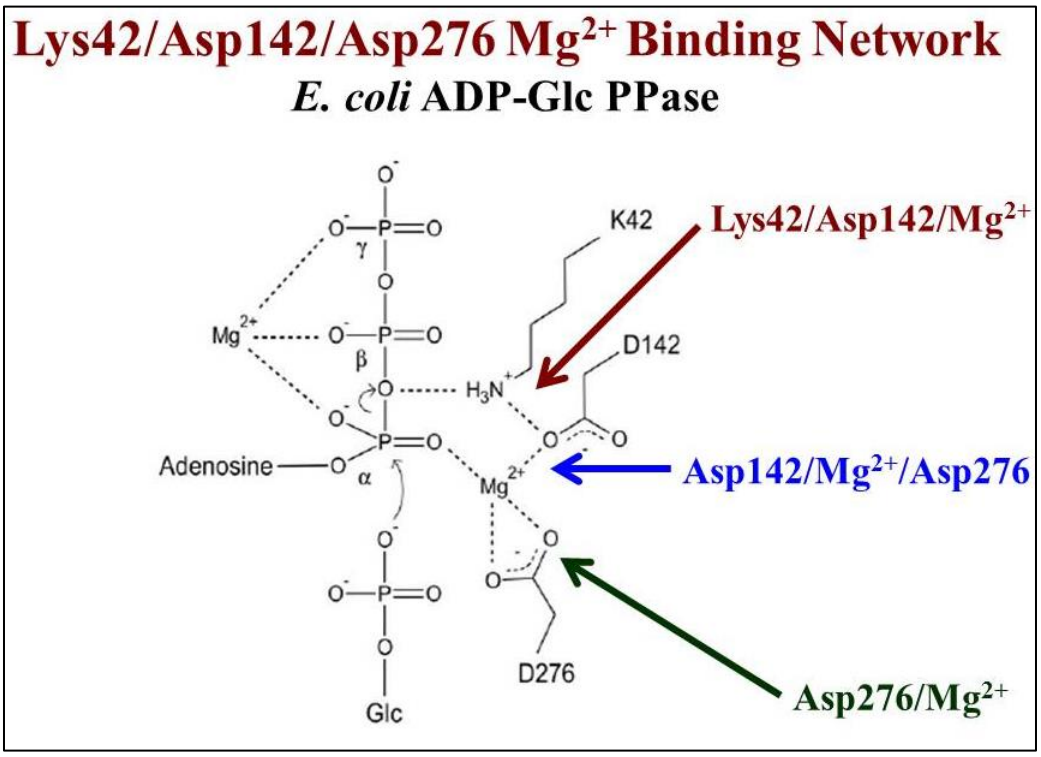

Figure 50. Lys42 and Mg^{2+} Binding Network.

Arg32/Lys42 Project Model and the Superfamily of NDP-Glc PPases

In 2005, Ballicora et al. highlighted the presence of a phylogenetic relationship among ADP-Glc PPase enzymes from photosynthetic eukaryotes. These enzymes consist of subunits often observed to be catalytic and non-catalytic (modulatory), with conserved residues. Both subunits are approximately fifty percent identical, giving credence to the notion of "common ancestry" among these two subunits (Ballicora, Iglesias et al. 2004, Ballicora, Erben et al. 2007, Ballicora, Iglesias et al. 2003). Here a question arose regarding the catalytic properties of two conserved N-terminus residues (Arg and Lys) within the catalytic S-subunits but not the modulatory (non-catalytic L-subunits) (Ballicora, Dubay et al. 2005, Crevillen, Ballicora et al. 2003, Kuhn, Falaschetti et al. 2009). The homotetrameric *E.coli* ADP-Glc PPase enzyme was an optimal candidate to model and empirically distinguish the then "uncharacterized" roles of these two conserved residues in question (equivalent to Arg32 and Lys42 of the *E. coli* enzyme). Overall, with this project, we were able to further characterized residues of the *E.coli* ADP-Glc PPase which includes Glc-1P substrate binding (Glu194, Ser212, Tyr216, Asp239, Phe240, Trp274 and Asp276), FBP activator binding (Lys39) and Allosteric signaling (Loop; Pro103, Gln106m Arg107, Trp113, Tyr114 and Arg115) (Figure 51). Additionally, most likely similar effects are in other NDP-Glc PPases – all residues conserved in the NDP-Glc PPase Family – with the exception of Large Subunits (Plant species). Conclusively, this project served as an advantageous model for better understanding all NDP-sugar PPases. NDP-sugar PPases are very common in metabolic pathways (Figures 1 and 52).

Glc-1P (substrate)	Binding FBP	Allosteric Signaling	Residues *for* Catalysis
Glu^{194}	*Lys*^{39}	*Pro*^{103}	*Asp*^{142} (Mg^{2+})
Ser^{212}		*Gln*^{106}	*Asp*^{276} (Mg^{2+})
Tyr^{216}		*Arg*^{107}	*Lys*^{42} ("General Acid Catalysis?")
Asp^{239}		*Trp*^{113}	*Arg*^{32} (Positioning of ATP)
Phe^{240}		*Tyr*^{114}	
Trp^{274}		*Arg*^{115}	
Asp^{276}			

Figure 51. *E.coli* ADP-Glc PPase Characterized Residues.

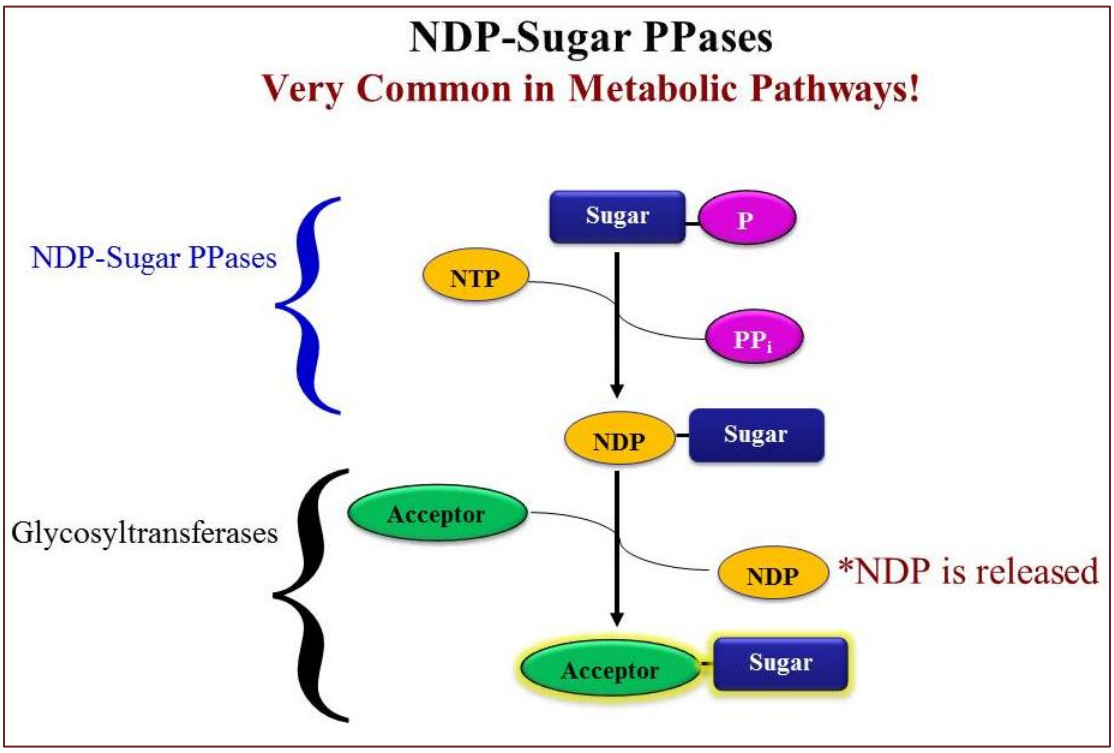

Figure 52. Model of NDP-Sugar PPases.

APPENDIX A

SUPPLEMENTAL INFORMATION

SUPPLEMENTAL INFORMATION

Table S1. Species and NCBI GI Accession numbers for Sequence Alignment of conserved Lys42 residue in *E. coli* ADP-Glc PPase and comparative enzymes.

Species	**GI Accession No.**
Escherichia coli	16131304
Agrobacterium tumefaciens sp. R. radiobacter	3241931
Acidovorax citrulli AAC00-1	120611645
Agrobacterium tumefaciens str. C58 (A. fabrum)	15890896
Alteromonas sp. SN2	333892129
Arthrospira maxima CS-328	209527099
Desulfobacterium autotrophicum HRM2	224369989
Desulfomonile tiedjei DSM 6799	392410016
Hydrocarboniphaga effusa AP103	392953280
Mahella australiensis 50-1 BON	332982541
Mycobacterium tuberculosis T85	289757310
Methylobacter tundripaludum SV96	344943819
Nitrosomonas europaea ATCC 19718	30249970
Nitrosococcus halophilus Nc4	292491590
Proteus penneri ATCC 35198	226330079
Rubrivivax gelatinosus IL144	383758760
Rhodospirillum rubrum ATCC 11170	83593581
Sorangium cellulosum	162453622
Treponema brennaborense DSM 12168	332298391
Thioalkalivibrio thiocyanoxidans ARh 4	350561659
Variovorax paradoxus S110	239813432
Solanum tuberosom	62738715
Glucose-1-phosphate thymidylyltransferase (RmlA) from E. coli	671701933
N-acetylglucosamine-1-phosphate uridyltransferase (GlmU) from E. coli	693351467

Table S2. Oligonucleotides* for mutagenesis of *E. coli* ADP-Glc PPase Lys42 mutants.

Name	Sequence[a]
5' WT -N-term (*"T7 Promoter"*)	5'-TAATACGACTCACTATAGGG-3'
5' WT -C-term (*"T7 Terminator"*)	5'-GCTAGTTATTGCTCAGCGG-3'
K42A - *"Forward"*	5'-CAATAAGCGAGCA**GCC**CCGGCCGTACACTT-3'
K42A - *"Reverse"*	5'-AAGTGTACGGCCGG**GGC**TGCTCGCTTATTG-3'
K42C - *"Forward"*	5'-CAATAAGCGAGCA**TGC**CCGGCCGTACACTT-3'
K42C - *"Reverse"*	5'-AAGTGTACGGCCGG**GCA**TGCTCGCTTATTG-3'
K42E - *"Forward"*	5'-CAATAAGCGAGCA**GAA**CCGGCCGTACACTT-3'
K42E - *"Reverse"*	5'-AAGTGTACGGCCGG**TTC**TGCTCGCTTATTG-3'
K42L - *"Forward"*	5'-CAATAAGCGAGCA**CTG**CCGGCCGTACACTT-3'
K42L - "Reverse"	5'-AAGTGTACGGCCGG**CAG**TGCTCGCTTATTG-3'
K42Q - *"Forward"*	5'-CAATAAGCGAGCA**CAG**CCGGCCGTACACTT-3'
K42Q- "Reverse"	5'-AAGTGTACGGCCGG**CTG**TGCTCGCTTATTG-3'
K42R - *"Forward"*	5'-CAATAAGCGAGCA**CGC**CCGGCCGTACACTT-3'
K42R - "Reverse"	5'-AAGTGTACGGCCGG**GCG**TGCTCGCTTATTG-3'
K42T - *"Forward"*	5'-CAATAAGCGAGCA**ACC**CCGGCCGTACACTT-3'
K42T - *"Reverse"*	5'-AAGTGTACGGCCGG**GGT**TGCTCGCTTATTG-3'

[a] Residue-42 genetic code mutations are in bold.

Table S3. Oligonucleotides* for mutagenesis of *E. coli* ADP-Glc PPase mutants.

Name	Sequence
5' WT -N-term (*"T7 Promoter"*)	5'-TAATACGACTCACTATAGGG-3'
5' WT -C-term (*"T7 Terminator"*)	5'-GCTAGTTATTGCTCAGCGG-3'
R32A - *"Forward"*	5'-GGACGTGGTACC**GCG**CTGAAGGATTTAACCAA-3'
R32A - *"Reverse"*	5'-TTGGTTAAATCCTTCAG**CGC**GGTACCACGTCC-3'
R32C - *"Forward"*	5'-GGACGTGGTACC**TGC**CTGAAGGATTTAACCAA-3'
R32C - *"Reverse"*	5'-TTGGTTAAATCCTTCAG**GCA**GGTACCACGTCC-3'
R32E - *"Forward"*	5'-GGACGTGGTACC**GAA**CTGAAGGATTTAACCAA-3'
R32E - *"Reverse"*	5'-TTGGTTAAATCCTTCAG**TTC**GGTACCACGTCC-3'
R32K - *"Forward"*	5'-GGACGTGGCACC**AAA**CTGAAGGATTTAACCAA-3'
R32K - "Reverse"	5'-TTGGTTAAATCCTTCAG**TTT**GGTGCCACGTCC-3'
R32L - *"Forward"*	5'-GGACGTGGTACC**CTG**CTGAAGGATTTAACCAA-3'
R32L - *"Reverse"*	5'-TTGGTTAAATCCTTCAG**GAC**GGTACCACGTCC-3'
R32Q - *"Forward"*	5'-GGACGTGGTACC**CAG**CTGAAGGATTTAACCAA-3'
R32Q - *"Reverse"*	5'-TTGGTTAAATCCTTCAG**CTG**GGTACCACGTCC-3'

* Residue-32 genetic code mutations are in bold.

Table S4. Oligonucleotides* for mutagenesis of *E. coli* ADP-Glc PPase Arg^{32}/Lys^{42} mutants.

Name	Sequence
5' WT -N-term (*"T7 Promoter"*)	5'-TAATACGACTCACTATAGGG-3'
5' WT -C-term (*"T7 Terminator"*)	5'-GCTAGTTATTGCTCAGCGG-3'
R32AK42A - *"Forward"*	5'-GGACGTGGTACC**GCG**CTGAAGGATTTAACCAA-3'
R32A/K42A - *"Reverse"*	5'-AAGTGTACGGCCGG**GGC**TGCTCGCTTATTG-3'
R32K/K42R - *"Forward"*	5'-GGACGTGGCACC**AAA**CTGAAGGATTTAACCAA-3'
R32K/K42R - *"Reverse"*	5'-AAGTGTACGGCCGG**GCG**TGCTCGCTTATTG-3'
R32E/K42E - *"Forward"*	5'-GGTACCGAACTGAAGGATTTAACCAATAAGC GAGCA**GAA**CCGGCCGTA-3'
R32E/K42E - *"Reverse"*	5'-TACGGCCGG**TTC**TGCTCGCTTATTGGTTAA ATCCTTCAGTTC GGTACC-3'

* Residues-32 and -42 genetic code mutations are in bold.

Table S5. Supporting Equations for Arg32 Analysis.

I) Derivation of a rapid equilibrium equation when the enzyme binary complex undergoes an isomerization process

The model involves the following rapid equilibrium reactions

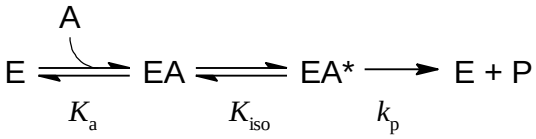

Where the initial velocity (v) is

$$v = \frac{dP}{dt} = k_p[EA^*]$$

The equilibria between enzyme complexes are

$$K_a = \frac{[A][E]}{[EA\,]};\ K_{iso} = \frac{[EA]}{[EA^*]}$$

Mass balance of all enzyme species

$$[E]_t = [E] + [EA] + [EA^*] = [E] + \frac{[A][E]}{K_a} + \frac{[A][E]}{K_a K_{iso}}$$

Then

$$\frac{[E]_t}{[E]} = 1 + \frac{[A]}{K_a} + \frac{[A]}{K_a K_{iso}}$$

The concentration of the binary complex that leads to products is

$$\frac{[EA^*]}{[E]} = \frac{[A]}{K_a K_{iso}}$$

Dividing the previous two equations

$$\frac{[EA^*]}{[E]_t} = \frac{\frac{[A]}{K_a K_{iso}}}{1 + \frac{[A]}{K_a} + \frac{[A]}{K_a K_{iso}}}$$

Replacing $[EA^*]$ by its equivalent v/k_p

$$\frac{v}{k_p[E]_t} = \frac{\frac{[A]}{K_a K_{iso}}}{1 + \frac{[A]}{K_a} + \frac{[A]}{K_a K_{iso}}}$$

Reordering

$$v = \frac{\left(\frac{k_p}{1 + K_{iso}}\right)[E]_t[A]}{K_a\left(\frac{K_{iso}}{1 + K_{iso}}\right) + [A]}$$

Then, the kinetic parameters depend on K_{iso} in the following manner:

$$V_m = \frac{k_p[E]_t}{1 + K_{iso}}$$

$$K_{mA} = K_a\left(\frac{K_{iso}}{1 + K_{iso}}\right)$$

$$\frac{V_m}{K_{mA}} = \frac{k_p[E]_t}{K_a K_{iso}}$$

Then if the isomerization process is perturbed, the corresponding catalytic efficiency would be

$$\frac{V'_m}{K'_{mA}} = \frac{k_p[E]_t}{K_a K'_{iso}}$$

And the ratio of catalytic efficiencies between the perturbed and unperturbed reaction

$$\frac{V'_m/K'_{mA}}{V_m/K_m} = \frac{K_{iso}}{K'_{iso}}$$

II) Derivation of a rapid equilibrium equation when the enzyme binary complex undergoes an isomerization process before binding a second substrate

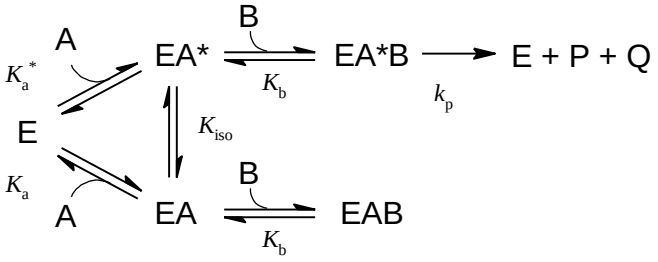

The equilibria between enzyme complexes are

$$K_a = \frac{[A][E]}{[EA\,]};\ K_{iso} = \frac{[EA]}{[EA^*]}; K_b = \frac{[EA][B]}{[EAB]};\ K_b = \frac{[EA^*][B]}{[EA^*B]}$$

Mass balance of all enzyme species

$$[E]_t = [E] + [EA] + [EA^*] + [EAB] + [EA^*B]$$

$$= [E] + \frac{[A][E]}{K_a} + \frac{[A][E]}{K_a K_{iso}} + \frac{[A][B][E]}{K_a K_b} + \frac{[A][B][E]}{K_a K_{iso} K_b}$$

Then

$$\frac{[E]_t}{[E]} = 1 + \frac{[A]}{K_a} + \frac{[A]}{K_a K_{iso}} + \frac{[A][B]}{K_a K_b} + \frac{[A][B]}{K_a K_{iso} K_b}$$

$$\frac{[E]_t}{[E]} = 1 + \frac{[A]}{K_a}\left(1 + \frac{1}{K_{iso}}\right) + \frac{[A][B]}{K_a K_b}\left(1 + \frac{1}{K_{iso}}\right)$$

The concentration of the binary complex that leads to products is

$$\frac{[EA^*B\,]}{[E]} = \frac{[A][B]}{K_a K_{iso} K_b}$$

Dividing by the previous equation

$$\frac{[EA^*B]}{[E]_t} = \frac{\frac{[A][B]}{K_a K_{iso} K_b}}{1 + \frac{[A]}{K_a}\left(1 + \frac{1}{K_{iso}}\right) + \frac{[A][B]}{K_a K_b}\left(1 + \frac{1}{K_{iso}}\right)}$$

Reordering

$$\frac{[EA^*B]}{[E]_t} = \frac{\frac{[A][B]}{K_a K_{iso} K_b}}{1 + \left(\frac{[A]}{K_a}\right)\left(\frac{K_{iso}+1}{K_{iso}}\right) + \left(\frac{[A][B]}{K_a K_b}\right)\left(\frac{K_{iso}+1}{K_{iso}}\right)}$$

$$\frac{[EA^*B]}{[E]_t} = \frac{\left(\frac{[B]}{[B]+K_b}\right)\left(\frac{1}{1+K_{iso}}\right)[A]}{K_a\left(\frac{K_b}{[B]+K_b}\right)\left(\frac{K_{iso}}{1+K_{iso}}\right) + [A]}$$

Replacing $[EA^*B]$ by its equivalent v/k_p

$$v = k_p[E]_t \frac{\left(\frac{[B]}{[B]+K_b}\right)\left(\frac{1}{1+K_{iso}}\right)[A]}{K_a\left(\frac{K_b}{[B]+K_b}\right)\left(\frac{K_{iso}}{1+K_{iso}}\right) + [A]}$$

Then, the kinetic parameters for the substrate A depend on K_{iso} in the following manner:

$$V_m = \frac{k_p[E]_t}{1+K_{iso}}\left(\frac{[B]}{[B]+K_b}\right)$$

$$K_{mA} = K_a\left(\frac{K_{iso}}{1+K_{iso}}\right)\left(\frac{K_b}{[B]+K_b}\right)$$

$$\frac{V_m}{K_{mA}} = \frac{k_p[B][E]_t}{K_a K_b K_{iso}}$$

Then if the isomerization process is perturbed, the corresponding catalytic efficiency would be

$$\frac{V'_m}{K'_{mA}} = \frac{k_p[B][E]_t}{K_a K_b K'_{iso}}$$

And the ratio of catalytic efficiencies between the perturbed and unperturbed reaction if [B] is maintained constant:

$$\frac{V'_m/K'_{mA}}{V_m/K_m} = \frac{K_{iso}}{K'_{iso}}$$

LIST OF REFERENCES

Aikawa, S., et al. "Synergistic Enhancement of Glycogen Production in Arthrospira Platensis by Optimization of Light Intensity and Nitrate Supply." *Bioresource technology* 108 (2012): 211-5. Print.

Aikawa, S., et al. "Direct Conversion of *Spirulina* to ethanol without Pretreatment Or enzymatic hydrolysis processes." *Energy and Environmental Science* 6 (2013): 1844-9. Print.

Aikawa, S., et al. "Glycogen Production for Biofuels by the Euryhaline Cyanobacteria Synechococcus Sp. Strain PCC 7002 from an Oceanic Environment." *Biotechnology for biofuels* 7 (2014): 88,6834-7-88. eCollection 2014. Print.

Alper, H., and G. Stephanopoulos. "Engineering for Biofuels: Exploiting Innate Microbial Capacity Or Importing Biosynthetic Potential?" *Nature reviews.Microbiology* 7.10 (2009): 715-23. Print.

Aoyama, K., et al. "Fermentative Metabolism to Produce Hydrogen Gas and Organic Compounds in a Cyanobacterium, Spirulina Platensis." *Journal of Fermentation and Bioengineering* 83 (1997): 17-20. Print.

Asencion Diez, M. D., et al. "A Novel Dual Allosteric Activation Mechanism of Escherichia Coli ADP-Glucose Pyrophosphorylase: The Role of Pyruvate." *PloS one* 9.8 (2014): e103888. Print.

Asencion Diez, M. D., et al. "The ADP-Glucose Pyrophosphorylase from *Streptococcus Mutans* Provides Evidence for the Regulation of Polysaccharide Biosynthesis in Firmicutes." *Molecular microbiology* 90.5 (2013): 1011-27. Print.

Atsumi, S., et al. "Metabolic Engineering of Escherichia Coli for 1-Butanol Production." *Metabolic engineering* 10.6 (2008): 305-11. Print.

Atsumi, S., T. Hanai, and J. C. Liao. "Non-Fermentative Pathways for Synthesis of Branched-Chain Higher Alcohols as Biofuels." *Nature* 451.7174 (2008): 86-9. Print.

Atsumi, S., W. Higashide, and J. C. Liao. "Direct Photosynthetic Recycling of Carbon Dioxide to Isobutyraldehyde." *Nature biotechnology* 27.12 (2009): 1177-80. Print.

Aw, T. Y., and D. P. Jones. "Control of Glucuronidation during Hypoxia. Limitation by UDP-Glucose Pyrophosphorylase." *The Biochemical journal* 219.3 (1984): 707-12. Print.

Ballicora, M. A., et al. "The Reductive Modulation of Chloroplast Fructose-1,6-Bisphosphatase by Tributylphosphine and Sodium Borohydride." *Cellular and molecular biology (Noisy-le-Grand, France)* 44.3 (1998): 431-7. Print.

Ballicora, M. A., et al. "Resurrecting the Ancestral Enzymatic Role of a Modulatory Subunit." *The Journal of biological chemistry* 280.11 (2005): 10189-95. Print.

Ballicora, M. A., et al. "Identification of Regions Critically Affecting Kinetics and Allosteric Regulation of the Escherichia Coli ADP-Glucose Pyrophosphorylase by Modeling and Pentapeptide-Scanning Mutagenesis." *Journal of Bacteriology* 189.14 (2007): 5325-33. Print.

Ballicora, M. A., et al. "Activation of the Potato Tuber ADP-Glucose Pyrophosphorylase by Thioredoxin." *The Journal of biological chemistry* 275.2 (2000): 1315-20. Print.

Ballicora, M. A., et al. "Heat Stability of the Potato Tuber ADP-Glucose Pyrophosphorylase: Role of Cys Residue 12 in the Small Subunit." *Biochemical and biophysical research communications* 257.3 (1999): 782-6. Print.

Ballicora, M. A., et al. "ADP-Glucose Pyrophosphorylase from Potato Tubers. Site-Directed Mutagenesis Studies of the Regulatory Sites." *Plant Physiology* 118.1 (1998): 265-74. Print.

Ballicora, M. A., A. A. Iglesias, and J. Preiss. "ADP-Glucose Pyrophosphorylase, a Regulatory Enzyme for Bacterial Glycogen Synthesis." *Microbiology and molecular biology reviews: MMBR* 67.2 (2003): 213,25, table of contents. Print.

Ballicora, M. A., et al. "ADP-Glucose Pyrophosphorylase: A Regulatory Enzyme for Plant Starch Synthesis." *Photosynthesis Research* 79.1 (2004): 1-24. Print.

Ballicora, M. A., et al. "Adenosine 5'-Diphosphate-Glucose Pyrophosphorylase from Potato Tuber. Significance of the N Terminus of the Small Subunit for Catalytic Properties and Heat Stability." *Plant Physiology* 109.1 (1995): 245-51. Print.

Ballicora, M. A., et al. "Characterization of Chimeric ADPglucose Pyrophosphorylases of Escherichia Coli and Agrobacterium Tumefaciens. Importance of the C-Terminus on the Selectivity for Allosteric Regulators." *Biochemistry* 41.30 (2002): 9431-7. Print.

Ballicora, M. A., and R. A. Wolosiuk. "Enhancement of the Reductive Activation of Chloroplast Fructose-1,6-Bisphosphatase by Modulators and Protein Perturbants." *European journal of biochemistry / FEBS* 222.2 (1994): 467-74. Print.

Barman, Thomas E., ed. *Enzyme Handbook Vol. I*. New York: Springer-Verlag Inc., 1969. Print.

Baroja-Fernandez, E., et al. "Most of ADP x Glucose Linked to Starch Biosynthesis Occurs Outside the Chloroplast in Source Leaves." *Proceedings of the National Academy of Sciences of the United States of America* 101.35 (2004): 13080-5. Print.

Bejar, C. M., et al. "The ADP-Glucose Pyrophosphorylase from Escherichia Coli Comprises Two Tightly Bound Distinct Domains." *FEBS letters* 573.1-3 (2004): 99-104. Print.

Bejar, C. M., et al. "ADPglucose Pyrophosphorylase's N-Terminus: Structural Role in Allosteric Regulation." *Biochemical and biophysical research communications* 343.1 (2006): 216-21. Print.

Bejar, C. M., et al. "Molecular Architecture of the Glucose 1-Phosphate Site in ADP-Glucose Pyrophosphorylases." *The Journal of biological chemistry* 281.52 (2006): 40473-84. Print.

Berg, J., J. Tymoczko, and L. Stryer, eds. *Biochemistry*. 7th ed. New York, NY: W.H. Freeman, 2012. Print.

Binderup, K., et al. "Crystallization and Preliminary X-Ray Diffraction Analysis of the Catalytic Subunit of ADP-Glucose Pyrophosphorylase from Potato Tuber." *Acta crystallographica.Section D, Biological crystallography* 56.Pt 2 (2000): 192-4. Print.

Blankenfeldt, W., et al. "The Structural Basis of the Catalytic Mechanism and Regulation of Glucose-1-Phosphate Thymidylyltransferase (RmlA)." *The EMBO journal* 19.24 (2000): 6652-63. Print.

Brown, K., et al. "Crystal Structure of the Bifunctional N-Acetylglucosamine 1-Phosphate Uridyltransferase from *Escherichia Coli*: A Paradigm for the Related Pyrophosphorylase Superfamily." *The EMBO journal* 18.15 (1999): 4096-107. Print.

Brynildsen, M. P., and J. C. Liao. "An Integrated Network Approach Identifies the Isobutanol Response Network of Escherichia Coli." *Molecular systems biology* 5 (2009): 277. Print.

Buehner, M., et al. "Three-Dimensional Structure of D-Glyceraldehyde-3-Phosphate Dehydrogenase." *Journal of Molecular Biology* 90.1 (1974): 25-49. Print.

Cardini, C. E., L. F. Leloir, and J. Chiriboga. "The Biosynthesis of Sucrose." *The Journal of biological chemistry* 214.1 (1955): 149-55. Print.

Castro, C., et al. "Nucleic Acid Polymerases use a General Acid for Nucleotidyl Transfer." *Nature structural & molecular biology* 16.2 (2009): 212-8. Print.

Charng, Y. Y., et al. "Molecular Cloning and Expression of the Gene Encoding ADP-Glucose Pyrophosphorylase from the Cyanobacterium Anabaena Sp. Strain PCC 7120." *Plant Molecular Biology* 20.1 (1992): 37-47. Print.

Charng, Y. Y., J. Sheng, and J. Preiss. "Mutagenesis of an Amino Acid Residue in the Activator-Binding Site of Cyanobacterial ADP-Glucose Pyrophosphorylase Causes Alteration in Activator Specificity." *Archives of Biochemistry and Biophysics* 318.2 (1995): 476-80. Print.

Choi, S. P., M. T. Nguyen, and S. J. Sim. "Enzymatic Pretreatment of *Chlamydomonas Reinhardtii* Biomass for Ethanol Production." *Bioresource Technology* 101 (2010): 5330-6. Print.

Conway, T. "The Entner-Doudoroff Pathway: History, Physiology and Molecular Biology." *FEMS microbiology reviews* 9.1 (1992): 1-27. Print.

Cortes, P., et al. "Effects of Early Diabetes on Uridine Diphosphosugar Synthesis in the Rat Renal Cortex." *Kidney international* 21.5 (1982): 676-82. Print.

Crevillen, P., et al. "The Different Large Subunit Isoforms of *Arabidopsis Thaliana* ADP-Glucose Pyrophosphorylase Confer Distinct Kinetic and Regulatory Properties to the Heterotetrameric Enzyme." *The Journal of biological chemistry* 278.31 (2003): 28508-15. Print.

Cupp-Vickery, J. R., R. Y. Igarashi, and C. R. Meyer. "Preliminary Crystallographic Analysis of ADP-Glucose Pyrophosphorylase from *Agrobacterium Tumefaciens*." *Acta crystallographica.Section F, Structural biology and crystallization communications* 61.Pt 3 (2005): 266-8. Print.

Cupp-Vickery, J. R., et al. "Structural Analysis of ADP-Glucose Pyrophosphorylase from the Bacterium *Agrobacterium Tumefaciens*." *Biochemistry* 47.15 (2008): 4439-51. Print.

Danishuddin, M., R. Chatrath, and R. Singh. "Insights of Interaction between Small and Large Subunits of ADP-Glucose Pyrophosphorylase from Bread Wheat (Triticum Aestivum L.)." *Bioinformation* 6.4 (2011): 144-8. Print.

Dawar, C., S. Jain, and S. Kumar. "Insight into the 3D Structure of ADP-Glucose Pyrophosphorylase from Rice (Oryza Sativa L.)." *Journal of molecular modeling* 19.8 (2013): 3351-67. Print.

De Philippis, R., C. Sili, and M. Vincenzini. "Glycogen and Poly-β-Hydroxybutyrate Synthesis in *Spirulina Maxima*." *Journal of General Microbiology* 138 (1992): 1623-8. Print.

Decker, D., et al. "Substrate Kinetics and Substrate Effects on the Quaternary Structure of Barley UDP-Glucose Pyrophosphorylase." *Phytochemistry* 79 (2012): 39-45. Print.

Degeest, B., and L. de Vuyst. "Correlation of Activities of the Enzymes Alpha-Phosphoglucomutase, UDP-Galactose 4-Epimerase, and UDP-Glucose Pyrophosphorylase with Exopolysaccharide Biosynthesis by Streptococcus Thermophilus LY03." *Applied and Environmental Microbiology* 66.8 (2000): 3519-27. Print.

Delmer, D. P., and P. Albersheim. "The Biosynthesis of Sucrose and Nucleoside Diphosphate Glucoses in Phaseolus Aureus." *Plant Physiology* 45.6 (1970): 782-6. Print.

Devillers, C. H., et al. "Characterization of the Branching Patterns of Glycogen Branching Enzyme Truncated on the N-Terminus." *Archives of Biochemistry and Biophysics* 418.1 (2003): 34-8. Print.

Dhalla, A. M., et al. "Regeneration of Catalytic Activity of Glutamine Synthetase Mutants by Chemical Activation: Exploration of the Role of Arginines 339 and 359 in Activity." *Protein science : a publication of the Protein Society* 3.3 (1994): 476-81. Print.

Diez, M. D., et al. "A Chimeric UDP-Glucose Pyrophosphorylase Produced by Protein Engineering Exhibits Sensitivity to Allosteric Regulators." *International journal of molecular sciences* 14.5 (2013): 9703-21. Print.

Ducat, D. C., J. C. Way, and P. A. Silver. "Engineering Cyanobacteria to Generate High-Value Products." *Trends in biotechnology* 29.2 (2011): 95-103. Print.

Erdrich, P., et al. "Cyanobacterial Biofuels: New Insights and Strain Design Strategies Revealed by Computational Modeling." *Microbial cell factories* 13 (2014): 128,014-0128-x. Print.

Ernst, A., and P. Boger. "Glycogen Accumulation and the Induction of Nitrogenase Activity in the Heterocyst-Forming Cyanobacterium Anabaena Variabilis." *Journal of General Microbiology* 131 (1985): 3147-53. Print.

Espada, J. "Enzymatic Synthesis of Adenosine Diphosphate Glucose from Glucose-1-Phosphate and Adenosine Triphosphate." *Journal of Biological Chemistry* 237.12 (1962): 3577-3581. Print.

Eswar, N., et al. "Comparative Protein Structure Modeling using MODELLER." *Current protocols in protein science / editorial board, John E.Coligan ...[et al.]* Chapter 2 (2007): Unit 2.9. Print.

Fersht, A., ed. *Structure and Mechanism in Protein Science: A Guide to Enzyme Catalysis and Protein Folding*. W.H. Freeman, 1999. Print.

Figueroa, C. M., et al. "The Unique Nucleotide Specificity of the Sucrose Synthase from Thermosynechococcus Elongatus." *FEBS letters* 587.2 (2013): 165-9. Print.

Figueroa, C. M., et al. "Understanding the Allosteric Trigger for the Fructose-1,6-Bisphosphate Regulation of the ADP-Glucose Pyrophosphorylase from Escherichia Coli." *Biochimie* 93.10 (2011): 1816-23. Print.

Figueroa, C. M., et al. "Unraveling the Activation Mechanism of the Potato Tuber ADP-Glucose Pyrophosphorylase." *PloS one* 8.6 (2013): e66824. Print.

Fox, J. D., R. B. Kapust, and D. S. Waugh. "Single Amino Acid Substitutions on the Surface of Escherichia Coli Maltose-Binding Protein can have a Profound Impact on the Solubility of Fusion Proteins." *Protein science: a publication of the Protein Society* 10.3 (2001): 622-30. Print.

Fox, J. D., et al. "Maltodextrin-Binding Proteins from Diverse Bacteria and Archaea are Potent Solubility Enhancers." *FEBS letters* 537.1-3 (2003): 53-7. Print.

Fredrick, J. F. "Biochemical Evolution of Glucosyl Transferase Isozymes in Algae." *Annals of the New York Academy of Sciences* 151.1 (1968): 413-23. Print.

Frueauf, J. B., M. A. Ballicora, and J. Preiss. "ADP-Glucose Pyrophosphorylase from Potato Tuber: Site-Directed Mutagenesis of Homologous Aspartic Acid Residues in

the Small and Large Subunits." *The Plant Journal: for cell and molecular biology* 33.3 (2003): 503-11. Print.

Frueauf, J. B., M. A. Ballicora, and J. Preiss. "Alteration of Inhibitor Selectivity by Site-Directed Mutagenesis of Arg(294) in the ADP-Glucose Pyrophosphorylase from Anabaena PCC 7120." *Archives of Biochemistry and Biophysics* 400.2 (2002): 208-14. Print.

Frueauf, J. B., M. A. Ballicora, and J. Preiss. "Aspartate Residue 142 is Important for Catalysis by ADP-Glucose Pyrophosphorylase from *Escherichia Coli*." *The Journal of biological chemistry* 276.49 (2001): 46319-25. Print.

Fu, Y., et al. "Mechanism of Reductive Activation of Potato Tuber ADP-Glucose Pyrophosphorylase." *The Journal of biological chemistry* 273.39 (1998): 25045-52. Print.

Fu, Y., M. A. Ballicora, and J. Preiss. "Mutagenesis of the Glucose-1-Phosphate-Binding Site of Potato Tuber ADP-Glucose Pyrophosphorylase." *Plant Physiology* 117.3 (1998): 989-96. Print.

Führing, J., et al. "Catalytic Mechanism and Allosteric Regulation of UDP-Glucose Pyrophosphorylase from *Leishmania Major*." *ACS Catalysis* 3 (2013): 2976-85. Print.

Führing, J. I., et al. "A Quaternary Mechanism Enables the Complex Biological Functions of Octameric Human UDP-Glucose Pyrophosphorylase, a Key Enzyme in Cell Metabolism." *Scientific reports* 5 (2015): 9618. Print.

Furlong, C. E., and J. Preiss. "Biosynthesis of Bacterial Glycogen. VII. Purification and Properties of the Adenosine Diphosphoglucose Pyrophosphorylase of Rhodospirillium Rubrum." *The Journal of biological chemistry* 244.10 (1969): 2539-48. Print.

Fusari, C., et al. "A Colorimetric Method for the Assay of ADP-Glucose Pyrophosphorylase." *Analytical Biochemistry* 352.1 (2006): 145-7. Print.

Gardiol, A., and J. Preiss. "*Escherichia Coli* E-39 ADPglucose Synthetase has Different Activation Kinetics from the Wild-Type Allosteric Enzyme." *Archives of Biochemistry and Biophysics* 280.1 (1990): 175-80. Print.

Ghosh, H. P., and J. Preiss. "Adenosine Diphosphate Glucose Pyrophosphorylase. A Regulatory Enzyme in the Biosynthesis of Starch in Spinach Leaf Chloroplasts." *The Journal of biological chemistry* 241.19 (1966): 4491-504. Print.

Gomez-Casati, D. F., et al. "Ultrasensitive Behavior in the Synthesis of Storage Polysaccharides in Cyanobacteria." *Planta* 216.6 (2003): 969-75. Print.

Gomez-Casati, D. F., et al. "Identification of Functionally Important Amino-Terminal Arginines of *Agrobacterium Tumefaciens* ADP-Glucose Pyrophosphorylase by Alanine Scanning Mutagenesis." *Biochemistry* 40.34 (2001): 10169-78. Print.

Gomez-Casati, D. F., and A. A. Iglesias. "ADP-Glucose Pyrophosphorylase from Wheat Endosperm. Purification and Characterization of an Enzyme with Novel Regulatory Properties." *Planta* 214.3 (2002): 428-34. Print.

Greenfield, N. J. "Using Circular Dichroism Spectra to Estimate Protein Secondary Structure." *Nature protocols* 1.6 (2006): 2876-90. Print.

Guerra, L. T., et al. "Natural Osmolytes are Much Less Effective Substrates than Glycogen for Catabolic Energy Production in the Marine Cyanobacterium Synechococcus Sp. Strain PCC 7002." *Journal of Biotechnology* 166.3 (2013): 65-75. Print.

Gutteridge, A., and J. M. Thornton. "Understanding Nature's Catalytic Toolkit." *Trends in biochemical sciences* 30.11 (2005): 622-9. Print.

Hall, T. A. "BioEdit: A User-Friendly Biological Sequence Alignment Editor and Analysis Program for Windows 95/98/NT." *Nucl. Acids. Symp. Ser.* 41 (1999): 95-8. Print.

Hanai, T., S. Atsumi, and J. C. Liao. "Engineered Synthetic Pathway for Isopropanol Production in Escherichia Coli." *Applied and Environmental Microbiology* 73.24 (2007): 7814-8. Print.

Hanes, C. "The Breakdown and Synthesis of Starch by an Enzyme System from Pea Seeds." *Proceedings of the Royal Society of London, B* 128 (1940): 421-50. Print.

Hanes, C. "The Reversible Formation of Starch from Glucose-1-Phosphate Catalysed by Potato Phosphorylase." *Proceedings of the Royal Society of London B* 129 (1940): 174-208. Print.

Harun, R., et al. "Exploring Alkaline Pre-Treatment of Microalgal Biomass for Bioethanol Production." *Applied Energy* 88 (2011): 3464-7. Print.

Hasunuma, T., et al. "Dynamic Metabolic Profiling of Cyanobacterial Glycogen Biosynthesis Under Conditions of Nitrate Depletion." *Journal of experimental botany* 64.10 (2013): 2943-54. Print.

Haugen, T. H., and J. Preiss. "Biosynthesis of Bacterial Glycogen. the Nature of the Binding of Substrates and Effectors to ADP-Glucose Synthase." *The Journal of biological chemistry* 254.1 (1979): 127-36. Print.

Heiniger, U., and G. and Franz. "The Role of NDP-Glucose Pyrophosphorylases in Growing Mung Bean Seedlings in Relation to Cell Wall Biosynthesis." *Plant Science Letters* 17 (1980): 443-50. Print.

Hendrickson, W. A. "Determination of Macromolecular Structures from Anomalous Diffraction of Synchrotron Radiation." *Science (New York, N.Y.)* 254.5028 (1991): 51-8. Print.

Hers, H. G., H. De Wulf, and and Van den Berghe, G. "The *in Vitro* and *in Vivo* Interconversion of the *a* and *b* Forms of Liver Glycogen Synthetase." *Sixth FEBS Symposium, Volume 19: Metabolic Regulation and Enzyme Action.* Ed. Sols, A. and Grisolía, S. New York and London: Academic Press, 1969. 161-170. Print.

Hill, B. L., et al. "Conserved Residues of the Pro103-Arg115 Loop are Involved in Triggering the Allosteric Response of the *Escherichia Coli* ADP-Glucose Pyrophosphorylase." *Protein science: a publication of the Protein Society* 24.5 (2015): 714-28. Print.

Hill, M. A., et al. "Biosynthesis of Bacterial Glycogen. Mutagenesis of a Catalytic Site Residue of ADP-Glucose Pyrophosphorylase from Escherichia Coli." *The Journal of biological chemistry* 266.19 (1991): 12455-60. Print.

Hind, G., H. Y. Nakatani, and S. Izawa. "Light-Dependent Redistribution of Ions in Suspensions of Chloroplast Thylakoid Membranes." *Proceedings of the National Academy of Sciences of the United States of America* 71.4 (1974): 1484-8. Print.

Ho, S. H., et al. "Bioprocess Development on Microalgae-Based CO2 Fixation and Bioethanol Production using Scenedesmus Obliquus CNW-N." *Bioresource Technology* 145 (2013): 142-9. Print.

Holliday, G. L., et al. "The Chemistry of Protein Catalysis." *Journal of Molecular Biology* 372.5 (2007): 1261-77. Print.

Holliday, G. L., J. B. Mitchell, and J. M. Thornton. "Understanding the Functional Roles of Amino Acid Residues in Enzyme Catalysis." *Journal of Molecular Biology* 390.3 (2009): 560-77. Print.

Hopkins, C. E., et al. "Chemical-Modification Rescue Assessed by Mass Spectrometry Demonstrates that Gamma-Thia-Lysine Yields the Same Activity as Lysine in

Aldolase." *Protein science : a publication of the Protein Society* 11.7 (2002): 1591-9. Print.

Humphrey, W., A. Dalke, and K. Schulten. "VMD: Visual Molecular Dynamics." *Journal of Molecular Graphics* 14.1 (1996): 33,8, 27-8. Print.

Hwang, S. K., S. Hamada, and T. W. Okita. "Catalytic Implications of the Higher Plant ADP-Glucose Pyrophosphorylase Large Subunit." *Phytochemistry* 68.4 (2007): 464-77. Print.

Hylton, C., and A. M. Smith. "The Rb Mutation of Peas Causes Structural and Regulatory Changes in ADP Glucose Pyrophosphorylase from Developing Embryos." *Plant Physiology* 99.4 (1992): 1626-34. Print.

Igarashi, R. Y., and C. R. Meyer. "Cloning and Sequencing of Glycogen Metabolism Genes from Rhodobacter Sphaeroides 2.4.1. Expression and Characterization of Recombinant ADP-Glucose Pyrophosphorylase." *Archives of Biochemistry and Biophysics* 376.1 (2000): 47-58. Print.

Iglesias, A. A., and J. Preiss. "Bacterial Glycogen and Plant Starch." *Biochemical Education* 20.4 (1992): 196-203. Print.

Iglesias, A. A., et al. "Domain Swapping between a Cyanobacterial and a Plant Subunit ADP-Glucose Pyrophosphorylase." *Plant & Cell Physiology* 47.4 (2006): 523-30. Print.

Ingram, L. O., et al. "Genetic Engineering of Ethanol Production in Escherichia Coli." *Applied and Environmental Microbiology* 53.10 (1987): 2420-5. Print.

Isom DG, Castañeda CA, Cannon BR and García-Moreno B. "Large Shifts in pKa Values of Lysine Residues Buried Inside a Protein." *Proc Natl Acad Sci U S A.* 108.13 (2011): 5260. Print.

Jin, X., et al. "Crystal Structure of Potato Tuber ADP-Glucose Pyrophosphorylase." *The EMBO journal* 24.4 (2005): 694-704. Print.

Kelly, S. M., and N. C. Price. "The use of Circular Dichroism in the Investigation of Protein Structure and Function." *Current Protein & Peptide Science* 1.4 (2000): 349-84. Print.

Kilian, A., et al. "Mapping of the ADP-Glucose Pyrophosphorylase Genes in Barley." *TAG.Theoretical and applied genetics.Theoretische und angewandte Genetik* 87.7 (1994): 869-71. Print.

Kimata, K., and S. Suzuki. "Studies on Cytidine Diphosphate Glucose Pyrophosphorylase and Related Enzymes of Azotobacter Vinelandii." *The Journal of biological chemistry* 241.5 (1966): 1099-113. Print.

Kleczkowski, L. A., et al. "UDP-Glucose Pyrophosphorylase. an Old Protein with New Tricks." *Plant Physiology* 134.3 (2004): 912-8. Print.

Konig, H., et al. "Glycogen in Thermoacidophilic Archaebacteria of the genera *Sulfolobus, Thermoproteus, Desulfurococcus* and*Thermococcus*." *Arch.Microbiol.* 132.4 (1982): 297-303. Print.

Kornfeld, S., and L. GLASER. "The Enzymic Synthesis of Thymidine-Linked Sugars. I. Thymidine Diphosphate Glucose." *The Journal of biological chemistry* 236 (1961): 1791-4. Print.

Koropatkin, N. M., W. W. Cleland, and H. M. Holden. "Kinetic and Structural Analysis of Alpha-D-Glucose-1-Phosphate Cytidylyltransferase from Salmonella Typhi." *The Journal of biological chemistry* 280.11 (2005): 10774-80. Print.

Kramer, E. B., and P. J. Farabaugh. "The Frequency of Translational Misreading Errors in E. Coli is Largely Determined by tRNA Competition." *RNA (New York, N.Y.)* 13.1 (2007): 87-96. Print.

Kuhn, M. L., C. A. Falaschetti, and M. A. Ballicora. "Ostreococcus Tauri ADP-Glucose Pyrophosphorylase Reveals Alternative Paths for the Evolution of Subunit Roles." *The Journal of biological chemistry* 284.49 (2009): 34092-102. Print.

Kuhn, M. L., et al. "Bi-National and Interdisciplinary Course in Enzyme Engineering." *Biochemistry and molecular biology education : a bimonthly publication of the International Union of Biochemistry and Molecular Biology* 38.6 (2010): 370-9. Print.

Kuhn, M. L., et al. "The Ancestral Activation Promiscuity of ADP-Glucose Pyrophosphorylases from Oxygenic Photosynthetic Organisms." *BMC evolutionary biology* 13 (2013): 51,2148-13-51. Print.

Kumar, A., et al. "Biosynthesis of Bacterial Glycogen. Determination of the Amino Acid Changes that Alter the Regulatory Properties of a Mutant Escherichia Coli ADP-Glucose Synthetase." *The Journal of biological chemistry* 264.18 (1989): 10464-71. Print.

Kumar, A., et al. "Biosynthesis of Bacterial Glycogen. use of Site-Directed Mutagenesis to Probe the Role of Tyrosine 114 in the Catalytic Mechanism of ADP-Glucose

Synthetase from Escherichia Coli." *The Journal of biological chemistry* 263.29 (1988): 14634-9. Print.

Larsen, C. E., Y. M. Lee, and J. Preiss. "Covalent Modification of the Inhibitor-Binding Site(s) of Escherichia Coli ADP-Glucose Synthetase. Isolation and Structural Characterization of 8-Azido-AMP-Incorporated Peptides." *The Journal of biological chemistry* 261.33 (1986): 15402-9. Print.

Lehmann, M., and G. Wober. "Accumulation, Mobilization and Turn-Over of Glycogen in the Blue-Green Bacterium Anacystis Nidulans." *Archives of Microbiology* 111.1-2 (1976): 93-7. Print.

Leloir, L. F., and C. E. Cardini. "Biosynthesis of Glycogen from Uridine Diphosphate Glucose." *J. Am. Chem. Soc.* 79 (1957): 6340. Print.

LELOIR, L. F., and C. E. CARDINI. "The Biosynthesis of Sucrose Phosphate." *The Journal of biological chemistry* 214.1 (1955): 157-65. Print.

Levi, C., and J. Preiss. "Regulatory Properties of the ADP-Glucose Pyrophosphorylase of the Blue-Green Bacterium Synechococcus 6301." *Plant Physiology* 58.6 (1976): 753-6. Print.

Levine, S., et al. "Uridine Diphosphate Glucose Pyrophosphorylase. II." *The Journal of biological chemistry* 244.20 (1969): 5729-34. Print.

Liu, T., and C. Khosla. "Genetic Engineering of Escherichia Coli for Biofuel Production." *Annual Review of Genetics* 44 (2010): 53-69. Print.

Liu, T., H. Vora, and C. Khosla. "Quantitative Analysis and Engineering of Fatty Acid Biosynthesis in E. Coli." *Metabolic engineering* 12.4 (2010): 378-86. Print.

Lopez, P. J., et al. "Prospects in Diatom Research." *Current opinion in biotechnology* 16.2 (2005): 180-6. Print.

Lu, X., H. Vora, and C. Khosla. "Overproduction of Free Fatty Acids in E. Coli: Implications for Biodiesel Production." *Metabolic engineering* 10.6 (2008): 333-9. Print.

Luthy, R., J. U. Bowie, and D. Eisenberg. "Assessment of Protein Models with Three-Dimensional Profiles." *Nature* 356.6364 (1992): 83-5. Print.

Machtey, M., et al. "Insights into Glycogen Metabolism in Chemolithoautotrophic Bacteria from Distinctive Kinetic and Regulatory Properties of ADP-Glucose

Pyrophosphorylase from *Nitrosomonas Europaea*." *Journal of Bacteriology* 194.22 (2012): 6056-65. Print.

Mackerell, A. D.,Jr, M. Feig, and C. L. Brooks 3rd. "Extending the Treatment of Backbone Energetics in Protein Force Fields: Limitations of Gas-Phase Quantum Mechanics in Reproducing Protein Conformational Distributions in Molecular Dynamics Simulations." *Journal of computational chemistry* 25.11 (2004): 1400-15. Print.

Malarkey, C. S., et al. "Evidence for Two Distinct Mg2+ Binding Sites in G(s Alpha) and G (i alpha1) Proteins." *Biochemical and biophysical research communications* 372.4 (2008): 866-9. Print.

Mangelsdorf, P. C., and D. F. Jones. "The Expression of Mendelian Factors in the Gametophyte of Maize." *Genetics* 11.5 (1926): 423-55. Print.

Martz, F., M. Wilczynska, and L. A. Kleczkowski. "Oligomerization Status, with the Monomer as Active Species, Defines Catalytic Efficiency of UDP-Glucose Pyrophosphorylase." *The Biochemical journal* 367.Pt 1 (2002): 295-300. Print.

Maruyama, D., et al. "Crystal Structure of Uridine-Diphospho-N-Acetylglucosamine Pyrophosphorylase from *Candida Albicans* and Catalytic Reaction Mechanism." *The Journal of biological chemistry* 282.23 (2007): 17221-30. Print.

Mazumdar, S., J. M. Clomburg, and R. Gonzalez. "Escherichia Coli Strains Engineered for Homofermentative Production of D-Lactic Acid from Glycerol." *Applied and Environmental Microbiology* 76.13 (2010): 4327-36. Print.

Melis, A. "Solar Energy Conversion Efficiencies in Photosynthesis: Minimizing the Chlorophyll Antennae to Maximize Efficiency." *Plant Science* 177 (2009): 272-80. Print.

Meng, M., et al. "UDP-Glucose Pyrophosphorylase is Not Rate Limiting, but is Essential in Arabidopsis." *Plant & Cell Physiology* 50.5 (2009): 998-1011. Print.

Minor, W., et al. "Crystal Structure of Soybean Lipoxygenase L-1 at 1.4 A Resolution." *Biochemistry* 35.33 (1996): 10687-701. Print.

Miranda, J. R., P. C. Passarinho, and L. Gouveia. "Pre-Treatment Optimization of Scenedesmus Obliquus Microalga for Bioethanol Production." *Bioresource technology* 104 (2012): 342-8. Print.

Mochalkin, I., et al. "Characterization of Substrate Binding and Catalysis in the Potential Antibacterial Target N-Acetylglucosamine-1-Phosphate Uridyltransferase (GlmU)." *Protein science: a publication of the Protein Society* 16.12 (2007): 2657-66. Print.

Mora-Garcia, S., M. A. Ballicora, and R. A. Wolosiuk. "Chloroplast Fructose-1,6-Bisphosphatase: Modification of Non-Covalent Interactions Promote the Activation by Chimeric Escherichia Coli Thioredoxins." *FEBS letters* 380.1-2 (1996): 123-6. Print.

Moretti, R., et al. "Expanding the Nucleotide and Sugar 1-Phosphate Promiscuity of Nucleotidyltransferase RmlA Via Directed Evolution." *Journal of Biological Chemistry* 286.15 (2011): 13235-43. Print.

Nelson, D. L., and M. M. Cox, eds. *Lehniger Principles of Biochemistry.* Third ed. New York: Worth Publishers, 2000. Print.

O'Brien, P. J., et al. "Arginine Coordination in Enzymatic Phosphoryl Transfer: Evaluation of the Effect of Arg166 Mutations in Escherichia Coli Alkaline Phosphatase." *Biochemistry* 47.29 (2008): 7663-72. Print.

Okita, T. W., R. L. Rodriguez, and J. Preiss. "Biosynthesis of Bacterial Glycogen. Cloning of the Glycogen Biosynthetic Enzyme Structural Genes of Escherichia Coli." *The Journal of biological chemistry* 256.13 (1981): 6944-52. Print.

Olsen, L. R., and S. L. Roderick. "Structure of the Escherichia Coli GlmU Pyrophosphorylase and Acetyltransferase Active Sites." *Biochemistry* 40.7 (2001): 1913-21. Print.

Ozbun, J. L., J. S. Hawker, and J. Preiss. "Soluble Adenosine Diphosphate Glucose- -1,4-Glucan -4-Glucosyltransferases from Spinach Leaves." *The Biochemical journal* 126.4 (1972): 953-63. Print.

Paule, M. R., and J. Preiss. "Biosynthesis of Bacterial Glycogen. X. the Kinetic Mechanism of Adenosine Diphosphoglucose Pyrophosphorylase from *Rhodospirillum Rubrum*." *Journal of Biological Chemistry* 246 (1971): 4602-9. Print.

Pelissier, M. C., et al. "Structural Insights into the Catalytic Mechanism of Bacterial Guanosine-Diphospho-D-Mannose Pyrophosphorylase and its Regulation by Divalent Ions." *The Journal of biological chemistry* 285.35 (2010): 27468-76. Print.

Pelroy, R. A., and J. A. Bassham. "Photosynthetic and Dark Carbon Metabolism in Unicellular Blue-Green Algae." *Archiv fur Mikrobiologie* 86.1 (1972): 25-38. Print.

Phillips, J. C., et al. "Scalable Molecular Dynamics with NAMD." *Journal of computational chemistry* 26.16 (2005): 1781-802. Print.

Planas, A., and J. F. Kirsch. "Reengineering the Catalytic Lysine of Aspartate Aminotransferase by Chemical Elaboration of a Genetically Introduced Cysteine." *Biochemistry* 30.33 (1991): 8268-76. Print.

Plaxton, W. C., and J. Preiss. "Purification and Properties of Nonproteolytic Degraded ADPglucose Pyrophosphorylase from Maize Endosperm." *Plant Physiology* 83.1 (1987): 105-12. Print.

Preiss, J., S. Yung, and P. A. and Baecker. "Regulation of Bacterial Glycogen Synthesis." *Molecular and Cellular Biochemistry* 57 (1983): 61-80. Print.

Preiss, J. "Adenosine Diphosphoryl Glucose Pyrophosphorylase." *The Enzymes, Vol. 8.* Ed. P. Boyer. 3rd ed. New York, N.Y.: Academic Press, 1973. 73-119. Print.

Preiss, J. *"The Biochemistry of Plants: A Comprehensive Treastise*. Volume 3 ed. New York, NY: Academic Press, 1980. Print.

Preiss, J. "Regulation of the Biosynthesis and Degradation of Starch." *Annual Review of Plant Physiology* 33 (1982): 431-454. Print.

Preiss, J., et al. "Biosynthesis of Bacterial Glycogen. IV. Activation and Inhibition of the Adenosine Diphosphate Glucose Pyrophosphorylase of *Escherichia Coli* B." *Biochemistry* 5.6 (1966): 1833-45. Print.

Preiss, J. "Bacterial Glycogen Synthesis and its Regulation." *Annual Review of Microbiology* 38 (1984): 419-58. Print.

Press, W. H., et al. *Numerical Recipes in C: The Art of Scientific Computing.* New York: Cambridge University Press, New York, 1988. Print.

Quintana, N., et al. "Renewable Energy from Cyanobacteria: Energy Production Optimization by Metabolic Pathway Engineering." *Applied Microbiology and Biotechnology* 91.3 (2011): 471-90. Print.

Recondo, E., M. Dankert, and L. F. Leloir. "Isolation of Adenosine Diphosphate D-Glucose from Corn Grains." *Biochemical and biophysical research communications* 12 (1963): 204-7. Print.

Recondo, E., and L. F. Leloir. "Adenosine Diphosphate Glucose and Starch Synthesis." *Biochemical and biophysical research communications* 6 (1961): 85-8. Print.

Revedin, A., et al. "Thirty Thousand-Year-Old Evidence of Plant Food Processing." *Proceedings of the National Academy of Sciences of the United States of America* 107.44 (2010): 18815-9. Print.

Robinson, K. A., et al. "Effects of Diabetes and Hyperglycemia on the Hexosamine Synthesis Pathway in Rat Muscle and Liver." *Diabetes* 44.12 (1995): 1438-46. Print.

Rosenberg, J. N., et al. "A Green Light for Engineered Algae: Redirecting Metabolism to Fuel a Biotechnology Revolution." *Current opinion in biotechnology* 19.5 (2008): 430-6. Print.

Rossmann, M. G., D. Moras, and K. W. Olsen. "Chemical and Biological Evolution of Nucleotide-Binding Protein." *Nature* 250.463 (1974): 194-9. Print.

Sali, A., and T. L. Blundell. "Comparative Protein Modelling by Satisfaction of Spatial Restraints." *Journal of Molecular Biology* 234.3 (1993): 779-815. Print.

Santarius, K. A., and U. Heber. "Changes in the Intracellular Levels of ATP, ADP, AMP and P1 and Regulatory Function of the Adenylate System in Leaf Cells during Photosynthesis." *Biochimica et biophysica acta* 102.1 (1965): 39-54. Print.

Sanwal, G. G., et al. "Regulation of Starch Biosynthesis in Plant Leaves: Activation and Inhibition of ADPglucose Pyrophosphorylase." *Plant Physiology* 43.3 (1968): 417-27. Print.

Sanwal, G. G., and J. Preiss. "Biosynthesis of Starch in Chlorella Pyrenoidosa. II. Regulation of ATP: Alpha-D-Glucose 1-Phosphate Adenyl Transferase (ADP-Glucose Pyrophosphorylase) by Inorganic Phosphate and 3-Phosphoglycerate." *Archives of Biochemistry and Biophysics* 119.1 (1967): 454-69. Print.

Saraste, M., P. R. Sibbald, and A. Wittinghofer. "The P-Loop--a Common Motif in ATP- and GTP-Binding Proteins." *Trends in biochemical sciences* 15.11 (1990): 430-4. Print.

Shen, L., and J. Preiss. "The Activation and Inhibition of Bacterial Adenosine-Diphosphoglucose Pyrophosphorylase." *Biochemical and Biophysical Research Communications* 17 (1964): 424-9. Print.

Shen, M. Y., and A. Sali. "Statistical Potential for Assessment and Prediction of Protein Structures." *Protein science: a publication of the Protein Society* 15.11 (2006): 2507-24. Print.

Sivaraman, J., et al. "Crystal Structure of *Escherichia Coli* Glucose-1-Phosphate Thymidylyltransferase (RffH) Complexed with dTTP and Mg2+." *The Journal of biological chemistry* 277.46 (2002): 44214-9. Print.

Slattery, C. J., I. H. Kavakli, and T. W. Okita. "Engineering Starch for Increased Quantity and Quality." *Trends in plant science* 5.7 (2000): 291-8. Print.

Smidansky, E. D., et al. "Enhanced ADP-Glucose Pyrophosphorylase Activity in Wheat Endosperm Increases Seed Yield." *Proceedings of the National Academy of Sciences of the United States of America* 99.3 (2002): 1724-9. Print.

Smith, H. B., and F. C. Hartman. "Restoration of Activity to Catalytically Deficient Mutants of Ribulosebisphosphate carboxylase/oxygenase by Aminoethylation." *The Journal of biological chemistry* 263.10 (1988): 4921-5. Print.

Spiro, M. J. "Effect of Diabetes on the Sugar Nucleotides in several Tissues of the Rat." *Diabetologia* 26.1 (1984): 70-5. Print.

Steen, E. J., et al. "Microbial Production of Fatty-Acid-Derived Fuels and Chemicals from Plant Biomass." *Nature* 463.7280 (2010): 559-62. Print.

Steiner, T., et al. "Open and Closed Structures of the UDP-Glucose Pyrophosphorylase from Leishmania Major." *The Journal of biological chemistry* 282.17 (2007): 13003-10. Print.

Stephanopoulos, G. "Challenges in Engineering Microbes for Biofuels Production." *Science (New York, N.Y.)* 315.5813 (2007): 801-4. Print.

Takata, H., et al. "Characterization of a Gene Cluster for Glycogen Biosynthesis and a Heterotetrameric ADP-Glucose Pyrophosphorylase from *Bacillus Stearothermophilus*." *Journal of Bacteriology* 179.15 (1997): 4689-98. Print.

Thoden, J. B., and H. M. Holden. "The Molecular Architecture of Glucose-1-Phosphate Uridylyltransferase." *Protein science : a publication of the Protein Society* 16.3 (2007): 432-40. Print.

Uttaro, A. D., et al. "Cloning and Expression of the glgC Gene from Agrobacterium Tumefaciens: Purification and Characterization of the ADPglucose Synthetase." *Archives of Biochemistry and Biophysics* 357.1 (1998): 13-21. Print.

Vaillancourt, P., ed. *E.Coli Gene Expressions Protocols (Methods in Molecular Biology)*. Vol 205 ed. New Jersey: Humana Press, 2003. Print.

Ventriglia, T., et al. "Regulatory Properties of Potato-Arabidopsis Hybrid ADP-Glucose Pyrophosphorylase." *Plant & Cell Physiology* 48.6 (2007): 875-80. Print.

Ventriglia, T., et al. "Two Arabidopsis ADP-Glucose Pyrophosphorylase Large Subunits (APL1 and APL2) are Catalytic." *Plant Physiology* 148.1 (2008): 65-76. Print.

Villand, P., et al. "ADP-Glucose Pyrophosphorylase Large Subunit cDNA from Barley Endosperm." *Plant Physiology* 100.3 (1992): 1617-8. Print.

Weissborn, A. C., et al. "UTP: Alpha-D-Glucose-1-Phosphate Uridylyltransferase of Escherichia Coli: Isolation and DNA Sequence of the galU Gene and Purification of the Enzyme." *Journal of Bacteriology* 176.9 (1994): 2611-8. Print.

Wentz, J. B. "Linkage between Sweet-Defective and Sugary Endosperm in Maize." *Genetics* 10.4 (1925): 395-401. Print.

Wolosiuk, R. A., M. A. Ballicora, and K. Hagelin. "The Reductive Pentose Phosphate Cycle for Photosynthetic CO2 Assimilation: Enzyme Modulation." *FASEB journal : official publication of the Federation of American Societies for Experimental Biology* 7.8 (1993): 622-37. Print.

Xu, Y., et al. "Altered Carbohydrate Metabolism in Glycogen Synthase Mutants of Synechococcus Sp. Strain PCC 7002: Cell Factories for Soluble Sugars." *Metabolic engineering* 16 (2013): 56-67. Print.

Yep, A., G. L. Kenyon, and M. J. McLeish. "Saturation Mutagenesis of Putative Catalytic Residues of Benzoylformate Decarboxylase Provides a Challenge to the Accepted Mechanism." *Proc Natl Acad Sci U S A.* 105 (2008): 5733-8. Print.

Yep, A., M. A. Ballicora, and J. Preiss. "The Active Site of the Escherichia Coli Glycogen Synthase is Similar to the Active Site of Retaining GT-B Glycosyltransferases." *Biochemical and biophysical research communications* 316.3 (2004): 960-6. Print.

The ADP-Glucose Binding Site of the Escherichia Coli Glycogen Synthase." *Archives of Biochemistry and Biophysics* 453.2 (2006): 188-96. Print.

Yep, A., et al. "Identification and Characterization of a Critical Region in the Glycogen Synthase from Escherichia Coli." *The Journal of biological chemistry* 279.9 (2004): 8359-67. Print.

Yep, A., et al. "An Assay for Adenosine 5'-Diphosphate (ADP)-Glucose Pyrophosphorylase that Measures the Synthesis of Radioactive ADP-Glucose with Glycogen Synthase." *Analytical Biochemistry* 324.1 (2004): 52-9. Print.

Yomano, L. P., et al. "Re-Engineering Escherichia Coli for Ethanol Production." *Biotechnology Letters* 30.12 (2008): 2097-103. Print.

Zhang, K., et al. "Expanding Metabolism for Biosynthesis of Nonnatural Alcohols." *Proceedings of the National Academy of Sciences of the United States of America* 105.52 (2008): 20653-8. Print.

Zhao, J., et al. "Homofermentative Production of Optically Pure L-Lactic Acid from Xylose by Genetically Engineered Escherichia Coli B." *Microbial cell factories* 12 (2013): 57,2859-12-57. Print.

Ziegler, A. J., et al. "Alkaline Phosphatase Inhibition by Vanadyl-Beta-Diketone Complexes: Electron Density Effects." *Journal of enzyme inhibition and medicinal chemistry* 24.1 (2009): 22-8. Print.

Zuccotti, S., et al. "Kinetic and Crystallographic Analyses Support a Sequential-Ordered Bi Bi Catalytic Mechanism for Escherichia Coli Glucose-1-Phosphate Thymidylyltransferase." *Journal of Molecular Biology* 313.4 (2001): 831-43. Print.

VITA

Angela L. Mahaffey was born in Cook County, IL. She attended the University of Chicago where she earned a Bachelor of Arts in Biological Sciences, in 2004. She was quickly recruited as an Instructor of Environmental Biology at East-West University. Continuing to fulfill her yearning for science, she enrolled part-time into the Graduate (Ph.D.) Program in the Department of Chemistry and Biochemistry at Loyola University Chicago, and later changed her status to fulltime.

While attending Loyola, Angela L. Mahaffey was the recipient of a DFI Fellowship (Illinois Board of Higher Education; IBHE) and the Robert Otremba Scholarship (Loyola University Chicago - Chemistry Dept.). In 2008, Mahaffey was inducted into the National Honor Society for Women in Chemistry (Iota Sigma Pi), and later became a member of the American Chemical Society and Biophysical Society. Mahaffey became the recipient of a number of national scientific conference awards for her superlative research presentations - some of which were also noted in select journal publications. Her work was exhibited at conferences hosted by the American Society of Biochemistry and Molecular Biology (ASBMB), National Organization for the Professional Advancement of Black Chemist and Chemical Engineers (NOBCChe), Biophysical Society Conference (BPS) and Midwest Enzyme Chemistry Conferences (MECC) Committees, Great Lakes BioInformatics (GLBIO*)* and a local DFI Fellowship

(IBHE) Conference – at the University of Illinois at Chicago, which she won awards and received notable recognitions in Journal Publications. Mahaffey was also featured in the Winter 2014 LOYOLA Magazine (both hardcopy and online), Loyola University Chicago (ORS) Endeavors Magazine (2011-2012): Women in Science Issue and the Loyola University Chicago Graduate School Quarterly Newsletter (on a number of occasions). Mahaffey, the dedicated humanitarian she is, initiated an on-site laboratory setting in the impoverished West Englewood area of Chicago, IL. Supporting Mahaffey's positive aspirations the Loyola University Chicago Dept. of Chemistry and Biochemistry decided to loan some scientific glassware, equipment and chemical solutions toward the inception of this Summer STEM program (entitled "Science Day"), on an annual basis. This STEM program exposed socioeconomically challenged students (K-12, who lacked the appropriate science curricula in their local schools) to applied science to applied chemical, environmental and biochemical sciences skills and techniques - whom lacked the proper science curricula in their local schools. In 2014, the STEM program abstract was submitted to the National Science Foundation entitled "An Approach to Youth STEM Education: Science Day Initiative' (Grades K-12) West Englewood Community – Chicago, IL (USA)". Weekly, Mahaffey currently volunteers with various non- profit Community-based Affiliates, Churches and Food-Pantry Distribution.

Presently, Angela L. Mahaffey is a Chemistry Laboratory Instructor and Coordinator in the Department of Chemistry and Biochemistry at Loyola University Chicago - and the Department of Chemistry at North Park University (Chicago, IL). She received her Ph.D. in Chemistry December 2015.